UNIVERSITA' DEGLI STUDI DI VERONA

DIPARTIMENTO DI BIOTECNOLOGIE

DOTTORATO DI RICERCA IN BIOTECNOLOGIE AGROINDUSTRIALI

CICLO XX

EXPRESSION OF MURINE AND VIRAL INTERLEUKIN-10 IN TOBACCO FOR IMMUNOMODULATION OF GALT FOR THE PREVENTION OF AUTOIMMUNE DISEASES

S.S.D. AGR/07

Coordinatore: Prof. Massimo Delledonne

Tutore: Prof. Mario Pezzotti

Co-tutori

Dr. Stefan Schillberg
Fraunhofer Institute for Molecular Biology and Applied Ecology, Aachen, Germany

Prof. Dr. Ralph Bock
Max Planck Institute of Molecular Plant Physiology, Potsdam-Golm, Germany

Dottorando: Dott.ssa Luisa Bortesi

TABLE OF CONTENTS

FIGURES

ABBREVIATIONS

α	anti, used in antibody abbreviations
ABTS	2,2'-Azino-di-(3-ethylbenzothiazoline sulphonate)
B cell	Bone-marrow-derived lymphocyte
BAP	6-Benzylaminopurine
BHK	Baby hamster kidney cell line
bp	base pair
BY-2	Bright Yellow-2 *N. tabacum* suspension cell cultures
cDNA	Complementary DNA
CHO	Chinese hamster ovary cell line
cv.	Cultivar
DMAE	2-Dimethylaminoethanol
DMSO	Dimethylsulfoxide
DNA	Deoxyribonucleic acid
dNTP	Deoxyribonucleoside triphosphate
dpi	days post infiltration / days post induction
DTT	Dithiothreitol
EDTA	Ethylene diaminether tetra-acetic acid
EGTA	Ethylene glycol tetraacetic acid
g	Relative centrifugal force (rcf)
GAPDH	Glyceraldehyde-3-phosphate-dehydrogenase
h	Hour(s)
HEPES	4-(2-Hydroxyethyl)-1-piperazineethanesulfonic acid
IPTG	Isopropyl-beta-D-thiogalactopyranosyde
kb	kilobase
kDa	kiloDalton
l	Liter
M	Molar
MES	Morpholineethanesulfonic acid
MHC	Major histocompatibility complex
min	Minute(s)
MS	Murashige and Skoog

NAA	Naphtaleneacetic acid
NBT-BCIP	Nitro-blue-tetrazolium-chloride/5-bromo 4-chloro-3-indolyl phosphate
NOD	Non obese diabetic
Nos	Nopaline synthase gene
NS0	mouse myeloma cell line
NSA	Nonenyl Succinic Anhydride
o/n	Overnight
OD	Optical density
ORF	Open reading frame
ori	origin of replication
PCR	Polymerase chain reaction
poly A	Polyadenylation signal
psi	Pound per square inch
PVPP	Poly Vinyl Poly Pyrrolidone
RNA	Ribonucleic acid
Rt	Room temperature
RT	Reverse transcription
T cell	Thymus-derived lymphocyte
Taq	*Thermus aquaticus*
UV	Ultraviolet
VCD	Vinyl cyclohexene dioxide
v/v	Volume per volume
w/v	Weight per volume
w/w	Weight per weight
wt	wild type

I INTRODUCTION

I.1 Plant molecular farming

Plant molecular farming (PMF) is the production of pharmaceutically important and commercially valuable proteins in plants (Franken et al., 1997). It exploits heterologous protein expression systems, such as plants, for the large-scale production of recombinant proteins that are therapeutically valuable, industrial enzymes, diagnostic and technical proteins.

I.1.1 Plant made pharmaceuticals (PMP)

The recombinant production of pharmaceuticals in plants is expected to challenge already established production technologies that currently are bacterial fermentation (*Escherichia coli*), yeast cell cultures (*Saccharomyces cerevisiae*, *Pichia pastoris*), insect cells, or mammalian cell cultures (NS0, BHK, CHO), for several reasons. First of all, molecular farming in plants provides an inexpensive and convenient way to produce biopharmaceutical molecules on a large scale. Using open-field cultivation, transgenic plants have superior advantages over all established expression systems in terms of capacity, flexibility, scalability, and production costs (Boehm, 2007). In fact, production of PMPs in whole plants needs simple and inexpensive inputs like sunlight, water and nutrients, it enables unsophisticated and rapid increase of production through increasing the area put to seed, and low technology harvest and processing for production of pharmaceuticals (Rigano and Walmsley, 2005). Therefore, the use of transgenic plants could be a valid solution to the need for a scale-up in the production capacity of recombinant proteins.

Another fundamental advantage of plants is the range and diversity of recombinant molecules that they can potentially produce. As higher eukaryotes, plants are able to synthesize small peptides, polypeptides and complex multimeric proteins, many of which cannot be made in microbial systems (Ma et al., 2003). For many molecules, such as antibodies, the presence of plant chaperones that are homologous to those in mammalian

cells is an important factor, as these chaperones control the efficiency of protein assembly and the extent of protein degradation. In addition, targeting recombinant proteins to the plant secretory pathway ensures that *N*-glycosylation and other post-translational modifications take place.

Unlike microbial or mammalian cell culture systems, plants ensure production of safe biopharmaceuticals, because they lack human pathogens, oncogenic DNA sequences, prions, and endotoxins (Commandeur et al., 2003).

Moreover, recombinant pharmaceutical proteins can be expressed in definite compartments or even targeted to storage organs such as seeds, where they remain stable for months at ambient temperatures, enormously reducing the costs of storage and distribution (Stoger et al., 2000).

Furthermore, plants can be exploited not only as production platforms for pharmaceutical proteins, but also as delivery systems for certain products when the plant tissue containing the recombinant protein is used as food, making extensive purification unnecessary and dramatically cutting down production costs (Lal et al., 2007).

Many pharmaceutical proteins of mammalian origin have been synthesized in plants. These range from blood products, such as human serum albumin for which there is an annual demand of more than 500 tonnes, to cytokines and other signaling molecules that are required in much smaller amounts (Giddings et al., 2000). Several full size immunoglobulines, secretory antibodies and further antibody derivatives have been expressed successfully in plants, including scFvs, diabodies, and antibody-fusion proteins (Ma et al., 2003 and references therein; Lienard et al., 2007). In the past 15 years, plant-made vaccines have also gained a lot of attention, and a long list of antigens that includes viral (Mason et al., 1996; Meyers et al., 2008; Santi et al., 2008), bacterial (Brennan et al., 1999; Walmsley et al., 2003; Frutos et al., 2008), enteric (Mason et al., 1998; Tacket, 2005) and nonenteric pathogen antigens (Mason et al., 1992; Lou et al., 2007) as well as autoimmune antigens (Fitchen et al., 1995; Avesani et al., 2003; Wang et al., 2008b) have been expressed in different plant and expression systems.

I.1.2 Edible vaccines

Problems with current vaccines include the need for multiple doses and boosters, the dependence on a functional cold chain and the potential infection hazards associated with unsafe injections. These problems are recognized by international agencies as a generic global barrier preventing the efficient delivery of all vaccines to those in developing countries with poor infrastructures (Tregoning et al., 2005). In response to these problems there has been increased interest in vaccination regimes that can be delivered without needles and have reduced dependence on the cold chain. One possible solution is to develop practical mucosal vaccines. Of particular relevance in the developing world is the development of vaccines expressed in plants.

Plant systems offer the oral delivery option of pharmaceuticals aimed at mucosal immunization or tolerance, overcoming the cost and inconvenience of injection of vaccines (Yusibov et al., 2002). In fact, plants are ideal not only as bioreactors but also as delivery systems for pharmaceuticals, given that the rigid cell walls protect the recombinant protein from the acidic environment in the stomach (Kong et al., 2001) and enable intact antigen to reach the gut-associated lymphoid tissue (GALT) (Rigano et al., 2003). Because protein purification costs can outweigh the economic advantage of any production system, the additional advantage of using transgenic plants for oral tolerance is that they allow to avoid extensive purification. Therefore, PMPs could undoubtedly assist vaccine programs in developing countries by simplifying immunization regimens and tremendously reducing the costs of vaccine production, purification, storage and administration (Nochi et al., 2007). In the beginning, consumption of antigen-bearing fruit and vegetables was proposed for this purpose. Considerations and hesitation about the regulatory requirements such as consistency between lots and uniformity of dosage have resulted in a refinement of the concept of “edible vaccines”. In fact, edible vaccines, as regulated products, would require controlled delivery of standardized doses, so some level of processing of the edible plant material would be required. This will not include complex purification, but is more likely to involve simple and inexpensive food processing techniques that are readily available, such as freeze drying, and batch processing (Ma et al., 2005). Therefore, if some regulatory issues like homogeneous vaccine dose per gram fresh weight can be solved satisfactorily, plant-derived vaccines will hold many promises for safe and cost-effective mass immunization of mankind much more than any other production system (Boehm, 2007).

Antigens already expressed as components of experimental plant-based vaccines include the B subunit of *E. coli* heat-labile enterotoxin (LTB) (Kim et al., 2007), Norwalk virus-like particles (Tacket et al., 2000) and hepatitis B surface antigen (Kong et al., 2001).

I.1.3 Plant expression strategies

I.1.3.1 Stable nuclear transformation

The most common approach to produce heterologous proteins in plants, that is applicable to a wide range of species, is to use agrobacteria or biolistics to generate stably transformed plants (Davey et al., 1989; Gelvin, 2003). *Agrobacterium*-mediated plant transformation at the moment is one of the most applicable and widespread methods of foreign genetic material transfer into plant cells. Extensive studies in the past years resulted in establishment of highly-effective recombinant *Agrobacterium* strains, vectors and protocols and considerably extended the range of hosts (Gelvin, 2003). By this method, recombinant gene sequences are integrated in the host plant's nuclear genome, and this approach can be routinely applied, even to complex multisubunit proteins, such as secretory antibodies (Ma et al., 1995).

Microparticle bombardment technologies were developed to circumvent the problems of incompatibility between tissues of many plant species, mainly monocotyledons, and the *Agrobacterium* vector (Smith et al., 2001). Conversely to agrotransformation, integration of exogenous DNA into the plant's genetic material following particle bombardment results in the majority of the cases in complex multicopy integrations and broken transgene integration (Christou, 1997; Finer et al., 1999; Smith et al., 2001). As there is evidence for correlation between increasing transgene copy number and transgene silencing (Taylor and Fauquet, 2002), enhanced *Agrobacterium* transformation systems are being developed for the major cereal crops, such as rice (Hiei and Komari, 2008; Sripriya et al., 2008), maize (Vega et al., 2008), wheat (Risacher et al., 2009; Wu et al., 2009), barley (Bartlett et al., 2008; Harwood et al., 2009), sorghum (Howe et al., 2006; Gurel et al., 2009) and oat (Gasparis et al., 2008), to overcome the drawbacks associated with biolistics transformation.

Transgenic plants require a rather long time for the generation and characterization of production lines and the generation of a sufficient amount of seed material. However, once this bottleneck is overcome, an almost unlimited and sustainable production capacity can be

reached using the established agricultural infrastructure in open-field or in greenhouses (Boehm, 2007). Stable integration of the transgene into the plant nuclear genome results in foreign protein levels usually not higher than 1 % of total soluble protein (TSP), although sometimes it reaches higher means if special strategies boosting gene expression and/or product accumulation have been applied. The major disadvantage of stable nuclear transformation is that the expression level of each gene is variable and difficult to control, because the integrated nuclear transgenes are highly sensitive to the surrounding chromatin environment, and there are also some regulatory concerns over the containment of nuclear transformed plants of which changes are inherited to new generations (Streatfield, 2006).

I.1.3.2 Transient expression

Transient gene expression systems in plants have several advantages over the generation of stably transformed transgenic plants. Transient expression is rapid and results on protein expression can be obtained within days (Kapila et al., 1997). This makes transient expression also suitable for verifying that the gene product is functional before moving on to the time-consuming generation of stable transgenic plants. A number of DNA transfer techniques, such as electroporation or particle bombardment, have been used for transient assays in plant tissue (To et al., 1996; Seki et al., 1999), but the two major transient expression systems to deliver a gene to a plant cell are either infiltration of intact tissue with recombinant agrobacteria (agroinfiltration), or infection with modified viral vectors.

Agroinfiltration uses recombinant *Agrobacterium tumefaciens* infiltrated into plant tissue. The transferred T-DNA does not integrate into the host chromosome but is present in the nucleus, where it is transcribed, and this leads to transient expression of the gene of interest which does not suffer from position effects (Kapila et al., 1997). Multiple genes, present in different populations of agrobacteria, can also be simultaneously expressed (Vaquero et al., 1999). It is a fast and flexible system, but it lacks the increases in production volume that can be achieved easily with stable transgenic plants (Sheludko, 2008).

Production of pharmaceuticals using plant viral vectors is also a very promising strategy (Pogue et al., 2002; Yusibov et al., 2006). To date, the most efficient means of achieving high level transient expression of foreign proteins in plants has involved the use of vectors based on RNA plant viruses (Giritch et al., 2006; Lindbo, 2007). Plant viruses are not infectious in humans or animals and can accumulate large quantities of heterologous

proteins in the plants. Two major strategies are ‘full virus’, which allows expression of large fusion proteins in the viral capsid, and a developing approach of ‘deconstructed virus’, which relies on *Agrobacterium* as a vector to deliver DNA of one or more viral RNA replicons to plant cells (Marillonnet et al., 2004; Gleba et al., 2007). Recently, a virus-based system that does not rely on viral replication has also been described (Sainsbury and Lomonossoff, 2008), that overcomes some of the major limitation of virus-mediated transgene expression, such as the issue of biocontainment and the restrictions on the size of the insert that can be accommodated without affecting replication.

I.1.3.3 Plastid transformation

A fast developing and promising technology in the PMF scenario is the synthesis of biopharmaceuticals and vaccines in plastids (Daniell, 2006). Owing to the polyploidy of the plastid genetic system with thousands of genome copies per cell, extraordinarily high levels of foreign protein accumulation can be achieved in chloroplasts (McBride et al., 1995; De Cosa et al., 2001), making transgenic plastids ideal expression factories for high-yield protein production (Bock, 2001). Besides the potential for high-level production of foreign proteins, other attractions of the technology include its effectiveness as a high-precision genetic engineering technique – owing to transgene integration exclusively via homologous recombination – , the absence from plastids of epigenetic effects and gene silencing mechanisms, and the increase in transgene containment provided by the maternal mode of chloroplast inheritance in most crop plants, which largely excludes chloroplasts from pollen transmission (Bock, 2007; Ruf et al., 2007). The major restrictions of using chloroplast transformation for production of recombinant proteins is the limited number of hosts in which the technique is routine, nowadays mostly tobacco and more recently tomato (Ruf et al., 2001; Zhou et al., 2008), carrot (Kumar et al., 2004) and lettuce (Lelivelt et al., 2005; Kanamoto et al., 2006), and the lack in the plastids of post-translational modifications such as *N*-glycosylation, that is strictly connected to and required for the stability, structural authenticity and functionality of some pharmaceuticals.

I.1.4 Optimization of recombinant protein expression in plants

The purpose of plant molecular farming is to produce large amounts of an active, safe pharmaceutical protein at an affordable price. Therefore, the development of an optimized

expression system and its scale up to economic levels of production are crucial stages. To achieve high yields, expression construct design must optimize all stages of gene expression, from transcription to protein stability.

For high-level transcription, the two most important elements are the promoter and the polyadenylation site, which are often derived from the 35S transcript of the *Cauliflower mosaic virus* (CaMV) for dicotyledonous plants (Kay et al., 1987) or the maize ubiquitin-1 gene for monocotyledonous plants (Christensen and Quail, 1996). Codon optimization, bringing the transgene codon usage in line with that of the host, might also result in increased accumulation levels of the recombinant protein (Adang et al., 1993). Other factors that influence transgene expression, including the position of transgene integration, the structure of the transgenic locus and the gene-copy number, cannot be controlled precisely through construct design, and several strategies have been adopted in the attempt to minimize variation in transgene expression. For example, surrounding the expression cassette by scaffold attachment regions (Breyne et al., 1992) or using viral genes to suppress gene silencing (Anandalakshmi et al., 1998) can notably increase transgene expression levels and minimize position effects (Butaye et al., 2004).

One of the most important factors governing the yield of recombinant proteins is subcellular targeting, which strongly affects the interlinked processes of folding, assembly and post-translational modification. The intracellular targeting of the recombinant protein is of great influence to protein yield and its biological properties mainly for two reasons. First, the subcellular environment in which the recombinant protein is synthesized is crucial for its correct folding and, usually, the more similar the environment to the native location, the more likely the protein will acquire the correct conformation and be functional. Second, proteolysis of the recombinant protein by host proteases and interferences between the recombinant molecule and the host molecular function may also lead to severe drawbacks and prevent to reach satisfactory accumulation levels (Barbante et al., 2008). At the current state of the art, the targeting of all intracellular compartments is feasible using known signal sequences that can be fused to the target gene. The cellular locations that have been tested and compared for foreign protein production include the cytosol, the endoplasmic reticulum (ER), the apoplast, the vacuole and the chloroplast. In comparative studies performed in tobacco (Fischer et al., 1999; Schillberg et al., 1999; Stoger et al., 2002) or rice (Torres et al., 1999), ER targeting gave rise to the highest yield of biologically active protein, most

likely due to the presence of chaperones, protein-disulfide isomerase, glycosylation enzymes and a reducing environment that favors protein stability in this compartment (Boehm, 2007). However, this is not the rule, as there is a number of proteins with pharmaceutical properties that are not satisfactorily produced in the endomembrane system or require the passage through the whole secretory pathway and the post-translational modifications therein to be functional (Vitale and Pedrazzini, 2005). A promising strategy to further increase protein stability in the unfavorable cytosolic and apoplastic environments, is to anchor the recombinant protein to the cytosolic face of the ER or to the outer side of the plasma membrane, and has already been successfully exploited (Schillberg et al., 2000; Barbante et al., 2008). Employing this strategy, interference of the recombinant protein with the host cell metabolism is avoided, and moreover the recombinant protein is rendered less susceptible to proteolytic degradation, leading to an overall increase in accumulation levels. In general, the lack of predictability of the best compartment for a given recombinant protein, implies a case-by-case experimental evaluation of different targeting strategies.

I.1.5 Tobacco as a model system for PMP

Tobacco is a non-food and non-feed crop that has an established history as a model system for molecular farming and is the most widely used species for the production of recombinant pharmaceutical proteins at the research laboratory level (Cramer et al., 1999; Fischer and Emans, 2000; Sorrentino et al., 2008; Villani et al., 2009). The main advantages of tobacco include the mature technology for gene transfer and expression, the high biomass yield (more than 100,000 kg per hectare for close-cropped tobacco), the potential for rapid scale-up owing to prolific seed production, and the availability of existing large-scale infrastructures for processing (Ma et al., 2003). Both nuclear and chloroplast genomes of tobacco have been transformed with relative ease. Although many tobacco cultivars produce high levels of toxic alkaloids, there are low-alkaloid varieties that can be used for the production of pharmaceutical proteins (Fischer and Emans, 2000).

Recombinant proteins can also be produced in plant cell cultures (Hellwig et al., 2004), and tobacco suspension cells are easily generated by the continuous agitation of friable callus tissue, which results in a homogeneous suspension of single cells and small clumps. This

approach is particularly advantageous when defined and sterile production conditions are required together with straightforward purification protocols (Ma et al., 2003).

I.2 Type-1 diabetes mellitus

Type-1 diabetes mellitus (T1DM) – also called insulin-dependent diabetes mellitus (IDDM) or juvenile diabetes – is one of the most common chronic diseases of childhood. It is an autoimmune disorder associated, in genetically susceptible individuals, with the generation and activation of autoreactive T cells recognizing pancreatic β cell autoantigens. Self-reactive CD4+ and CD8+ lymphocytes infiltrate the pancreas (insulitis) and selectively destroy the insulin producing β cells in the islets. This destruction occurs silently and progressively and may stay undetected for many years. By the time the first clinical symptoms become apparent, nearly 80 % of the patients' β cells have been destroyed and there is little hope of curing the disease. It is diagnosed in nearly 0.3% of all children, but clinical signs can appear at any age (Kidambi and Patel, 2008). T1DM incidence is growing by 3% per year in children and adolescents, and at an alarming 5% per year among pre-school children (International Diabetes Federation 2007).

It is the cause of severe and debilitating disability in many individuals worldwide. The chronic hyperglycemia of diabetes mellitus is associated with long-term damage, dysfunction, and failure of various organs, especially the eyes, kidneys, nerves, heart, and blood vessels (Schuster and Duvuuri, 2002). At present, there is no clinically useful preventive measure against developing type 1 diabetes, nor does exist a cure, and people that suffer from it must take insulin by injection or insulin pump throughout their life to survive, generating also a great deal of health care cost, which is bound to increase with time and inflation. Unfortunately, in many parts of the world, insulin is not even available because of cost or economic geography (International Diabetes Federation, 2007).

The principal T1DM-associated autoantigens known to date are insulin itself, the 65 kDa isoform of glutamic acid decarboxylase (GAD65) and tyrosine phosphatase-like IA-2. Susceptibility to T1DM is genetically determined, as certain alleles of major histocompatibility complex (MHC)-loci, are associated with either a high or a low risk to develop type-1 diabetes. Although the development of the disease is greatly influenced by

environmental factors, the events that lead to the breakdown of self-tolerance to pancreatic β cells are still poorly understood (Hanninen, 2000).

Ideally, autoimmune disease therapies would uniquely target the specific autoreactive lymphocyte populations while leaving the rest of the immune system unaltered. Traditionally, tolerance has been achieved through the use of anti-inflammatory and immunosuppressive drugs, most notably corticosteroids, which must be taken indefinitely. Unfortunately, such immunosuppressive regimens non-specifically suppress the entire immune system, thus exposing patients to increased risk of infections and cancer. Recent efforts aimed at achieving tolerance through elimination of only the pathogenic immune response, leaving the other functions of the immune system unperturbed, investigated newer and more tailored tolerance therapies, such as the induction of oral tolerance (Wolfraim, 2006).

I.3 Oral tolerance and the role of T regulatory cells

Antigens elicit qualitatively distinct immune responses based on their portal of entry, and antigens introduced at mucosal surfaces, such as the gastrointestinal tract, often elicit active and systemic inhibition of the immune response to those antigens (Mayer and Shao, 2004). The gut-associated lymphoid tissue (GALT) is one of the largest and most complex parts of the immune system. Not only does it encounter a larger variety of antigens than any other part of the organism, it must also discriminate between pathogenic organisms and harmless antigens, such as food proteins and commensal bacteria. Most human pathogens enter the body through the intestine, and strong immune responses are required to protect this essential organ. By contrast, active immunity against nonpathogenic antigens would be wasteful, and hypersensitivity responses against dietary antigens or commensal bacteria can lead to inflammatory disorders, such as celiac disease and Crohn's disease, respectively (Garside et al., 1999).

Under normal conditions, immune responses to harmless gut antigens lead to the induction of local and systemic immunological tolerance, known as oral tolerance. Oral tolerance can also be exploited for therapeutic use, as the induction of antigen-specific systemic immunological unresponsiveness by feeding protein antigens represents a simple and practical mean to prevent or treat autoimmune diseases and chronic inflammatory

conditions, and an attractive alternative to immunosuppressive medical interventions that have undesirable side-effects (Wolfraim, 2006). Oral administration of antigens is thought to lead to immune tolerance through one of two distinct mechanisms, depending upon dose. High doses of orally fed antigen lead to deletion or anergy of Th cells, which may occur when the T cell receptor (TCR) engages the major histocompatibility comples (MHC)-antigen complex in the absence of proper costimulation, whereas repeated low doses lead to the more long lasting induction of T-regulatory (Treg) cells (Wolfraim, 2006).

One of the several mechanisms developed by the immune system to maintain peripheral tolerance is indeed the active suppression of undesired immune responses mediated by Treg cells (Battaglia and Roncarolo, 2004). Many different Treg cell subsets have been shown to play a central role in intestinal immunity. In particular, the Treg cell subset that plays a role in oral tolerance is represented by the T-regulatory type-1 cells (Treg1). Treg1 cells have been described both for murine and human animal models (Larche and Wraith, 2005). They display a unique profile of cytokine production that is distinct from that of other T cells. The main cytokines produced by Treg1 cells are IL-10 and TGF-β, which downregulate immune responses mediated by naive and memory T cells.

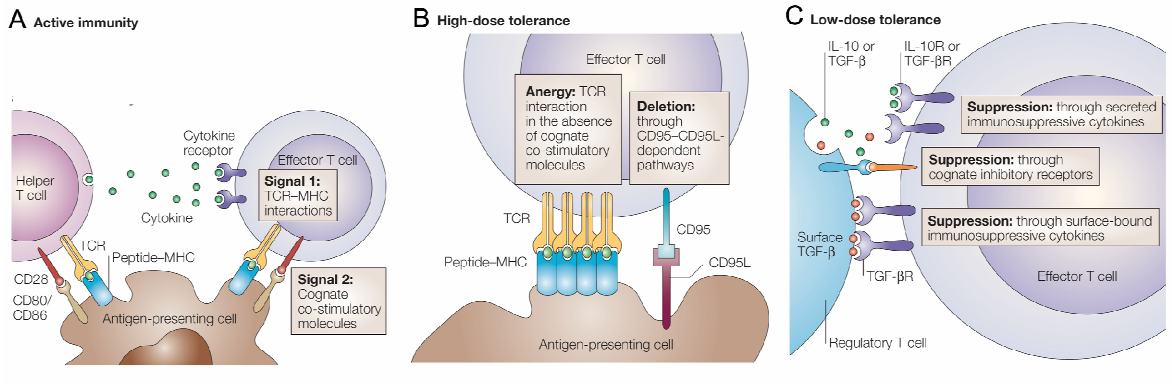

Figure 1: Potential mechanisms of oral tolerance.

(**A**) The generation of an immune response requires ligation of the T-cell receptor (TCR) with peptide-MHC complexes. In the context of appropriate co-stimulatory molecules (CD80 and CD86) and cytokines, an active immune response is generated. (**B**) However, with high doses of oral antigen, TCR crosslinking can occur in the absence of co-stimulation, or concurrently in the presence of inhibitory ligands (CD95 and CD95 ligand, CD95L), leading to immunosuppressive responses such as anergy and deletion. (**C**) Low doses of oral antigen lead to the activation of regulatory T cells, which suppress immune responses by cognate interactions, and soluble (interleukin-10, IL-10, and transforming growth factor-β, TGF-β) or cell-surface-associated suppressive cytokines. R, receptor. (From Mayer and Shao, 2004)

Treg1 cells have been extensively characterized and today are considered to be a specialized subset of Treg cells able to prevent immune-mediated diseases and to maintain immunological tolerance. For example, high doses of IL-10 and repeated TCR stimulation are sufficient to induce a population of murine CD4+ cells containing a high number of Treg1 cells with the ability to suppress immune responses both *in vitro* and *in vivo* in a model of inflammatory bowel disease (IBD) (Groux et al., 1996). Moreover, it has been shown that oral administration of antigens in combination with IL-10 is one mechanism, among many, for the *in vivo* differentiation of Treg1 cells, and this can be envisaged as a novel strategy for oral tolerance induction (Battaglia and Roncarolo, 2004).

An intriguing feature of Treg1 cells is that, although they can be activated in an antigen-specific manner, they can suppress immune responses in the immediate surrounding area in an antigen non-specific manner, a phenomenon known as bystander suppression (Mayer and Shao, 2004). The ability to control this phenomenon is a potentially powerful therapeutic tool for controlling autoimmune/inflammatory conditions.

Several successful therapeutic trials of oral tolerance induction in animal models have supported a limited number of human clinical trials, and, in general, oral tolerance was more effective as a prophylactic measure than it was in reversing ongoing diseases. Unfortunately, in humans, heterogeneity in the design and results of these trials have made efficacy still difficult to discern (reviewed in Mayer and Shao, 2004).

I.3.1 Use of immunoregulatory molecules in oral tolerance induction

The potential benefits of mucosal autoantigen administration in the treatment or prevention of autoimmune diseases are indisputable. In spite of this, the simultaneous induction of possibly detrimental immune responses cannot be overlooked, and mucosal tolerance at the present may still be a ‘two-edged sword’ with potential hazards that we are not yet able to completely control. How can we then be convinced that we are inducing tolerance and *only* tolerance if we give autoantigens via mucosal routes? Ways should be found to efficiently control the induction of detrimental immune responses while not blocking the induction of tolerance (Hanninen, 2000).

Several ways of manipulating oral tolerance exist, some of them enhancing and others preventing tolerance. A strategy to improve the effect of orally administered antigens is the

use of mucosal immunomodulators/adjuvants, that can enhance the oral tolerance of co-administered antigens by targeting small amounts of protein antigens to specialized antigen-presenting cells of the GALT (Sun et al., 1996). Thus, reduced quantities of the co-administered autoantigen would be sufficient to induce oral tolerance. This would represent a great advantage, because a major problem recognized with the oral tolerance strategy is that it requires feeding large if not massive doses of autoantigens. In particular, a combination therapy of an autoantigen along with one or more regulatory anti-inflammatory cytokines given orally to enhance protection may represent an important new strategy in the prevention of autoimmune diseases for several reasons. First of all, it should establish a form of forced manipulation of antigen-specific Th1:Th2 T cell populations, and possibly also induce regulatory immunity (Ma et al., 2004). Additionally, being endogenous molecules (unlike other mucosal adjuvants like the cholera toxin B subunit (CTB) that is of bacterial origin), cytokines should not induce neutralizing antibody responses which could limit their usefulness in oral tolerance, particularly if prolonged or repeated administration is required to initiate or maintain tolerance (Ma et al., 2004). Moreover, as already mentioned, because adjuvants facilitate tolerance induction, their use would lower the required quantities of co-administered autoantigens and therefore notably reduce the costs of this therapeutic or prophylactic approach.

I.4 Interleukin-10

The anti-inflammatory cytokine interleukin-10 (IL-10), is a multifunctional Th2-type cytokine with diverse effects on most hemopoietic cell types (Sprang and Bazan, 1993). The open reading frames (ORF) of the IL-10 cDNAs encode secreted proteins of ~178 amino acids, including hydrophobic leader sequences (Moore et al., 1990; Vieira et al., 1991), with rather well conserved sequences – murine IL-10 (mIL-10) and human IL-10 (hIL-10) are ~73% identical – consistent with an α-helical bundle structure (Sprang and Bazan, 1993). Human IL-10 is an 18 kDa polypeptide, which is not glycosylated. In contrast, both recombinant and T cell-derived murine IL-10 are heterogeneously *N*-glycosylated at a site near the *N*-terminus (Moore et al., 1990; Mosmann et al., 1990). IL-10 is biologically active as an homodimer and the crystal structure of hIL-10 (Figure 2) demonstrates α-helices within each subunit of a homodimer (Walter and Nagabhushan, 1995; Zdanov et al., 1995).

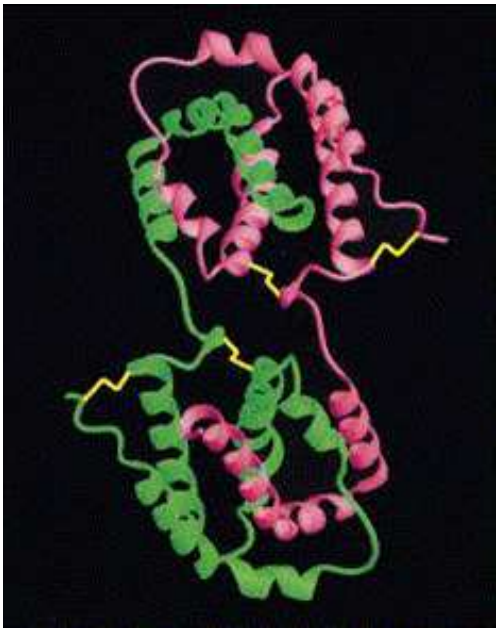

Figure 2: Ribbon diagram of the intertwined human IL-10 homodimer.

The two IL-10 monomers are represented in green and pink, respectively. Intermolecular disulfide bonds are shown in yellow (http://www.pdb.org).

While it plays a complex role in the immune system, the major activities of IL-10 are to inhibit cytokine production by macrophages and to suppress their accessory functions during T-cell activation (de Waal Malefyt et al., 1991; Fiorentino et al., 1991). Since this causes the termination of inflammatory responses, IL-10 is widely considered as an immunosuppressive and anti-inflammatory cytokine, and many investigations of IL-10 expression *in vitro*, in animal models and in human patients have indicated a significant role in inflammatory, malignant and autoimmune diseases, highlighting the potential clinical value of this cytokine (Asadullah et al., 2003). However, mammalian IL-10, including the human one, also presents several immunostimulatory properties (e.g., activation of dendritic cells, NK cells, and some T cells) which appear not to be negligible when IL-10 is used *in vivo* to induce tolerance (Wakkach et al., 2000).

I.4.1 Viral IL-10

Interestingly, IL-10 has orthologs in several virus genomes, and the IL-10 variant produced by Epstein-Barr virus (vIL-10) is particularly closely related to its human counterpart (71% and 84% identity at the nucleotide and amino acid sequence levels, respectively) and binds to both human and murine receptors (Moore et al., 2001). Despite the sequence similarity,

vIL-10 exhibits primarily the immune-inhibitory properties associated with the cellular cytokine (e.g., suppression of Th1-polarized responses and monocyte inhibition) but lacks many of the immunostimulatory properties associated with the human IL-10 and murine IL-10, such as costimulation of thymocyte or mast cell proliferation, and enhancement of class II MHC expression on B cells (Lucas and McFadden, 2004). This exacerbated inhibitory effect of vIL-10 makes it an even more attractive therapeutic candidate for tolerance induction, as the viral cytokine could have a profoundly different effect on the outcome of an *in viv*o immune response compared to hIL-10/mIL-10 (Moore et al., 2001).

I.4.2 IL-10 as an adjuvant for oral tolerance induction

IL-10 has been extensively investigated as an immudomodulatory agent for the prevention or cure for T1DM. Depending on the time and site of administration, IL-10 alone can exert distinct effects on diabetes development in mice. Early systemic treatment with exogenous murine IL-10 inhibits T1DM in NOD mice, whereas exposure of NOD mice to IL-10 during the effector phase of the disease did not inhibit the diabetogenic potential of the T-cells (Balasa et al., 2000), and local expression of IL-10 (intraislets) even accelerated the onset of the disease in the same animal model (Wogensen et al., 1994).

One promising immunomodulatory application of IL-10 is to enhance the induction of oral tolerance to co-administered auto-antigens, leading to the prevention or treatment of autoimmune diseases with lower doses of tolerizing protein. For instance, induction of oral tolerance for the prevention of type-1 diabetes mellitus (T1DM) could be achieved by repeated oral administration of small doses of one of the major auto-antigens associated with the disease, the 65 kDa isoform of the enzyme glutamic acid decarboxylase (GAD65). The characterization of transgenic tobacco plants producing immunoreactive GAD65 has already been reported (Avesani et al., 2003), although feeding studies in a mouse model have not yet been possible due to the low protein expression levels, requiring the consumption of unrealistically large amounts of plant material in order to achieve an oral tolerizing effect. However, simultaneous feeding with plant material containing IL-10 may reduce the amount of GAD65 necessary to induce oral tolerance. In fact, as Th1 cells are clearly implicated in the T1DM pathology, an immunoregulatory cytokine strongly promoting Th2 immune responses like IL-10, could augment tolerance to co-administered autoantigens such as GAD65. Additionally, IL-10 inducing the formation of Treg1 cells (Wakkach et al., 2000), should also drive the immune response towards active rather than a

passive tolerance, which should in turn provide a more robust and long-lasting protection from the onset of the autoimmune disease.

I.4.3 Production of IL-10 in plants

Currently, recombinant murine IL-10 (BD Pharmingen) is produced in insect cells, while the human (Schering-Plough) and viral IL-10 (R&D Systems) are produced in *E. coli* and refolded *in vitro* to reconstitute the dimers.

These expression systems suffer from several limitations, mainly related to the necessity of refolding the protein after purification and to deliver an endotoxin-free product, which result in an extremely high price of IL-10 on the market and render the costs of research or treatment unsustainable in some cases. For example, it has been reported that early studies on the treatment of psoriasis with IL-10 suggested good efficacy (Asadullah et al., 2001; Kimball et al., 2002), but the outcome was not considered sufficiently cost-effective to justify further development of the cytokine for treatment of people with this disease (Walsh and Shear, 2004).

As the interest in the use of IL-10 as a potential therapeutic agent continues to increase, a more efficient production system providing sufficient amounts of biologically active IL-10 at low cost is becoming highly desirable (Wang et al., 2008a). In particular, the use of this cytokine either orally or topically for the cure of inflammatory diseases would require large amounts of recombinant protein for each treatment. This need led to the interest in transgenic plants as a source of low cost recombinant IL-10.

Human IL-10 has been produced in stably transformed tobacco plants, and the ability of plant-produced human IL-10 to induce anti-inflammatory responses has also been demonstrated (Menassa et al., 2007). In two different works, Menassa and colleagues investigated several subcellular localizations of the recombinant protein, and among the compartments where human IL-10 was targeted to (apoplast, ER, chloroplast, mitochondrion), the ER turned out to be the most favorable one, where the protein accumulated to the highest levels (up to 0.0055 % TSP) (Menassa et al., 2001; Menassa et al., 2004). However, these yields were not satisfactory, and far below the 1 % threshold that has been proposed for plant-made pharmaceuticals to be economically competitive with current recombinant production systems (Twyman et al., 2005). In an attempt to increase the

stability and thus the yield of the cytokine, they subsequently generated a fusion protein of hIL-10 with a 27mer ELP-tag, and reached accumulation levels of 0.27 % TSP (Patel et al., 2007).

I.5 Objective and strategy of the study

I.5.1 Objective of the study

Transgenic plants are attractive systems for production of therapeutic proteins because of the ability to produce the target protein at large scale and at low cost, and the low maintenance requirements. They are highly amenable to oral administration and could become effective delivery systems without extensive protein purification.

We are interested in the induction of oral tolerance for the prevention of type-1 diabetes mellitus (T1DM) which could be achieved by repeated oral administration of small doses of plant material expressing one of the major auto-antigens associated with the disease, GAD65.

The production and characterization of transgenic tobacco plants producing immunoreactive GAD65 has already been reported (Porceddu *et al.*, 1999; Avesani *et al.*, 2003). However, accumulation levels of the recombinant protein were too low for an oral tolerizing effect using plant tissue directly.

A strategy to improve the effect of orally administered antigens is the combined use of immunomodulators, such as IL-10, which should enhance the induction of oral tolerance to co-administered auto-antigens, leading to the prevention or treatment of autoimmune diseases with lower doses of tolerizing protein.

We therefore set out to investigate the ability of tobacco plants to produce high levels of biologically active viral and murine IL-10. We focused on the expression of the viral IL-10 from Epstein Barr virus because, lacking some of the immunostimulatory properties of the mammalian counterparts, it is an even better candidate for the induction of oral tolerance to co-fed autoantigens, and the murine IL-10 was also investigated as a reference, because the final aim is to test the recombinant cytokine in a mouse model of T1DM. In fact, a comparative study, feeding either recombinant vIL-10 or the recombinant endogenous mIL-10 together with the GAD65 auto-antigen to NOD mice, would allow to evaluate and

assess the outcome of the different immunomodulatory properties of the viral cytokine in inducing oral tolerance in the animal model, and to evaluate the possibility of exploiting vIL-10 for the prevention of T1DM.

I.5.2 Experimental design

The task of this thesis was to determine whether biologically active viral and murine IL-10 could be produced in tobacco by (i) identifying the best expression strategy, (ii) performing a biochemical characterization of the plant-derived recombinant proteins, and (iii) confirming their biological activity and functionality.

To reach high accumulation levels of the recombinant proteins, different targeting strategies of the nuclear encoded recombinant protein were investigated as well as plastid transformation with the IL-10 genes.

The aim of the study was achieved by the following approaches:

- Identification of the best strategy for the production of IL-10 in tobacco

  - Targeting strategies: Different constructs for targeting IL-10 to specific plant sub-cellular compartments (ER retained, membrane-anchored facing the apoplast and membrane-anchored facing the cytosol) with a C-terminal His6-tag were generated. The best targeting strategy was evaluated through transient expression, and nuclear stable transformation of tobacco plants with the most promising construct was performed.
  - Chloroplast (plastid) transformation: Chloroplast transformation was carried out by biolistic particle bombardment of *N. tabacum* leaves using gold particles coated with plasmid DNA coding for a His6-tagged version of either murine or viral IL-10. Primary spectinomycin-resistant transformants were passed through several additional rounds of selection and regeneration to obtain homoplasmic transplastomic tissue from which shoots were regenerated.
  - BY2 transformation and inducible transgene expression: Although it was not planned in the beginning of the study, stable transformation of tobacco suspension cell cultures was also investigated as an alternative approach to identify the most

suitable production platform, given the difficulties encountered during the experimental work in obtaining high accumulation levels of the viral IL-10. In this expression system, viral IL-10 expression under the control of a constitutive as well as an inducible promoter was performed and evaluated.

- Characterization of transgenic plants and plant-produced IL-10: Determination of recombinant IL-10 accumulation levels was done by ELISA and/or immunoblot analyses. Validation of the selected targeting strategy was carried out by immunogold labeling and electron microscopy on the highest IL-10 producing plants. Purification of His6-tagged IL-10 was performed for subsequent N-terminal sequence determination, *N*-glycosylation analysis, assessment of plant-produced IL-10's biological activity by *in vitro* assays using a murine macrophage cell line, and stability studies.

A schematic representation of the experimental design is presented in Figure 3.

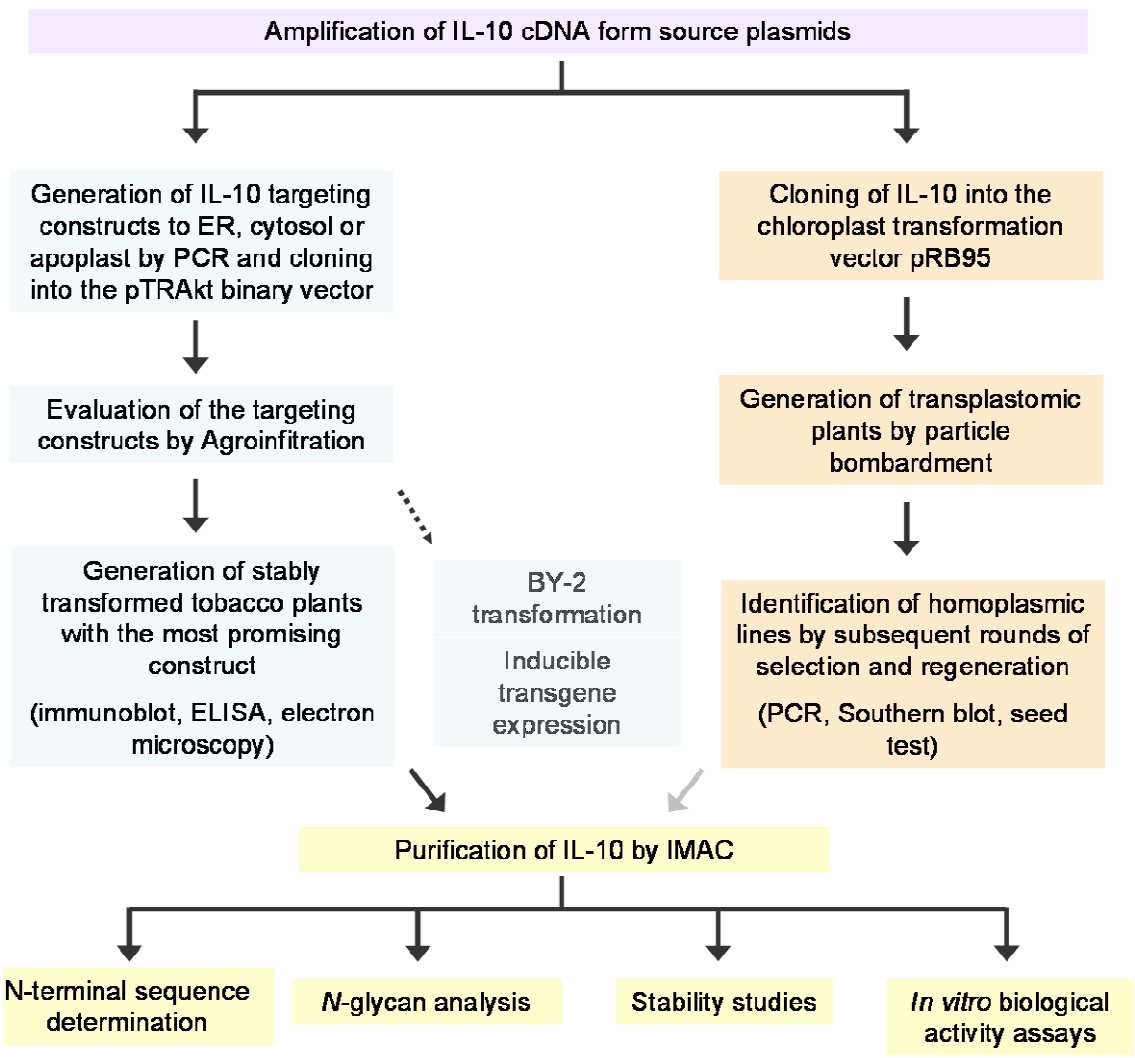

Figure 3: Schematic representation of the experimental design.

II MATERIALS AND METHODS

II.1 Materials

II.1.1 Organisms

II.1.1.1 Plant material

- *Nicotiana tabacum* L. cv. Petit Havana, used for chloroplast transformation
- *Nicotiana tabacum* L. cv. Petit Havana SR1, used for agro-mediated transient expression and stable nuclear transformation
- *Nicotiana tabacum* L. cv. Bright Yellow 2 (BY-2) cell suspension culture

II.1.1.2 Bacterial strains

Table 1: Bacterial strains

Strain		Reference
Escherichia coli DH5α	*rec*A1, *end*A1, *hsdR*17 (r_k^- m_k^+), Δ(*Lac*ZYA-*arg*F) *U*169, *supE*44, Φ*80d* LacZΔM15, *thi*-1, *gyr*A96, *relA1* λ, *deoR*; cloning	(Ausubel *et al.*, 1994)
Agrobacterium tumefaciens GV3101 pMP90RK	RK Gm^R, Km^R, Rif^R; gene transfer in *N. tabacum* SR1 and BY-2 cells with the pTRA vectors	(Koncz and Schell, 1986)
Agrobacterium tumefaciens GV2260	Rif^R, $Carb^R$; gene transfer in BY-2 cells with the pBinHyg vector	(Deblaere *et al.*, 1985)

II.1.1.3 Animal cell line

- J774 murine macrophage cell line, kindly provided by Dr. V. Kruys, Université Libre de Brussels, Belgium, was used to assess IL-10 biological activity *in vitro*.

II.1.2 Nucleic acids

II.1.2.1 Vectors

- TOPO Cloning TA vector pCR®2.1TOPO® (Invitrogen, Karlsruhe, D): 3931 bp, pUC based cloning vector, *Lac*Zα, T7 promoter, *bla*, *nptII*.
- pTRAkt-gfp (Thomas Rademacher, Institute for Biology VII, RWTH Aachen, Germany): 8352 bp, [Amp^R, $Carb^R$, Kan^R] binary plant expression vector, derivative of the pPAM expression vector (GenBank: AY027531). It contains the 35S promoter with duplicated enhancer region (Kay et al., 1987) and the pA35S terminator from the *Cauliflower mosaic virus* (CaMV); the 5' untranslated region (UTR) from the *Tobacco etch virus* (TEV); two Scaffold Attachment Regions (SAR) from tobacco flanking the expression cassette, for optimized transgene expression *in planta* (Breyne et al., 1992). This vector was used for cloning of the IL-10 cDNA and *A. tumefaciens* mediated transformation of tobacco.
- TRAkc-rTPrfp (Thomas Rademacher): 8406 bp, [Amp^R, $Carb^R$, Kan^R], contains the 5' untranslated region from the chalcone synthetase gene from *Petunia hortense* and the gene encoding the DsRed reporter molecule (Jach *et al.*, 2001). The vector was used as control during agroinfiltration experiments.
- pBinHygTX: 12095 bp (GenBank: Z37515), [Kan^R, Hyg^R] derivative of the binary vector pBIB (Becker, 1990), harbours an expression cassette with the CaMV 35S promoter containing three TET-Repressor binding sites. This vector was as used for cloning of the IL-10 cDNA and Tc-inducible expression of transgenes.
- pTRAhDsRed_eTX-vIL-10 (Thomas Rademacher): 11627 bp, [Amp^R, $Carb^R$, Hyg^R], contains the sequence encoding DsRed under the control of a constitutive CaMV 35S promoter, in tandem with the sequence encoding the His-tagged ER-retained version of vIL-10 under the control of the modified CaMV35S promoter containing three TET-Repressor binding sites and the duplicated enhancer region; the two expression cassettes are flanked and interspaced by SARs. This vector was used for Tc-inducible expression of transgenes with a visible screenable marker for selection of transgenic clones.

- pHK20 (Pal Maliga, Rutgers University, Piscataway, NJ, USA): [Amp^R]; was used as intermediate plasmid in the generation of the chloroplast transformation vector, to clone the IL-10 sequences in the expression cassette consisting of the ribosomal RNA operon promoter fused to the 5' untranslated region (5'UTR) from gene 10 of phage T7 and the downstream box (DB) from *E. coli* (P*rrn-T7g*10-DB), and the 3'UTR of the plastid *rbcL* gene (T*rbcL*) (Kuroda and Maliga, 2001).
- pRB95: 6810 bp, [Amp^R, Kan^R, Spec^R] chloroplast transformation vector (GenBank: AJ312393) harbouring the *aadA* gene for Spec/Strep resistance in *E. coli* and in plant chloroplasts (Ruf et al., 2001).

II.1.2.2 Oligonucleotides

All oligonucleotides used in this study were synthesized and HPLC purified by Invitrogen or MWG Biotech (Ebersberg, D). Stock solutions of 200 pmol in autoclaved ddH_2O were prepared and stored at -20 °C.

Name	Sequence (5'→3') [1]	Orientation
mIL-10 cloning		
m-SP_f	CAT GCC ATG GCA CCT GGC TCA GCA CTG CTA TGC GCT CTA GAC GGT TTA GAG CTC ATC TTT CTC AGA	(+)
m-HisKDEL_r	GTG ATG GTG ATG GTG ATG GCT TTT CAT TTT GAT CAT CAT GTA TGC GAT GGT GGC AGA CAG GAC CCC TTG CTG GTA GGA	(-)
m-TcR_r1	CAC CGA GGT AAA GCC ACA GTC TGC TCT ACC GCT TTT CAT TTT GAT CAT CAT GTA TGC AAC ACA AGG GCG CTG ACC AGC ACA GCA TAC AGG	(-)
m-TcR_r2	GTG GCC TTC CCT AGC AGG ATC TCA TAG AGG ATG GTG GCA GAC AGG ACC CC GCT CTA GAC GGT TTA GTG ATG GTG ATG GTG ATG	(-)
m-TcRHis_r3	GAA ATC CTT TCT CTT GAC CAT TGC CAT CAA CAC AAG GGC GCT GAC CAG C	(-)
m-cytb5_f	TTG TCA TGA GCA GGG GCC AGT ACA GCC G	(+)
m-Hiscytb5_r1	ATG GCT GGG ATC ACC CAG TTG GTC CAC CAA CTG GAA TTA GAC TCG ACG TGA TGG TGA TGG TGA TGG CTT TTC ATT TTG ATC ATC ATG TAT GC	(-)
m-cytb5_r2	GCT CTA GAC GGT TTA ATC TTC TGC CAT GTA GAG GCG ATA CAT CAG AGC TAC CAC CAG GGC TGA GAT GGC TGG GAT CAC CCA GTT GG	(-)
Ch_m_f	GGA ATT CCA TAT GAG CAG GGG CCA GTA CAG C	(+)
Ch_m_His_r	GCT CTA GAT TTA GTG ATG GTG ATG GTG ATG GCT TTT CAT TTT GAT CAT CAT GTA TG	(-)
vIL-10 cloning		
v-SP_f	CAT GCC ATG GAG CGA AGG TTA GTG GTC ACT CTG CAG TGC	(+)
v-HisKDEL_r	GCT CTA GAC GGT TTA GAG CTC ATC TTT CTC AGA GTG ATG GTG ATG GTG ATG CCT GGC TTT AAT TGT CAT GTA TGC	(-)

v-TcR_r1	ATG GTG GCA GAC AGG ACC CCT TGC TGG TAG GACA CCG AGG TAA AGC CAC AGT CTG CTC TAC CCC TGG CTT TAA TTG TCA TGT ATG CTT CTA TGT AGT T	(-)
v-TcR_r2	ACA CAA GGG CGC TGA CCA GCA CAG CAT ACA GGG TGG CCT TCC CTA GCA GGA TCT CAT AGA GGA TGG TGG CAG ACA GGA CCC C	(-)
v-TcRHis_r3	GCT CTA GAC GGT TTA GTG ATG GTG ATG GTG ATG GAA ATC CTT TCT CTT GAC CAT TGC CAT CAA CAC AAG GGC GCT GAC CAG C	(-)
v-cytb5_f1	TAC TTC TAT TGC AGC AAT TTA AAT CAT TTC TTT TAA AGC AAA AGC AAT TTT CAC CAT GCA ATG TGA CAA TTT TCC CCA AAT G	(+)
v-cytb5_f2	GGA ATT CCT CAA CAC AAC ATA TAC AAA ACA AAC GAA TCT CAA GCA ATC AAG CAT TCT ACT TCT ATT GCA GCA ATT TAA ATC ATT TC	(+)
v-Hiscytb5_r1	TGG CTG GGA TCA CCC AGT TGG TCC ACC AAC TGG AAT TAG ACT CGA CGT GAT GGT GAT GGT GAT GCC TGG CTT TAA TTG TCA TGT ATG CTT C	(-)
v-cytb5_r2	GCT CTA GAC GGT TTA ATC TTC TGC CAT GTA GAG GCG ATA CAT CAG AGC TAC CAC CAG GGC TGA GAT GGC TGG GAT CAC CCA GTT GG	(-)
Ch_v_f	GGA ATC CAT ATG CAA TGT GAC AAT TTT CCC CAA ATG	(+)
Ch_v_His_r	GCT CTA GAT TTA GTG ATG GTG ATG GTG ATG CCT GGC TTT AAT TGT CAT GTA TGC	(-)
Analysis of transplastomics		
P5'RB70	GGA TTT GGT ATA GTT GGC C	(+)
P3'RB70	CTT GTT TAC CTA TTA GTT TTC AGT	(-)
paadA136	TCG ATG ACG CCA ACT ACC	(+)
Biological activity		
SOCS3_f	CCT TTG TAG ACT TCA CGG CT	(+)
SOCS3_r	TTT GGA GCT GAA GGT CTT GAG	(-)
GAPDH_f	TGG CCT CCA AGG AGT AAG AA	(+)
GAPDH_r	GGT CTG GGA TGG AAA TTG TG	(-)
Sequencing		
m-int_f	GCC AGG TGA AGA CTT TC	(+)
m-int_r	GCC TTG CTC TTA TTT TCA C	(-)
v-int_f	CCT AAG AGA TGC CTT CAG	(+)
v-int_r	CCT GCA GCT TGT TAA AGG	(-)
pSS5'	ATC CTT CGC AAG ACC CTT CCT CT	(+)
pSS3'	AGA GAG AGA TAG ATT TGT AGA GA	(-)
Universe	GTT GTA AAA CGA CGG CCA GT	(+) or (-)
Reverse	ACA CAG GAA ACA GCT ATG AC	(+) or (-)

[1]Underlined sequences represent clamps that do not hybridize to the starting DNA template

II.1.3 Antibodies

Antibody	Epitope	Characteristics	Reference
Primary antibodies			
Rat-anti-mIL-10	Mouse IL-10	Monoclonal	BD Pharmingen (Erembodegem, B)
Rat-anti mIL-10	Mouse IL-10	Monoclonal, biotinylated	BD Pharmingen
Rabbit-anti-mIL-10	Mouse IL-10	Polyclonal	ACRIS (Herford, D)
Rat-anti-h and vIL-10	Human and viral IL-10	Monoclonal	BD Pharmingen
Rat-anti-h and vIL-10	Human and viral IL-10	Monoclonal, biotinylated	BD Pharmingen
Goat-anti-vIL-10	Viral IL-10	Polyclonal	R&D Systems (Wiesbaden, D)
Rabbit-anti-penta His	C-terminal His-tag	Polyclonal	Cell Signaling (Denver, MA, USA)
Mouse-anti-KDEL	C-terminal KDEL tag	Monoclonal	Assay Design (Ann Harbor, MI, USA)
Mouse-anti-STAT3	STAT3	Monoclonal	Cell Signaling
Rabbit-anti-phospho-STAT-3	STAT3 phosphorylated on Tyr705	Polyclonal	Cell Signaling
Rabbit-anti-SOCS3	SOCS3, NH_2 terminus	Polyclonal	IBL (Tokio, J)
Mouse-anti-GAPDH	GAPDH	Monoclonal	IBL
Secondary antibodies			
Rabbit-anti-rat (RAR^{AP})	Rat IgG (H+L)	Polyclonal, conjugated to alkaline phosphatase	SIGMA (Deisenhofen, D)
Rabbit-anti-rat (RAR^{HRP})	Rat IgG (H+L)	Polyclonal, conjugated to horse radish peroxidase	SIGMA
Goat-anti-rabbit (GAR^{AP})	Rabbit IgG (H+L)	Polyclonal, conjugated to alkaline phosphatase	Jackson ImmunoResearch (Suffolk, UK)
Goat-anti mouse (GAM^{AP})	Mouse IgG (H+L)	Polyclonal, conjugated to alkaline phosphatase	Jackson ImmunoResearch
Rabbit-anti-goat (RAG^{10})	Goat IgG (H + L)	Polyclonal, conjugated to 10 nm gold particles	BBInternational (Cardiff, UK)
Goat-anti-rabbit (GAR^{10})	Rabbit IgG (H + L)	Polyclonal, conjugated to 10 nm gold particles	BBInternational
Goat-anti-rabbit (GAR^{680})	Rabbit IgG (H+L)	Polyclonal, conjugated to Alexa Fluor®680	Invitrogen
Goat-anti-mouse (GAM^{800})	Mouse IgG (H+L)	Polyclonal, conjugated to IRDye™800	Rockland (Gilbertsville, PA, USA)

II.1.4 Chemicals and consumables

The chemicals and consumables used throughout the work were purchased from the following companies: Acris, Ambion (Austin, TX, USA), Amicon (Witten, D), Assay Design, BB International, BD Pharmingen, Biochrom Seromed (Berlin, D), Bio-Rad (Munich, D), Bio-Whittaker, (Verviers, B), Cell Signaling, Duchefa (Haarlem, NL), Eppendorf (Hamburg, D), Fluka (Neu-Ulm, D), Fuji Film (Dusseldorf, D), GE Healthcare

(Uppsala, S), Gibco BRL (Eggenstein, D), Greiner Bio-One (Frickenhausen, D), IBL, Invitrogen (Karlsruhe, D), InvivoGen (San Diego, CA, USA), Jackson ImmunoResearch, Kodak (Stuttgart, D), Macherey-Nagel (Düren, D), Merck (Darmstadt, D), Millipore (Eschborn, D), R&D Systems, Roche (Mannheim, D), Rockland (Gilbertsville, PA, USA), Roth (Karlsruhe, D), Schleicher&Schuell (Dassel, D), Schott Glaswerke (Mainz, D), Serva (Heidelberg, D), Sigma, Whatman (Bender & Hobein, Bruchsal, D).

II.1.5 Stock solutions, buffers and additives

Standard media, buffers and stock solutions were prepared according to standard procedures (Ausubel et al., 1998; Sambrook and Russel, 2001) using deionized water. Solutions were sterilized by autoclaving (20min/121°C/2bar). Heat-sensitive components, such as antibiotics, were prepared as stock solutions, filter-sterilized (0.2 μm) and added to the medium/buffer after cooling to 50°C.

II.1.5.1 Antibiotics

Antibiotics	Final concentration	Stock solution
***Escherichia coli* medium**		
Ampicillin (Amp)	100 mg l^{-1}	100 mg ml^{-1} H_2O
Kanamycin (Kan)	25 mg l^{-1}	100 mg ml^{-1} H_2O
***Agrobacterium tumefaciens* medium**		
Rifampicin (Rif)	100 mg l^{-1}	100 mg ml^{-1} DMSO
Kanamycin (Kan)	25 mg l^{-1}	100 mg ml^{-1} H_2O
Carbenicillin (Carb)	100 mg l^{-1}	100 mg ml^{-1} EtOH 50% (v/v)
Plant medium		
Kanamycin (Kan)	50 mg l^{-1}	100 mg ml^{-1} H_2O
Claforan	250 mg l^{-1}	200 mg ml^{-1} H_2O
Hygromycin	60 mg l^{-1}	100 mg ml^{-1} H_2O
Streptomycin (Strep)	500 mg l^{-1}	500 mg ml^{-1} H_2O
Spectinomycin (Spec)	500 mg l^{-1}	500 mg ml^{-1} H_2O
Tetracyclin (anhydrotetracyclin hydrochloride)	4.64 mg l^{-1}	2.32 mg ml^{-1} H_2O

II.1.6 Enzymes and reaction kits

Restriction enzymes either from New England Biolabs, GibcoBRL or Roche were used for DNA digestion. HighFidelity Taq Polymerase (Invitrogen) was used for PCR amplification of the constructs, while *Taq*DNA polymerase produced in-house (home-made Taq) was used for check-PCR reactions. The following kits were used:

Kit	Supplier
QIAquick® Gel Extraction Kit	Qiagen
QIAprep® Spin Miniprep Kit	Qiagen
QIAquick® PCR-Purification Kit	Qiagen
RNeasy RNA mini	Qiagen
Megaprime DNA labelling kit	GE Healthcare

II.1.7 Matrices and membranes

- Hybond™-C nitrocellulose membrane (0.45 µm, GE Healthcare) and Whatman N°1 paper from Whatman (Maidstone) were used for immunoblot analyses using alkaline phosphatase substrate for detection (II.2.4.9).
- Immobilion-P PVDF membrane (0.45 µm) from Millipore was used for western blot preparation using chemiluminescence detection (II.2.4.10).
- Hybond™-XL nylon membrane (0.45 µm, GE Healthcare) for RFLP (II.2.1.11) and northern blot analyses (II.2.1.14).
- Ni-NTA agarose resin (Qiagen) was used for the purification of recombinant IL-10 fused to the His_6-tag from plant protein extracts (II.2.4.13).

II.1.8 Equipment and applications

- **Centrifuges**: Eppendorf 5415 D and 5415 R, Avanti™ J-26 XPI (Beckman Coulter, Krefeld, D), Multifuge 3 S-R (Heraeus, Hanau, D),. Rotors: JA-10 and JA 25.50 (Beckman), 75006445 and 3057 (Hereaeus).
- **DNA gel electrophoresis:** wide mini and mini cells for DNA agarose electrophoresis and power supplies (Bio-Rad, Muenchen, D).
- **Drilling device**: Stirrer RZR1 C63-1000 (Heidolph, Schwabach, D)
- **Electron microscope:** EM-400 transmission electron microscope (Philips, Hamburg, D).

- **Electroporation apparatus:** Gene pulser™, Pulse controller unit, Estender unit (Bio-Rad) and 0.2 cm cuvettes (Bio-Rad).
- **Fluorescence microscope:** Olympus BX40 (Muenchen, D).
- **Freeze-dryer**: Alpha 1-4 LSC (Christ, Osterode, D).
- **Gel filtration apparatus:** ÄKTAprime™ plus purification system with a Superdex 200 pre-packed glass column (GE Healthcare).
- **Incubator:** Innova™ 4340 incubator shaker (New Brunswick scientific, Nuertingen, D).
- **Infrared fluorescence detector:** ODYSSEY® Infrared Imaging system (LI-COR, Bad Homburg, D).
- **Luminescent image analyzer:** LAS 3000 (Fuji Film, Duesseldorf, D).
- **Mass spectrometer:** quadrupole time-of-flight Ultima Global mass spectrometer (Waters Micromass, Vienna, AT).
- **Microtiterplate reader:** synergy HT (Bio-TEK, Bad Friedrichshall, D).
- **Mixer mill:** Mixer Mill MM200 (Retsch, Haan, D).
- **Particle bombardment system:** Biolistic PDS-1000/He system (BioRad).
- **PCR Termocyclers:** Primus and Primus 96 plus (MWG-Biotech), PE Biosystems GeneAmp PCR Systems 9600 (Weiterstadt, D).
- **Photometer:** Eppendorf Biophotometer (Eppendorf).
- **Phosphor autoradiography imager:** Typhoon Trio+ variable mode imager (GE Healthcare).
- **Probe sonicator:** UW2070 (Bandelin electronic, Berlin, D), Microtip Titan MS72.
- **Protein gel electrophoresis equipment:** Mini PROTEAN II™ (Bio-Rad).
- **Protein gel transfer equipment:** Min Trans-blot transfer cell (Bio-Rad).
- **Ultramicrotome:** Ultracut E (Leica, Wetzlar, D).
- **UV-crosslinker:** BLX-254 (Vilber Lourmat, Eberhardzell, D)
- **UV-Transilluminators**: wavelength 302 nm and UVT-20M (Herolab, Wiesloch, D) UV-chamber (Bio-Rad).

II.2 Methods

II.2.1 Nucleic acid technologies

II.2.1.1 PCR amplification

Polymerase Chain Reaction (PCR) was performed either to amplify the genes of interest from template DNA, directly fusing the sequences necessary to create and clone the different targeting constructs into the plant transformation vectors (II.1.2.1), or to identify positive clones after bacterial transformation (II.2.2.7). DNA amplification was carried out in a final volume of 50 µl, containing 1x PCR buffer, 1.5 mM $MgCl_2$, 0.25 mM of each dNTP, 10 pmol of each primer, 2.5 units of *Taq* DNA polymerase and 10-100 ng template DNA. The PCR reaction was performed in a GeneAmp PCR Systems 9600 (PE Biosystems) as follows: one denaturation step at 94°C for 3 min; 30 cycles of denaturation at 94°C for 30 sec, annealing at T_m-5°C for 30 sec, extension at 72°C 1 min, followed by a final extension step at 72°C for 7 min.

10x PCR buffer (for home-made *Taq*)	100 mM Tris-HCl, pH 9.0 500 mM KCl 1 % (v/v) Triton X-100

II.2.1.2 Nucleic acids quantification

The DNA (or RNA) concentration was determined by optical density measurement (1 OD_{260nm} unit = 50 µg ml^{-1} of double stranded DNA or 40 µg ml^{-1} of RNA) as described (Jefferson et al., 1987). The DNA (or RNA) purity was controlled by the OD_{260nm}/OD_{280nm} ratio.

II.2.1.3 DNA sequencing

DNA sequences were determined by the DNA Analysis core facility at the Fraunhofer IME using an Applied Biosystems (Weiterstadt, Germany) Abi Prism 3730 sequencer and the BigDye™-terminator v3.1 chemistry. Premixed reagents were from Applied Biosystems. Sequence analyses were carried out with the Wisconsin Package v10.2 (Genetics Computer Group, Madison, WI, USA).

II.2.1.4 Agarose gel electrophoresis of DNA

Analytical as well as preparative gel electrophoresis of DNA was performed as described (Sambrook et al., 1996) in 0.8-1.2 % (w/v) agarose gels prepared with TBE buffer and containing 0.1 µg/ml ethidium bromide. Known amounts of DNA molecular markers, such as 1 Kb ladder (Fermentas) or Lambda/*Pst*I marker (Fermentas), were used for evaluation of DNA concentration and size. The DNA samples were loaded after the addition of DNA loading buffer, and the electrophoretic run was carried out in TBE buffer at 5-10 V/cm. Visualization of the DNA bands and documentation of the gels were performed using a UV transilluminator at 302 nm and a black and white E.A.S.Y 429K camera (Herolab). In preparative electrophoresis, for purification of a particular DNA fragment from a mixture after restriction enzyme digestion, the DNA fragment of interest was excised from the gel on an UV transilluminator with a clean scalpel. The DNA extraction was performed with the QIAquick® gel extraction kit (Qiagen) according to the manufacturer's instructions. The concentration of the recovered DNA was measured spectrophotometrically (II.2.1.2), and the quality of the extraction was assessed by agarose gel electrophoresis.

10x TBE electrophoresis buffer	900 mM Tris-base 900 mM Boric acid 25 mM EDTA, pH 8.3
6x DNA loading buffer	0.025 % (w/v) Bromphenol blue 0.025 % (w/v) Xylencyanol 50 % (v/v) Glycerol in 2x TBE buffer

II.2.1.5 Restriction digestion of DNA

Restriction enzyme digestions were carried out in the buffer supplied with the enzyme, in accordance with the manufacturer's recommendations for temperature and duration of the digestion. For 1 µg DNA 1-2 units of the appropriate enzyme were used and the mixture was incubated 1-3 h at the enzyme's optimal temperature. For double digestions, combination of the two enzymes at the most suitable buffer was performed. If combination of the two enzymes was not possible, sequential digestions were performed, and DNA was purified via the QIAquick® PCR purification kit (Qiagen) in between to exchange reaction buffer and remove the first enzyme. Reactions were stopped by heat inactivation, when

applicable, or the DNA was directly purified either by gel extraction (II.2.1.4) or PCR purification kit (Qiagen).

II.2.1.6 Dephosphorylation of DNA

Dephosphorylation of restricted vector DNA was done with Calf Intestine Phosphatase (NEB) according to the manufacturer's protocol.

II.2.1.7 Ligation of DNA

DNA ligation was carried out in a total volume of 20 µl. Concentration of the DNA fragments was determined (II.2.1.2), the vector DNA dephosphorylated (II.2.1.6) and the reaction was set up mixing around 100 ng of vector in a 1:3 molar ratio with the insert, with either 80 U T4 DNA-Ligase or 1 µl Quick T4 DNA-Ligase (NEB) and the appropriate ligase buffer. Sticky-end ligations were carried out at 22°C for 30-180 min, and blunt-end ligations overnight (o/n) at 16°C. Ligation product was used directly to transform *E. coli* by heat-shock (II.2.2.3).

II.2.1.8 Isolation of plasmid DNA from *E. coli* with a commercial kit

Plasmid DNA was purified using QIAprep Spin Miniprep Kit or the Plasmid Midi Kit (Qiagen) according to the manufacturer's instructions. Quality and yield of plasmid DNA were examined by spectrophotometric analysis (II.2.1.2) and agarose gel electrophoresis (II.2.1.13). Isolated DNA was stored at -20°C.

II.2.1.9 Isolation of plasmid DNA from *E. coli* with the boiling-prep method

For simultaneous screening of numerous clones, the boiling-prep method (Holmes and Quigley, 1981) was used to isolate DNA from recombinant *E. coli*. One ml of a 5 ml o/n culture (II.2.2.1) was harvested by centrifugation at 16000 g, for 5 min, at room temperature (Rt) and the pellet resuspended in 150 µl of STETL buffer by vigorous vortexing. The suspension was incubated 5 min at Rt, boiled for 30-45 s and then centrifuged 10 min at 16000 g at Rt. The white pellet was removed with a toothpick and the DNA was precipitated with 150 µl of ice-cold isopropanol centrifuging 20 min at 16000 g at 4°C. The pellet was washed once with 70 % (v/v) ice-cold ethanol, dried and resuspended in bi-distilled water (ddH_2O) containing 0.1 mg/ml RNase-A.

STETL buffer	8 % (w/v) Sucrose 5 % (v/v) Triton X-100 50 mM EDTA, pH 8.0 50 mM Tris-HCl, pH 8.0 autoclave and store at 4°C + 0.5 mg/ml lysozyme prior to use

II.2.1.10 Isolation of DNA from plant material

High quality total DNA for restriction fragment length polymorphism (RFLP) analysis (II.2.1.11) was purified from plant tissue (leaf or callus) as follows. Around 100 mg of material were collected in a 2 ml tube and snap frozen in liquid nitrogen. The frozen tissue was pulverized with metal beads using a Retsch mill (1 min shaking, 20 ν), resuspended in 200 µl CTAB-buffer and incubated 30 min at 60°C, vortexing twice. DNA was extracted with 80 µl of chloroform/isoamyl alcohol (24:1) and centrifuged 10 min at 13400 g and 4°C. The aqueous upper phase was transferred in a new tube and RNA digestion was carried out by adding DNase-free RNase at a final concentration of 20 µg/ml and incubating 15 min at 37°C. Another extraction step was then performed, adding 60 µl of chlorophorm/isoamyl alcohol (24:1) to the mixture and centrifuging 10 min at 13400 g and 4°C. Around 150 µl of upper phase were transferred to a new tube, and DNA was precipitated adding 0.8-0.9 volumes of isopropanol, placed 15 min on ice and then centrifuged 30 min at 13400 g and 4°C. The supernatant was carefully removed, and after washing the pellet with 70 % (v/v) ethanol, DNA was resuspended in ddH_2O and stored at 4°C until use.

CTAB-buffer	2 % (w/v) CTAB 1.4 M NaCl 20 mM EDTA, pH 8.0 100 mM Tris-HCl, pH 8.0 100 mM β-Mercaptoethanol

II.2.1.11 RFLP analysis

Total DNA was extracted from leaf samples of transplastomic tobacco lines (II.2.3.2) using the CTAB method (II.2.1.10), and 5 µg were digested o/n with the restriction enzyme *Bgl*II (II.2.1.5). Digested DNAs were separated by electrophoresis on a 0.8 % (w/v) agarose gel (II.2.1.4), transferred onto a Hybond-XL nylon membrane by upward capillary blotting in 20x SSC buffer using standard protocols (Sambrook et al., 1996), and DNA was UV cross-linked onto the air-dried membrane (1x 0.120 J/cm^2). The blot was pre-hybridized for

2 h in Church buffer, and then incubated with 25 ng of *PsaB* probe produced from a 540 bp PsaB photosystem I core protein nucleotide sequence using a [^{32}P]CTP Megaprime labeling kit (GE Healthcare) following the manufacturer's instructions, o/n at 65°C, rotating. Excess probe was removed with two 20 min washes in 2x SSC, 0.1 % (w/v) SDS and then 0.5x SSC, 0.1 % (w/v) SDS. The washed membrane was placed in a cassette with a phosphor screen and after 2-4 h incubation at Rt, the hybridization signals were detected using a Typhoon™ Trio+ phosphoimager (GE Healthcare).

20x SSC buffer	3 M NaCl 0.3 M Sodium citrate pH 7.0
Church buffer	1 % (v/v) BSA 1 mM EDTA 7 % (w/v) SDS 0.5 M $NaHPO_4$ pH 7.2

II.2.1.12 Isolation of total RNA from plant material

To isolate total RNA from plant tissue, around 100 mg of material were collected in a 2 ml tube and snap frozen in liquid nitrogen. The frozen tissue was pulverized with metal beads using a Retsch mill (1 min shaking, 20 ν) and extracted with PeqGOLD TriFast™ reagent (Peqlab) following the manufacturer's instructions. RNA was finally resuspended in 20 µl ddH_2O, its concentration was determined spectrophotometrically (II.2.1.2) and the integrity checked by agarose gel electrophoresis (II.2.1.4). RNA was stored at -80°C until use.

II.2.1.13 Agarose formaldehyde gel electrophoresis of RNA

RNA was separated by gel electrophoresis under denaturing conditions in the presence of formaldehyde. Briefly, a 1 % (w/v) agarose gel containing 1 % (v/v) formaldehyde was prepared with MOPS buffer, and the RNA sample was denatured 10 min at 75°C in 1x RNA loading buffer before loading onto the gel. The electrophoresis run was performed in MOPS buffer, first at 30 V for 30 min, and then at 5 V/cm.

10x MOPS buffer	0.2 M MOPS 0.05 M Sodium Acetate 0.01 M EDTA pH 5.5-7.0

RNA loading buffer	50 % (v/v) Formamide, deionized 6.5 % (v/v) Formaldehyde 20 % Glycerol 1.25 mM EDTA, pH 8.0 0.005 % (v/v) Ethidiumbromide 0.1% (w/v) Xylene cyanol 0.1 % (w/v) Bromphenol blue in 1x MOPS aliquot and store at -80°C

II.2.1.14 Northern blot analysis

Ten µg of total RNA isolated from transplastomic tobacco leaves were separated by agarose formaldehyde gel electrophoresis (II.2.1.13) and transferred onto a Hybond-XL nylon membrane by upward capillary blotting in 20x SSC buffer using standard protocols (Sambrook et al., 1996). RNA was UV cross-linked onto the air-dried membrane (1x 0.120 J/cm^2). The blot was pre-hybridized for 2 h in Church buffer, and then incubated with 25 ng of either murine or viral IL-10 probes produced from a 540 bp mIL-10 or a 468 bp vIL-10 cDNA sequence (II.1.2.2; Ch_m_f and Ch_m_His_r, Ch_v_f and Ch_v_His_r), respectively, using a [^{32}P]CTP Megaprime labeling kit (GE Healthcare) following the manufacturer's instructions, o/n at 65°C, rotating. Excess probe was removed with two 20 min washes in 2x SSC, 0.1 % (w/v) SDS and then 0.5x SSC, 0.1 % (w/v) SDS. The washed membrane was placed in a cassette with a phosphor screen and after 2-12 h incubation at Rt, the hybridization signals were detected using a Typhoon™ Trio+ phosphoimager (GE Healthcare).

II.2.1.15 Isolation of RNA from mammalian cell cultures

J774 cells were scraped from the wells, washed once with PBS and resuspended in RLT buffer (Qiagen). After vigorous vortexing, samples were completely homogenized using a 1 ml disposable syringe with 20-gauge needle 5-8 times, and total RNA was extracted using the RNeasy kit (Qiagen), following the manufacturer's instructions. RNA was immediately checked for integrity by gel electrophoresis (II.2.1.13) and quantified (II.2.1.2), then stored at -80°C until use.

II.2.1.16 Real Time RT-PCR

Reverse transcription of RNA isolated from J774 macrophage cells (II.2.1.15) was carried out using SuperScript II (Invitrogen) following the manufacturer's instructions. Real time

RT-PCR was performed in triplicate from 10 ng cDNA for each sample, using the SYBR Green real-time master mix "SYBR Premix Ex Taq™" (Takara Bio Inc, Shiga, J), in the presence of 200 nM specific primer pairs purchased from Invitrogen (SOCS3_f and SOCS_r; GAPDH_f and GAPDH_r, II.1.2.2). The reaction conditions performed by the DNA Engine Opticon 2 System (MJ Research, Waltham, MA, USA), were as follows: 95°C for 10 s, followed by 40 cycles of 95°C for 10 s and 60°C for 40 s. Data were calculated with LinReg PCR 7.0 and Q-Gene software (http://www.gene-quantification.de/download.html) and then expressed as mean normalized expression (MNE) units after GAPDH normalization.

II.2.2 Manipulation of recombinant bacteria

II.2.2.1 Growth of *E. coli* and glycerol stock preparation

Single *E. coli* colonies were examined for plasmid integration by PCR (II.2.1.1). Selected clones were grown at 37°C either in LB medium on a shaker incubator at 180 rpm, or on LB-agar plates (1.5 % (w/v)), containing the appropriate antibiotics (II.1.5.1). For long-term storage, 600 µl of an o/n liquid culture was mixed with an equal volume of 40% (v/v) glycerol and stored at -80°C.

LB medium	1% (w/v) NaCl 1 % (w/v) Trypton 0.5 % (w/v) Yeast extract pH 7.4

II.2.2.2 Preparation of competent *E. coli* cells for heat-shock transformation

E. coli strain DH5α (II.1.1.2) competent cells were prepared for RbCl-mediated heat shock transformation. A single bacterial colony was inoculated in 5 ml of LB medium and cultured at 37°C, 180 rpm o/n. 100 ml of LB medium were inoculated 1:100 with the o/n culture, the cells were cultured at 37°C for 3-4 hours until the OD_{600nm} reached 0.4-0.5 and then transferred to an ice-cold tube. After 10 min on ice, the cells were recovered by centrifugation (2000 g/4°C/10 min). The pellet was gently dissolved in 30 ml ice-cold TfB-I solution and kept on ice for 10 min. The cells were recovered by centrifugation and resuspended in 4 ml ice-cold TfB-II buffer. 200 µl aliquots of the suspension were

dispensed into pre-chilled 1.5 ml tubes, frozen immediately in liquid nitrogen and stored at -80°C.

TfB-I	100 mM RbCl 75 mM $MnCl_2$ 10 mM $CaCl_2$ 0.5 mM LiCl 35 mM K acetate 15 % (v/v) Glycerol pH 5.8
TfB-II	10 mM RbCl 75 mM $CaCl_2$ 15 % (v/v) Glycerol 10 mM MOPS pH 6.8

II.2.2.3 Transformation of *E. coli* by heat-shock

As soon as the competent cells were thawed on ice, around 20-100 ng plasmid DNA (II.2.1.8) or ligation products (II.2.1.7), diluted in sterile dH_2O if necessary, were mixed gently with the competent cells and stored on ice for 30 min. The cells were then incubated for 90 seconds at 42°C and immediately placed on ice for 2 min. 800 µl of SOC medium were added to the tube and the transformed cells were incubated at 37°C for 45 min. 200 µl of cells were plated onto LB-agar plates supplemented with the appropriate antibiotics and incubated o/n at 37°C. Single colonies were inoculated in 5 ml of LB selective medium and cultivated o/n at 37°C, shaking at 180 rpm. An aliquot of the culture was then used for plasmid extraction by the boiling-prep method (II.2.1.9), and the correctness of the insert size was assessed digesting the plasmid DNA with appropriate restriction enzymes (II.2.1.5) and evaluating the digestion profile after electrophoretic separation of the fragments on 1.2 % (w/v) agarose gel (II.2.1.4). Plasmid DNA from the positive clones was then extracted with commercial kits (II.2.1.8) and sent for sequencing (II.2.1.3).

SOC medium	1 % (w/v) Bacto tryptone 0,5 % (w/v) Yeast extract 10 mM NaCl 2.5 mM KCl autoclave, then add sterile $MgCl_2$ to 10 mM sterile $MgSO_4$ to 10 mM sterile Glucose to 20 mM

II.2.2.4 Growth of *A. tumefaciens* and preparation of glycerol stocks

Single *A. tumefaciens* colonies were examined for plasmid integration by PCR (II.2.2.7). The selected positive clones were grown at 28°C either in YEB medium on a shaker incubator at 180 rpm, or on YEB-agar plates (1.5 % (w/v)) containing the appropriate antibiotics (II.1.5.1). For long-term storage, 800 µl of a saturated culture was mixed with 400 µl of glycerol and stored at -80°C.

II.2.2.5 Preparation of competent *A. tumefaciens* cells for electroporation

A single colony of *A. tumefaciens* grown on a YEB-agar plate containing Rif and Kan (YEB-Rif-Kan) was inoculated in 5 ml of YEB-Rif-Kan medium in a 100 ml Erlenmeyer flask and incubated at 28°C for two days shaking (180 rpm). One ml of the culture was then transferred into 100 ml of YEB-Rif-Kan medium, and cultivated at 28°C for 15-20 h shaking (180 rpm) until the OD_{600nm} reached 1-1.5. The cells were chilled on ice for 15 min and centrifuged for 5 min at 4000 g, 4°C. The cell pellet was washed tree times with 10 ml of ddH_2O and finally resuspended in 500 µl of sterile 10 % (v/v) glycerol. The suspension was dispensed as 45 µl aliquots into pre-chilled 1.5 ml tubes, immediately frozen in liquid nitrogen and stored at -80C.

II.2.2.6 Transformation of *A. tumefaciens* by electroporation

0.2-1.0 µg of plasmid DNA (II.2.1.8) in sterile ddH_2O was added to a thawed aliquot of *A. tumefaciens* electrocompetent cells (II.2.2.5), placed on ice for 3 min and then the cell/DNA mixture was transferred into a pre-chilled electroporation cuvette (0.2 cm). After application of the pulse (25 µF, 2.5 kV, 200 Ω), the cells were diluted in 1 ml of YEB medium and incubated for 1 h at 28°C, shaking (180 rpm). One to 10 µl of the culture were plated on YEB-Rif-Kan-Carb agar plates and incubated at 28°C for 2-3 days. Single colonies were examined for plasmid integration by colony PCR (II.2.1.1).

II.2.2.7 Identification of recombinant agrobacteria

For rapid identification and verification of the foreign gene in recombinant agrobacteria, isolated single colonies were picked from selective plates using sterile tips and directly inoculated in a 0.2 ml PCR tube containing the PCR mix, while the plates were incubated at 28°C o/n to let the colonies regrow. PCR reaction was carried out as described (II.2.1.1)

using a home-made *Taq* DNA polymerase, and the PCR products were resolved on a 1.2 % (w/v) agarose gel by electrophoresis (II.2.1.4).

II.2.3 Transformation of plants and plant suspension cultures

II.2.3.1 Growth and maintenance of *N. tabacum* L. cv. Petit Havana

Sterile tobacco plants were grown in either plastic Magenta boxes or glass Weck containers on MS medium (containing the appropriate antibiotics for selection, if transgenic) in a controlled growth chamber with 20-25°C, 16 h photoperiod (7000 lux).

Non-sterile tobacco plants were grown in a greenhouse in ED73 standard soil (Patzer) with 0-30 % (v/v) sand under supplementary illumination of 10000 lux (plus the sun light), 70-90 % humidity and 16 h photoperiod at 24°C (or higher, depending on the outside temperature). To prevent cross-pollination, flowers were covered with plastic bags with micro pores. Mature, dried seeds were stored in paper bags at Rt.

MS medium	0.44 % (w/v) MS salts with vitamins 1 % (w/v) Glucose 0.7 % (w/v) Agar, pH 5.8

II.2.3.2 Transformation of *N. tabacum* chloroplasts by particle bombardment

N. tabacum cv. Petit Havana wild type (wt) plants grown in sterile culture (II.2.3.1) were used for chloroplast transformation by particle bombardment. The youngest leaves from ~ 6-8 cm high plants were taken and laid adaxial face upwards, on petri dishes containing RMOP medium. For each shot, 1.5 mg of gold particles (0.6 µm) were coated with 20 µg of plasmid DNA, prepared at a concentration of 2.5 µg/µl with commercial kits (II.2.1.8). Leaf bombardment was performed with a PDS-1000/He System (BioRad) at 1360 psi helium pressure, using 1100 psi rupture disks and a hepta adaptor, with a distance from the target of 9 cm. After shooting, the leaves were cut into 5x5 mm squares and placed adaxial face downwards onto RMOP medium containing spectinomycin (500 mg l^{-1}) at 20-25°C, 16 h photoperiod (7000 lux), until green calli appeared (4-8 weeks). The calli were then transferred onto fresh RMOP-Spec plates until small shoots appeared (4-8 weeks). When leaves appeared, they were cut into small pieces (~ 2 x 2 mm) and transferred onto new RMOP-Spec plates for the first regeneration round. A double-selection test, placing small leaf pieces on RMOP plates containing spectinomycin and streptomycin (both at 500 mg ml^{-1}) was also performed to exclude spontaneous resistant mutants. After regeneration of

shoots, leaf samples were collected and tested for homoplasmy by RFLP analysis (II.2.1.11). The plantlets were subjected to additional regeneration rounds, if necessary, until homoplasmic, and they were then transferred in Magenta boxes containing RM-Spec for rooting. True homoplasmic transplastomic plants were put in soil and transferred to the greenhouse, where they were kept under transparent plastic lids for 1-2 weeks to gradually decrease the humidity, and then grown normally. Transplastomic plants were self pollinated or, if male-sterile, hand-fertilized with wt pollen, and the seeds were germinated on RM-Spec and RM-Spec-Strep medium to confirm homoplasmy of the parental transplastomic plant (Figure 5B).

RM macro	0.44 % (w/v) $CaCl_2$ x $2H_2O$ 0.17 % (w/v) KH_2PO_4 1.9 % (w/v) KNO_3 0.37 % (w/v) $MgSO_4$ x 7 H_2O 1.65 % (w/v) NH_4NO_3
RM micro	0.169 % (w/v) $MnSO_4$ 0.086 % (w/v) $ZnSO_4$ x 7 H_2O 0.062 % (w/v) H_3BO_3 0.0083 % (w/v) KI 0.0025 % (w/v) Na_2MoO_4 x 2 H_2O 0.00025 % (w/v) $CuSO_4$ x 5 H_2O 0.00025 % (w/v) $CoCl_2$ x 6 H_2O
RMOP medium, pH 5.8 (1 L)	100 ml RM macro 10 ml RM micro 5 ml FeNaEDTA 1 % (w/v) 30 g Sucrose 100 mg Myo-inositol 1 ml Thiamine HCl 0.001 % (w/v) 0.1 ml NAA 0.01 % (w/v) 1 ml BAP 0.1 % (w/v) 5.4 g Agar
RM medium, pH 5.75 (1 L)	100 ml RM macro 10 ml RM micro 5 ml FeNaEDTA 1 % (w/v) 30 g Sucrose 5.6 g Agar

II.2.3.3 Vacuum agroinfiltration of *N. tabacum* leaves

The preparation and vacuum infiltration of tobacco leaves with recombinant *A. tumefaciens* (II.2.2.7) was carried out essentially as described by Kapila *et al*. (1997). A pre-culture of

recombinant agrobacteria (5 µl) from glycerol stock (II.2.2.4), carrying the desired plant expression vector of the pTRAkt series (II.1.2.1) was grown in 5 ml YEB-Rif-Carb-Kan selection medium (II.2.2.4) for two days at 28°C, shaking (180 rpm). On the third day, this saturated culture was used to inoculate 20-100 ml of YEB-Carb-Kan medium 1:100, and the suspension was allowed to grow o/n at 28°C, shaking (180 rpm). On the fourth day, the culture was induced adding acetosyringone to 20 µM , glucose to 10 mM and MES (pH 5.6) to 10 mM, and grown as usual. On the fifth day, the OD_{600nm} of the culture was determined (approx. 5.0), the bacterial culture was adjusted to OD_{600nm} ~1.0 with 2x infiltration medium and water, and induced for an additional 2 h with 200 µM acetosyringone. *N. tabacum* cv. Petit Havana SR1 wt leaves, freshly harvested, were vacuum-infiltrated at 70 mbar for 20 min in the bacterial suspension, then placed with the adaxial side upwards in plastic trays with moistened Whatman paper. The trays were sealed with Saran wrap and incubated at 20-25°C with a 16 h photoperiod (7000 lux), for 3 days.

2x Infiltration medium	10 % (w/v) Sucrose 20 mM Glucose 0.86 % (w/v) MS salts pH 5.6, prepare fresh

II.2.3.4 Syringe agroinfiltration of *N. tabacum* plants

Five ml of YEB-Rif-Carb-Kan were inoculated with 5 µl of recombinant agrobacteria from a glycerol stock (II.2.2.4) carrying a plant expression vector of the pTRAkt series (II.1.2.1) and grown o/n at 28°C, 180 rpm. On the second day, the culture was induced adding acetosyringone to 20 µM, glucose to 10 mM, MES pH 5.6 to 10 mM, and grown as usual. The following day, the OD_{600nm} of the culture was determined (approx. 3.0), the bacterial culture was adjusted to OD_{600nm} ~1.0 with 2x infiltration medium and water, and induced for an additional 2 h with 200 µM acetosyringone. The agro-suspension was infiltrated with the aid of a 1 ml syringe, without needle, into the leaves of intact *N. tabacum* cv. Petit Havana SR1 wt plants. The infiltrated plants were grown at 20-25°C, 16 h photoperiod (7000 lux), for 3-5 days.

II.2.3.5 Stable nuclear transformation of *N. tabacum* plants

Stable nuclear transformation of *N. tabacum* cv. Petit Havana SR1 was performed according to the leaf disc method, using recombinant *A. tumefaciens* (II.2.2.7), and transgenic T_0

plants were regenerated from transformed calli (Fraley et al., 1983; Horsch et al., 1985). Briefly, wt plants were grown in sterile conditions on MS medium in Weck glasses (II.2.3.1) and the youngest leaves (length up to 6 cm) were used for transformation. The agrobacteria suspension was prepared inoculating 100 ml of YEB-Rif-Carb-Kan medium with 100 µl of glycerol stock of the selected clone and growing the culture o/n at 28°C, shaking at 180 rpm. On the next day the cells were pelletted by centrifugation at 5000 g for 10 min, resuspended in 250 ml of induction medium and cultivated o/n at 28°C, shaking at 180 rpm. Agrobacteria cells were centrifuged 15 min at 5000 g, resuspended in 50 ml of MMA buffer, and kept at Rt for 2 h. The OD_{600nm} was adjusted to 1.0. The leaves were cut into small pieces, transferred into Weck glasses containing 50-100 ml of recombinant agrobacteria suspension and incubated for 30 min at Rt. The leaf pieces were then transferred onto sterile pre-wetted Whatman filters in petri dishes, closed with saran wrap and incubated at 25°C in the dark for two days. Afterwards, they were transferred onto MS-II plates and incubated first at 25°C in the dark for 3 days, and then with a 16 h photoperiod until shoots appeared, transferring them onto fresh plates every 2 weeks. When shoots appeared, they were transferred onto MS-III plates, incubated at 20-25°C with a 16 h photoperiod (7000 lux), until roots developed and finally transferred into soil and grown in the greenhouse (II.2.3.1).

Induction medium	YEB medium 10 mM MES pH 5.6
MMA buffer	0.43 % (w/v) 10 mM MES 2 % (w/v) Sucrose 200 µM Acetosyringone (added just before use) pH 5.6
MS-II medium	MS medium with 1 mg l^{-1} BAP 100 mg l^{-1} Kanamycin 200-500 mg l^{-1} Claforan
MS-III medium	MS medium with 100 mg l^{-1} Kanamycin 200-500 mg l^{-1} Claforan

II.2.3.6 Growth and maintenance of *Nicotiana tabacum* cv. BY-2 cells

N. tabacum cv. BY-2 suspension cells and calli were cultivated in BY-2 medium at 26°C in the dark, shaking at 160 rpm for the suspension cultures. Suspension cells were sub-cultured weekly using a 2 % (v/v) inoculum, while pinpoint-sized clumps of callus cells were transferred to fresh plates monthly.

BY-2 medium (1L)	4.43 g MSMO 30 g Sucrose 100 µl 2,4-D (2 mg/ml) 150 µl Thiamine-HCl (4 mg/ml) 0.2 g KH_2PO_4 (2 g (w/v) Agar)

II.2.3.7 Stable transformation of *N. tabacum* cv. BY-2 cells

N. tabacum cv. BY-2 cells were transformed by co-cultivation with recombinant *A. tumefaciens* as follows. 100 ml of BY-2 medium were inoculated with 2 % (v/v) BY-2 wt cells 3 days ahead of the transformation date, and 10 ml of YEB-Rif-Kan-Carb medium were inoculated 1:100 with a glycerol stock of recombinant agrobacteria (II.2.2.4) and grown at 28°C, shaking (180 rpm) for 2 days. On the day of transformation, three ml of BY-2 culture, induced with 200 µM acetosyringone, were co-inoculated with 150 µl of agrobacteria (OD_{600nm} ~1) in a small petri dish (5 cm). After incubation for 3 days in the dark at 24°C, the cells were transferred to centrifuge tubes and sedimented (3min/100g/Rt). The cells were gently resuspended in 2 ml of BY-2 medium containing 200µg/ml claforan, and around 500-700 µl of the resuspended cells were transferred onto a BY-2 medium plate containing 100 µg/ml Kan and 200 µg/ml claforan; other 500 µl of BY-2 medium were added to facilitate an even distribution of the cells on the plate. After the liquid medium had mostly evaporated, the plates were sealed with parafilm and incubated at 24°C in the dark for 3-4 weeks, until transgenic calli appeared.

II.2.3.8 Identification of transformants by visualization of DsRed fluorescence

The fluorescence of the reporter protein DsRed was visualized by incubating the transiently infiltrated tobacco leaves (II.2.3.4) or the stably transformed BY-2 cells (II.2.3.7) with an

LCD lamp with glass fibre optic (Leica KL1500), an additional filter for green excitation (BP545/30) and a coloured foil (# 182, light red).

II.2.4 Protein analysis

II.2.4.1 Isolation of total soluble proteins from tobacco leaves

For screening purposes, around 100 mg leaf tissue were collected into a 1.5 ml tube and extracted in 3 volumes of pre-cooled protein extraction buffer with a drilling device. Aqueous supernatant was collected after centrifugation at 16000 g for 30 min at 4 °C, and the samples either used immediately or stored at -20°C.

Plant protein extraction buffer	PBS, pH 7.4 0.05 % (v/v) Tween 20 5 mM EDTA 2 % (w/v) PVPP

For large scale extraction for IL-10 purification, leaf material, deprived of the midrib, was ground to a fine powder using a mortar and pestel in liquid nitrogen. The recovered material was weighed and homogenized with 3 volumes of IL-10 extraction buffer and further processed according to the IL-10 purification protocol (II.2.4.13).

IL-10 extraction buffer	PBS pH 6.0 5 mM Ascorbic Acid 5 mM β-Mercaptoethanol)

II.2.4.2 Isolation of total soluble proteins from BY-2 cells

For screening purposes, around 200 mg of either callus or cell pellet from a liquid culture (10 min at 16000 g, 4°C) were weighed in a 2 ml plastic tube, and sonicated on ice for 1 min, 9 x 10 % cycle, 35 % power with 2 volumes of BY-2 extraction buffer. Clear supernatant was separated from cell debris by centrifugation at 16000 g for 30 min at 4°C.

BY-2 extraction buffer	PBS pH 7.4 0.05 % (v/v) Tween-20 5 mM EDTA pH 8.0 1 % (v/v) DMSO – freshly added

For large scale extraction for IL-10 purification, the BY-2 cell pellet (15 min at 5000 g, 4°C) from 250 ml of a 5 days old liquid culture was washed once with PBS (pH 7.4) and then homogenized with 2 volumes of IL-10 extraction buffer (II.2.4.1) with a dip-in blender in a metal beaker placed on ice. The extract was further processed according to the IL-10 purification protocol (II.2.4.13).

II.2.4.3 Isolation of total soluble proteins from animal cell cultures

After stimulation (II.2.6.2, II.2.6.4), J774 cells (~1 x 10^5/well) were diluted in ice-cold PBS and centrifuged twice for 5 min at 500 g, 4°C. Cells were then resuspended in lysis buffer containing inhibitors of proteases (5 µg/ml leupeptin, 5 µg/ml pepstatin A, 1 mM PMSF, 1 mg/ml α1-antitrypsin) and phosphatases (1 mM Na_3VO_4, 10 mM NaF, 10 µM phenylarsin oxide), and following a 15 min incubation on ice, cell debris were spun down (12000 g, 20 min, 4°C) and the supernatants were frozen and stored at -80°C until use. Small aliquots of the various extracts were used for protein content determination (II.2.4.4).

Lysis buffer	20 mM HEPES, pH 7.9 420 mM NaCl 1 mM EDTA 1 mM EGTA 1 % (v/v) Nonidet P-40 20 % (v/v) Glycerol 1 mM DTT

II.2.4.4 Total soluble protein quantification

Bradford reagent Roti®-Quant (Roth) was used to determine the concentration of total soluble proteins (Bradford, 1976). Standard protein solutions were prepared ranging from 250 to 31 µg/ml using bovine serum albumin (BSA) to determine the calibration curve. Then, 10 µl of a 1/20 and 1/40 dilution of protein extract in PBS (pH 7.4) were mixed with 200 µl of 1/5 diluted Bradford reagent in a 96-well (flat bottom, low binding) microtiterplate (Greiner Bio-one). All samples were assayed in duplicate, the spectrophotometer was blanked with 1/5 diluted Bradford reagent alone and absorbance was read at 595 nm on a microtiterplate reader (Bio-TEK). Protein concentration was then calculated by comparing the OD_{595nm} of each sample with the OD_{595nm} of the standard protein (BSA) curve.

II.2.4.5 SDS-PAGE with Tris-Glycine gels

Proteins were electrophoretically separated by discontinuous SDS-PAGE as described (Laemmli, 1970).

Running gel (2 gels)	**7.5 %**	**12 %**	**17 %**
ddH2O	4.8 ml	3.3 ml	1.63 ml
1.5 M Tris-HCl, pH 8.8	2.5 ml	2.5 ml	2.5 ml
SDS 10 % (w/v)	100 µl	100 µl	100 µl
Acrylamyde 30 % (w/v)	2.5 ml	4 ml	5.66 ml
TEMED	8 µl	4 µl	4 µl
APS 20 % (w/v)	50 µl	50 µl	50 µl

Stacking gel (2 gels)	
ddH_2O	3.645 ml
1 M Tris-HCl, pH 6.8	625 µl
SDS 10 % (w/v)	50 µl
Acrylamyde 30 % (w/v)	830 µl
TEMED	5 µl
APS 20 % (w/v)	15 µl

Before loading, proteins were denatured and solubilised in either reducing or non-reducing 1x SDS sample buffer at 100°C for 10 min. Electrophoresis was carried out in SDS running buffer, with a constant voltage of 20 V/cm.

Proteins were visualised by staining with Coomassie brilliant blue (II.2.4.7), Silver (II.2.4.8) or transferred by tank-blotting (90 min at 180 V) onto either nitrocellulose or PVDF membranes for immunoblot analysis.

5x Reducing SDS sample buffer	62.5 mM Tris-HCl pH 6.8 30 % (v/v) Glycerol 4 % (v/v) SDS 0.05 % (w/v) Bromphenol blue 10 % (v/v) β-Mercaptoethanol
5x Non-reducing SDS sample buffer	62.5 mM Tris-HCl pH 6.8 30 % (v/v) Glycerol 4 % (v/v) SDS 0.05 % (w/v) Bromphenol blue
5x SDS running buffer	125 mM Tris-base 960 mM Glycine 0.5 % (w/v) SDS

II.2.4.6 SDS-PAGE with Tris-Tricine gels

For total soluble protein separation in the range from 1 to 100 kDa, Tricine-SDS-PAGE was performed (Schagger and von Jagow, 1987).

	10 % Separating gel (2 gels)	Stacking gel (2 gels)
Rotiphorese® Gel A	3.25 ml	650 µl
Rotiphorese® Gel B	1.5 ml	300 µl
3M Tris HCl, pH 8.45	3.334 ml	1.25 ml
10 % (w/v) SDS	100 µl	37.3 µl
80 % (v/v) Glycerol	1.326 ml	-
ddH_2O	450 µl	2.72 ml
TEMED	3.6 µl	4 µl
10 % (w/v) APS	36 µl	40 µl

Before loading, proteins were denatured and solubilised in Tricine-sample buffer at 100°C for 10 min. Electrophoresis was carried out with the appropriate anode and cathode buffers, at 30 V for 1 h and then at 70 V constant for 13 h, with a buffer cooling system. Proteins were visualised by staining with Coomassie brilliant blue (II.2.4.7).

2x Tricine-sample buffer	0.1 M Tris-HCl, pH 6.8 24 % (v/v) Glycerol 8 % SDS (w/v) 0.2 M DTT 0.02 % (w/v) Coomassie Blue $_{G250}$
10x Anode buffer	2 M Tris-HCl, pH 8.9
10x Cathode buffer	1 M Tris-base 1 M Tricine 1 % (w/v) SDS pH ~ 8.25 (do not adjust)

II.2.4.7 Coomassie brilliant blue staining

Proteins separated by SDS-PAGE (II.2.4.5, II.2.4.6) were visualized by Coomassie brilliant blue staining as described (Fairbanks et al., 1971). The gel was stained with 100 ml of Fairbanks A solution, heated in a microwave (1000 W) until boiling point (ca. 2 min), and then let cool down at Rt for ca. 5 min, gently shaking. The solution was discarded, the gel briefly rinsed with dH_2O, 100 ml of Fairbanks D solution were added and then heated in a microwave until boiling point (ca. 1min 20 sec). A piece of kimwipe was added to absorb the stain, and the solution was allowed to cool down at Rt for ca. 5 min, gently shaking. The

solution was then replaced with fresh Fairbanks D solution, and kept gently shaking until the gel background became transparent. The gel was eventually dried between cellophane sheets for documentation purposes.

Fairbanks A (staining solution)	0.05 % (w/v) Coomassie R-250 25 % (v/v) Isopropanol 10 % (v/v) Acetic acid
Fairbanks D (destaining solution)	10 % (v/v) Acetic acid

II.2.4.8 Silver staining

For higher sensitivity and to detect small amounts of proteins, SDS-polyacrylamide (SDS-PAA) gels were silver stained according to the protocol from Shevchenko (Shevchenko *et al.*, 1996), summarized as follows:

Step	Solution	Time	250 ml (2 minigels)
Fixation	50 % (v/v) Methanol 5% (v/v) Acetic acid	20 min	125 ml 12.5 ml
Wash	50 % (v/v) Methanol dH_2O	10 min 10 min	125 ml 250 ml
Sensitizing	0.02 % (w/v) $Na_2S_2O_3$	1 min	0.05 g
Silver Reaction	0.1 % (w/v) $AgNO_3$	20 min, 4°C	0.25 g
Wash	dH_2O	2 x 1 min	
Developing	0.04 % (v/v) Formaldehyde (37 %) 2 % (w/v) Na_2CO_3		750 µl 5 g
→ keep shaking gently while developing → when the solution is yellow discard it and replace it with a fresh portion → the solution has to be transparent			
Stopping	5 % (v/v) Acetic acid	10 min	12.5 ml
Storing	1 % (v/v) Acetic acid, 4°C		2.5 ml

II.2.4.9 Immunoblot with AP detection system

Electrophoretically separated proteins were transferred from a SDS-PAA gel onto a Hybond^{TM}-C nitrocellulose membrane (45 µm) in the presence of transfer buffer for 90 min at 180 V. The membrane was blocked with 5 % (w/v) skim milk in PBST for 1 h at Rt, and then blotted proteins were probed with the primary antibody o/n at 4°C. The bound antibody

was detected by the addition of the appropriate secondary polyclonal antibody coupled to alkaline phosphatase (AP) (II.1.3). Both primary and secondary antibodies were diluted in PBST. To remove unspecifically bound antibodies, the membranes were extensively washed with PBST in between each step. The target proteins were finally revealed by addition of the substrate NBT/BCIP dissolved in AP buffer.

Blotting buffer	25 mM Tris-HCl, pH 8.3 192 mM Glycine 20 % (v/v) Methanol
10x PBS	1.37 mM NaCl 27 mM KCl 81 mM $Na_2HPO_4x\ 12H_2O$ 15 mM KH_2PO_4
PBST	1x PBS, pH 7.4 0.05 % (v/v) Tween 20
AP Buffer	100 mM Tris-HCl, pH 9.6 100 mM NaCl 5 mM $MgCl_2$

II.2.4.10 Immunoblot with HRP detection system

Electrophoretically separated proteins were transferred from a SDS-PAA gel onto a PVDF membrane (45 µm), pre-activated in methanol, in the presence of transfer buffer for 90 min at 180 V. The membrane was blocked with 5 % (w/v) skim milk in PBST for 1 h at Rt, and then blotted proteins were probed with the primary antibody o/n at 4°C. The bound antibody was detected by the addition of the appropriate secondary polyclonal antibody coupled to horse radish peroxidase (HRP). Both primary and secondary antibodies were diluted in PBST. To remove unspecifically bound antibodies, the membranes were extensively washed with PBST in between each step. The target protein were finally revealed with the ECL Plus Western Blotting Detection kit (GE Healthcare) and the signal was either captured with a LAS 3000 imaging system (Fujifilm) or using a BioMax autoradiography film (Kodak).

II.2.4.11 Dot blot analysis

Dot blot analysis was used to screen either the transgenic plants or the transgenic calli for IL-10 production. Two to 20 µl of row extract and 20 or 100 ng of commercial murine (BD Pharmingen) or viral IL.10 (R&D Systems), respectively, as positive control were dotted directly onto a nitrocellulose membrane. The membrane was blocked with 5 % (w/v) skim milk in PBST for 1 h and the primary antibody (1:2000 for the anti murine and 1:1000 for the anti viral IL-10, in PBST) was applied o/n, at 4°C. The membrane was then incubated with the secondary RAR^{AP} antibody (1:5000 in PBST) for 1 h at Rt, and the signal detected with the NBT/BCIP substrate.

II.2.4.12 IL-10 quantification by ELISA

Determination of the concentration of IL-10, in either row extracts or elution fractions after Ni-NTA purification, was performed by sandwich enzyme-linked immunosorbent assay (ELISA) according to the following protocol (in between each steps, the plates were washed 3 times with PBST):

- **Capture antibody**: 96-well, flat bottom, high binding microtiterplates (Greiner Bio-One) were coated o/n at 4°C with 100 µl of the respective antibodies diluted in the appropriate coating buffer:

mIL-10: monoclonal anti-mIL-10 Ab (BD Pharmingen) diluted to 2 µg/ml in

mIL-10 Coating buffer

Na_2HPO_4 11.8 g
NaH_2PO_4 16.1 g
dH_2O to 1000 ml
Adjust the pH 6.5, store at 4°C

vIL-10: monoclonal anti- v-IL-10 (BD Biosciences) diluted to 0.5 µg/ml in

vIL-10 Coating buffer

Na_2CO_3 1.59 g
NaH_2CO_3 2.93 g
NaN_3 0.2 g
dH_2O to 1000 ml
Adjust the pH 9.6 with acetic acid, store at 4°C

- **Blocking:** the wells were incubated with 200 µl blocking buffer (1 % (w/v) BSA in PBST buffer) for 1 h at Rt.

- **Sample application:** samples were brought to the appropriate dilution with PBS and applied to the 96 well plate using a multichannel pipettor and incubated o/n at 4°C. Standards for the calibration curve were 12 2-fold serial dilutions of, respectively: mIL-10 (BD Pharmingen) diluted to 50 ng/ml starting concentration in PBS, and vIL-10 (R&D Systems) diluted to 1 ng/ml starting concentration in PBS.
- **Detection biotinylated antibody**: 100 µl of either biotinylated monoclonal rat anti-mIL-10 (BD Pharmingen) or biotinylated monoclonal rat anti-vIL-10 (BD Pharmingen), diluted to 1 µg/ml in blocking buffer, were applied to each well and incubated for 1h at Rt.
- **Streptavidin-AP conjugated**: 100 µl of Streptavidin-AP (Jackson ImmunoResearch) diluted 1:5000 in blocking buffer were applied to each well and incubated for 30 min at Rt.
- **Detection**: 100 µl of the substrate para-nitrophenylphosphate (SIGMA, #104-105) diluted to 1 mg/ml in substrate buffer were added to each well, the colour reaction developed at Rt until yellow, and the OD of the plate read at 405 nm using the microtiterplate reader.

Substrate buffer	0.1M Diethanolamine 150 mM NaCl 1 mM $MgCl_2$ pH 9.6

II.2.4.13 Ni-NTA purification

His_6-tagged IL-10 was affinity purified from either plant leaves or BY-2 cell pellet by immobilized metal ion affinity chromatography (IMAC). 1 ml of Ni-NTA-agarose matrix (QIAGEN) was poured in a disposable Econo-Pac column (BioRad) and used for purification. After cell disruption (II.2.4.1, II.2.4.2), row extract was centrifuged at 15000 g for 15 min, and the supernatant filtered through a paper filter (Macherey-Nagel, #615). Afterwards, the filtrate was adjusted to 500 mM NaCl, 5 mM Imidazole, pH 8.0, and incubated on ice for 1 h, gently shaking. The extract was then centrifuged at 30000 g for 30 min, 4°C, the supernatant filtered through miracloth material and then loaded onto the column, previously equilibrated with wash buffer. The flow rate for the loading was adjusted to 2 ml/min. The column was extensively washed with at least 20 column volumes of wash buffer, and elution was performed with 2-3 volumes of elution buffer. All steps

were performed at 4°C. The collected elution fractions were dialyzed o/n at 4°C against water, and then lyophilized using an Alpha 1-4 LSC freeze-dryer (Christ). Lyophilized material was then dissolved in PBS (pH 7.4), the preparation was centrifuged to remove residual insoluble material, and IL-10 concentration in the supernatant was determined by ELISA (II.2.4.12).

Wash buffer	1x PBS 500 mM NaCl 5 mM Imidazole pH 8.0
Elution buffer	1x PBS 500 mM NaCl 500 mM Imidazole pH 8.0

II.2.4.14 Gel filtration

To assess whether plant produced mIL-10 was completely in the dimeric state, the IMAC purified protein (II.2.4.13) was analyzed by gel filtration using an ÄKTAprime™ plus purification apparatus (GE Healthcare) and a Superdex 200 column (10/30, GE Healthcare), with PBS (pH 7.4) as eluent and a flow rate of 0.35 ml/min. 450 ng of purified recombinant mIL-10 were loaded on the column, and 1 ml (elution volumes 7-12 and 17-28 ml) and 0.2 ml fractions (elution volumes 12-17 ml) were collected. The elution fractions were analyzed for IL-10 concentration by ELISA (II.2.4.12).

II.2.4.15 Mass spectrometry

Murine and viral IL-10, purified from either leaf material or BY-2 cell pellet by IMAC (II.2.4.13), were separated on a 17 % gel by SDS-PAGE (II.2.1.4), and the proteins were visualized by Coomassie brilliant blue staining (II.2.4.7). The bands were then excised, destained, carbamidomethylated, digested with trypsin and extracted from gel pieces as previously described (Kolarich and Altmann, 2000; Kolarich *et al.*, 2006). Subsequent fractionation of the peptides by capillary reversed-phase chromatography, with detection by a quadrupole time-of-flight (Q-TOF) Ultima Global mass spectrometer (Waters Micromass, Manchester, UK), was performed as described previously (Van Droogenbroeck *et al.*, 2007). The MS data from the tryptic peptides were compared with data sets generated by *in silico* tryptic digestion of the recombinant protein sequences using the PeptideMass program

(http://www.expasy.org/tools/peptide-mass.html). Sequences of the N-terminal peptides were confirmed by tandem MS experiments. Data were analyzed with MassLynx 4.0 SP4 Software (Waters Micromass, Mildford, MA, USA). The MS-analyses were performed by Johannes Stadlmann from the BOKU, Wien, Austria.

II.2.5 Electron microscopy

II.2.5.1 Specimen processing for ultrastructure analysis

Tobacco leaves were cut into small squares of around 1 mm^2 with a razor blade and fixed o/n at 4°C in fixative solution (2 % (w/v) paraformaldehyde, 2.5 % (v/v) glutaraldehyde in 0.1 M phosphate buffer (pH 7.4). Specimens were then washed five times for 15 min with 0.1 M phosphate buffer (pH 7.4) at 4°C. Samples were post-fixed in a 1 % (w/v) osmium tetroxide and 0.8 % (w/v) potassium ferricyanide solution in 0.1 M phosphate buffer (pH 7.4) for 3 h at 4°C, and the samples were then washed five times for 15 min with 0.1 M phosphate buffer (pH 7.4). Dehydration was carried out passing the specimens through an acetone series (50 % (v/v), 1 x 10 min; 70 % (v/v), 2 x 10 min; 90 % (v/v), 3 x 10 min; 96 % (v/v), 3 x 10 min, and 100 % (v/v), 3 x 15 min) at 4°C. Specimens were then infiltrated in Spurr epoxy resin, in a series 1:3, 2:2, 3:1 resin:acetone (v/v), for 3 h each, and 100 % (v/v) resin o/n at 4°C. The specimens were then transferred into Beem capsules (SPI Supplies) filled with freshly prepared Spurr resin, and allowed to polymerize at 60°C for 48 h. Thin sections showing silver interferences were obtained using a Ultracut E ultramicrotome (Leica) and were mounted on Formvar-coated 200 mesh gold grids (Sigma). The sections were stained for 10 min at Rt with an aqueous 2 % (w/v) uranyl acetate solution, washed with ddH_2O and air-dried. They were analyzed with a EM 400 transmission electron microscope (Philips) running at 80 kV by Elsa Arcalis from the RWTH, Aachen, Germany.

0.1 M Phosphate buffer, pH 7.4	19 % (v/v) 200 mM NaH_2PO_4 81 % (v/v) 9.9 mM Na_2HPO_4
Spurr resin	12 % (w/v) DER. 736 Resin 0.8 % (w/v) DMAE 49 % (w/v) NSA 20 % (w/v) VCD

II.2.5.2 Specimen processing for immunolocalization

Tobacco leaves were cut into small squares of around 1 mm^2 with a razor blade and fixed o/n at 4°C in fixative solution (4 % (w/v) paraformaldehyde, 0.2 % (v/v) glutaraldehyde in 0.1 M phosphate buffer, pH 7.4). Specimens were then washed five times for 15 min with 0.1 M phosphate buffer (pH 7.4) at 4°C. Dehydration was carried out first by immersing the specimens in a 50 % (v/v) ethanol solution at 4°C for 30 min, then passing the specimens through an ethanol series (70 % (v/v), 96 % (v/v) and 100 % (v/v), for 30 min each) at -20°C. Specimens were then infiltrated in LR White Resin (London Resin Company), containing 0.5 % (w/v) benzoin methyl ether, in a series 1:3, 2:2, 3:1 resin:ethanol (v/v), for 1 h each, and 100 % (v/v) resin o/n at -20°C. The specimens were then transferred into Beem capsules (SPI Supplies) filled with freshly prepared LR White resin, and allowed to polymerize under UV light at -20°C for 24 h in an automatic freeze substitution unit (Leica). Then, thin sections showing silver interferences were obtained using a Ultracut E ultramicrotome (Leica) and were mounted on Formvar-coated 200 mesh gold grids (Sigma).

II.2.5.3 Immunogold labeling

For immunogold labeling, grids carrying ultra thin sections of LRW-embedded specimens (II.2.5.2) were floated on drops of 6 % (w/v) BSA in phosphate buffer (0.1 M, pH 7.4) for 20 min at Rt. The sections were incubated o/n at 4°C with either a goat anti-vIL-10 (1:100 in 0.1 M phosphate buffer; R&D Systems) or a rabbit anti-mIL-10 (1:300 in 0.05 % (v/v) Tween 20, 0.1 M phosphate buffer; Acris) antibody, both pre-adsorbed 1:10 in wt extract. After washing wit 0.1 M phosphate buffer supplemented with 0.5 % Tween 20 (v/v), the sections were incubated with the secondary antibody conjugated to 10-nm gold particles (Molecular Probes) diluted 1:30 in phosphate buffer and incubated at Rt for 1 h. The grids were then washed with phosphate buffer and water, air-dried and stained with an aqueous 2 % (w/v) uranyl acetate solution at Rt for 10 min. Electron microscopy was carried out on a EM 400 transmission electron microscope (Philips) running at 80 kV, and was performed by Elsa Arcalis from the RWTH, Aachen, Germany.

II.2.6 Biological activity assays

II.2.6.1 Maintenance of the mouse macrophage cell line

The mouse macrophage cell line J774 was maintained in Dulbecco's modified Eagle's medium (DMEM) (Bio-Whittaker) supplemented with 5 % (w/v) low endotoxin fetal bovine serum (FBS) (Biochrom Seromed), at 37°C in atmosphere containing 5% (v/v) CO_2, and passaged twice weekly.

II.2.6.2 STAT3 phosphorylation assay

J774 cells were seeded at a density of ~ 8 x 10^5 cells/well in a 24-well tissue culture plate and then stimulated with either commercial murine IL-10 (BD Pharmingen) or viral IL-10 (R&D Systems), increasing doses of plant purified murine or viral IL-10, or purified extract from wt leaves as negative control. After 20 min incubation, the cells were immediately blocked with ice-cold PBS, then proteins extracted (II.2.4.3) and quantified (II.2.4.4). For tyrosine-phosphorylated and total STAT3 detection, 40 µg of protein extracts were separated on a 7.5 % (w/v) gel by SDS-PAGE (II.2.4.5), and two color immunoblots were performed with rabbit anti-phospho-STAT3 (Tyr705) and mouse anti-STAT3 124H6 antibodies (Cell Signaling), respectively, both diluted 1:1000. Detection was simultaneously carried out with Alexa Fluor®680 goat anti-rabbit (1:5000, Invitrogen) and IRDye™800-conjugated goat anti-mouse (1:2500, Rockland) secondary antibodies. Blotted proteins were detected and quantified using the Odyssey infrared imaging system (LI-COR Biosciences) and software provided by the manufacturer.

II.2.6.3 LPS-induced TNFα inhibition assay

J774 cells were seeded at a density of ~ 4 x 10^5 cells/well in a 48-well tissue culture plate and stimulated with 100 ng/ml ultrapure *E. coli* LPS (0111:B4 strain, InvivoGen) for 18 h in presence or absence of either commercial or plant produced murine or viral IL-10. Cells were then spun down by centrifugation, and determination of TNFα levels in cell-free supernatants was performed using a commercial ELISA kit (DY410; R&D Systems), according to the manufacturer's instructions.

II.2.6.4 Analysis of SOCS3 expression

J774 cells were seeded at a density of ~ 4 x 10^5 cells/well in a 48-well tissue culture plate and stimulated with 100 ng/ml LPS for 18 h in presence or absence of either commercial or

plant produced murine or viral IL-10. For *SOCS3* gene expression analysis, total RNA was extracted (II.2.1.15), reverse transcription was carried out and real time RT-PCR was performed in triplicate from 10 ng cDNA for each sample (II.2.1.16). For determination of SOCS3 protein amounts, proteins were extracted from the cells (II.2.4.3) and quantified (II.2.4.4), and 50 µg of total protein extracts were separated on a 7.5 % (w/v) gel by SDS-PAGE (II.2.4.5). Two color immunoblots were performed with rabbit anti-NH_2 terminus SOCS3 (1:150, IBL) and mouse anti-GAPDH antibodies (1:4000, Ambion). Detection was simultaneously carried out with Alexa Fluor®680 goat anti-rabbit (1:5000, Invitrogen) and IRDye™800-conjugated goat anti-mouse (1:2500, Rockland) secondary antibodies. Blotted proteins were detected and quantified using the Odyssey infrared imaging system (LI-COR Biosciences) and software provided by the manufacturer.

II.2.7 Simulated gastrointestinal digestion

The stability of plant-produced murine and viral IL-10, either embedded in the lyophilized tobacco tissue or purified from tobacco leaves (II.2.4.13), was compared, along with the commercial counterparts, in *in vitro* gastrointestinal simulation conditions. The experiments were conducted over a range of time points (0 s, 15 s, 30 s, 1 min, 5 min, 15 min, 30 min, 1 h) at 37°C. Purified IL-10 was digested in either simulated gastric fluid (SGF) or simulated intestinal fluid (SIF) at a concentration of 1 ng/ml. At each time point, 10-ng aliquots were taken and the digestion reaction was stopped by either adding Na_2CO_3 to a final concentration of 45 mM, for the SGF, or EDTA to a final concentration of 10 mM, for the SIF. Samples were then analyzed by ELISA (II.2.4.12) for IL-10 quantification.

For the analysis of the protective effect of leaf tissue on murine and viral IL-10, stable transgenic leaves expressing the recombinant protein (II.2.3.1) were snap-frozen in liquid nitrogen, ground with mortar and pestle and freeze-dried as 0.1 g aliquots in 1.5 ml tubes. For each time point, a single aliquot of leaf tissue was incubated with 700 µl of either SGF or SIF, and the reaction quenched at the appropriate time, as described. After digestion, the leaf powder was extracted with 2 volumes of buffer (II.2.4.1) and the IL-10 content in the extract was determined by ELISA (II.2.4.12).

Simulated gastric fluid (SGF)	3.2 g/l Pepsin 2 g/l NaCl pH 1.2
Simulated intestinal fluid (SIF)	10 g/l Pancreatin 7.8 g/l NaH_2PO_4 x H_2O pH 6.8

II.2.8 Statistical analysis

Statistical changes in TNFα production and *SOCS3* mRNA expression levels were determined using the one-way ANOVA with α set to 0.05, according to the Newman-Keuls test.

III RESULTS

III.1 Expression of IL-10 in tobacco chloroplasts

III.1.1 Generation of transplastomic plants

The constructs for chloroplast transformation were generated amplifying the m/vIL-10 mature sequences by PCR (II.2.1.1) using primers designed to introduce a His_6-tag at the C-terminus, and to create *Nde*I and *Xba*I recognition sites at the 5' and 3' ends, respectively (II.1.2.2, Ch_m_f and Ch_m_His_r for the murine, and Ch_v_f and Ch_v_His_r for the viral IL-10). The resulting amplification products were digested with the appropriate restriction enzymes and inserted into the chloroplast expression cassette of the pHK20 plasmid (II.1.2.1), replacing the *nptII* coding region. The correctness of the inserted fragments was confirmed by sequencing, and the expression cassettes containing the m/vIL-10 cDNA were excised digesting the pHK20/IL-10 vectors with *Sac*I and *Hind*III.

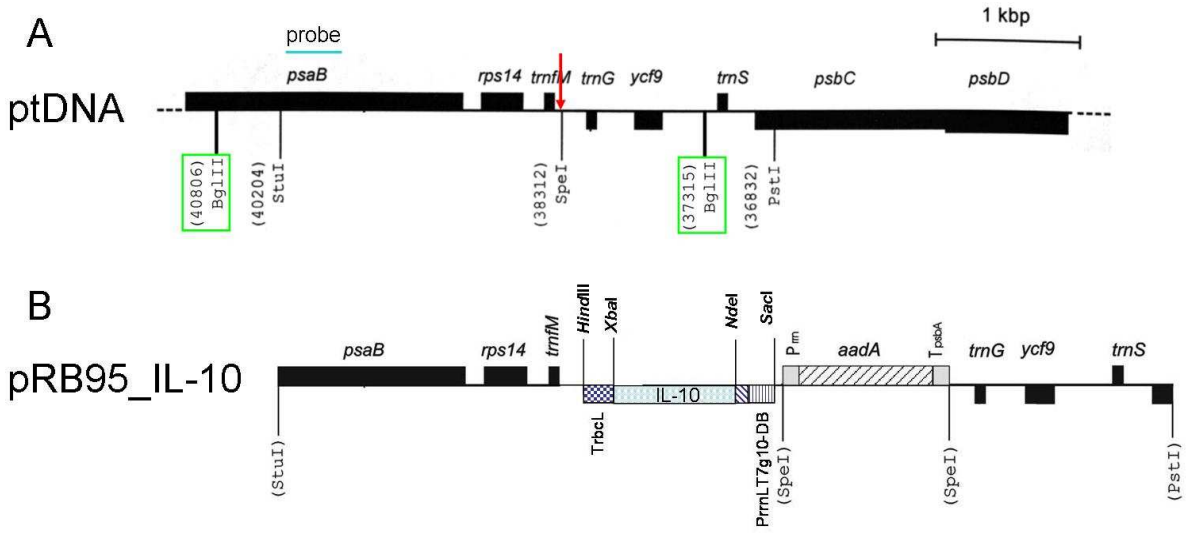

Figure 4: Map of the chloroplast transformation vector and its integration site in the tobacco plastome.

(**A**) Physical map of the chloroplast genome region into which the pRB95 vector (II.1.2.1) integrates by homologous recombination. The transgenes are targeted to the intergenic region between the *trnfM* and *trnG* genes (Ruf et al., 2001). Selected relevant restriction sites are marked. The *Bgl*II restriction sites and the hybridization position of the probe used for RFLP analyses (II.2.1.11) are indicated. (**B**) Structure of the plastid transformation vector pRB95_IL-10. The transgene expression cassette consists of the ribosomal RNA operon promoter fused to the 5' untranslated region (5'UTR) from gene 10 of phage 7 (P*rrn-T7g10*) and the 3'UTR of the plastid *rbcL* gene (T*rbcL*). The selectable marker gene aadA is driven by a chimeric ribosomal RNA operon promoter (P*rrn*) and fused to the 3'UTR from the plastid psbA gene (T*psbA*).

Finally, the inserts were cloned into the similarly digested chloroplast transformation vector pRB95 (II.1.2.1), which allows single copy insertion of the transgene in a defined DNA sequence of the tobacco plastome by homologous recombination (Figure 4), and contains the *aadA* gene as selectable marker, conferring resistance to the aminoglycoside-type antibiotics spectinomycin and streptomycin.

Chloroplast transformation of *N. tabacum* cv. Petit Havana was achieved by biolistic bombardment of young sterile tobacco leaves with plasmid DNA-coated gold particles (II.2.3.2).

III.1.2 Selection of homoplasmic lines

Primary Spec-resistant lines were identified as green calli or regenerating shoots on medium containing the antibiotic. During selection of the plant tissue on spectinomycin-containing medium, however, spontaneous resistance to the antibiotic can arise by specific point mutations in the chloroplast 16S rRNA gene (Svab and Maliga, 1991). To eliminate the spontaneous mutants, the leaf pieces were exposed to double selection on medium containing both spectinomycin and streptomycin (II.2.3.2). The *aadA* gene, if inserted, confers resistance to both aminoglycoside-type antibiotics, while the spontaneous point mutations confer only resistance to spectinomycin (Figure 5A).

For the murine construct, 5 spectinomycin-resistant lines were obtained, only one of which (line #4) survived the double selection test. Line #4 was confirmed to be a true transformant containing the *aadA* and the *mIL-10* genes by PCR analysis (II.2.1.1, PaadA136 and m-int_r primers, not shown). Homoplasmy of this line was assessed by restriction fragment length polymorphism (RFLP) analysis (II.2.1.11) on a few plants derived from the first regeneration round, which gave the expected hybridization pattern and demonstrated that the line was already in homoplasmic state (not shown). Seeds from two of these plants (C and D) were tested by germination on spectinomycin-containing medium (Figure 5B) and the T_1 plantlets were also analyzed by RFLP analysis (Figure 6A), both assays confirming again the homoplasmic state of this transplastomic line.

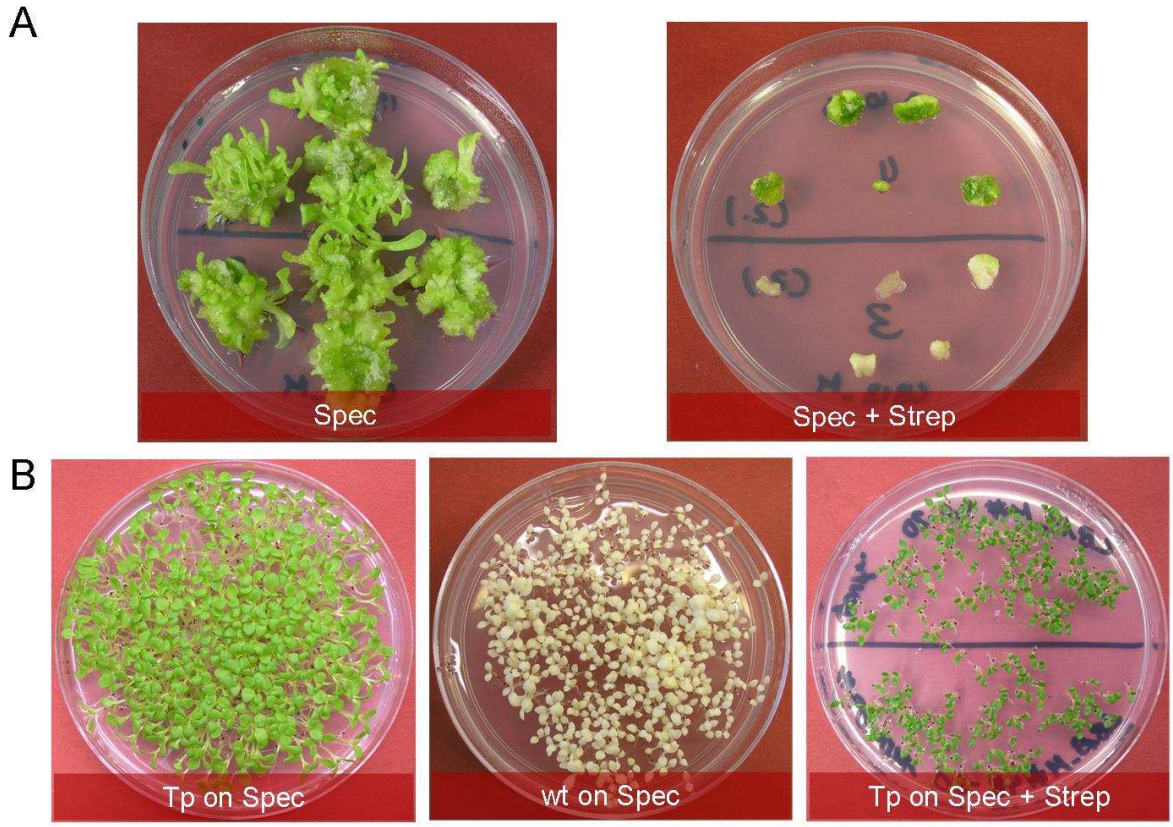

Figure 5: Selection of true transplastomic lines on antibiotic-containing medium.

(**A**): During the regeneration of chloroplast transformants on spectinomycin-containing medium, spontaneous resistance to the antibiotic can occur through acquisition of specific point mutations in the chloroplast 16S rRNA gene. Spontaneous spectinomycin-resistant mutant lines were effectively eliminated by selection on synthetic medium containing both spectinomycin (Spec) and streptomycin (Strep), because the point mutation does not confer resistance to both antibiotics. When exposed to the double-selective medium, leaf pieces from spontaneous Spec-resistant lines bleached out (lower half of the plates), whereas leaf pieces from true chloroplast transformants remained green (upper half of the plates). (**B**): Seeds from transplastomic (Tp) plants were tested for germination on spectinomycin-containing medium to confirm the homoplasmic state. Homoplasmic lines give rise to 100% spectinomycin-resistant progeny (left), while seedlings free of the chloroplast transgene would bleach out like the wt (middle). To ultimately exclude spectinomycin-resistant mutants, some seeds from the same transplastomic batch were also tested by germination on double-selective medium containing spectinomycin and streptomycin (right). The germinated seedlings, although resistant, do not grow nicely due to the high total antibiotic concentration, and are usually discarded afterwards.

For the viral construct, only three spectinomycin-resistant lines could be regenerated after bombardment, and of these, only one (line #2) passed the double selection test and turned out positive for transgene insertion in PCR analysis (II.1.2.2, paadA136 and v-int_r, not shown). Obtainment of vIL-10 homoplasmic transplastomic plants from this line was finally confirmed by RFLP analysis on leaf tissue from plants of both the first and second regeneration rounds (Figure 6B). As often happens when plants are kept long in tissue culture, the transplastomic plants transformed with the vIL-10 construct were male sterile,

and they had to be cross fertilized with wt pollen. However, this is not a problem in the case of transplastomic plants, due to uniparentally maternal plastid inheritance, which should ensure transmission of the transgene to the whole progeny. In fact, as expected, all the seeds germinated on spectinomycin-containing medium were resistant to the antibiotics (Figure 5), confirming both homoplasmy of the parental line and lack of pollen transmission of chloroplast transgenes. Molecular analysis of the T_1 generation plantlets ultimately confirmed that they were homoplasmic, as no hybridization signal with the wt plastome was detected for all the transplastomic plants analyzed (Figure 6B).

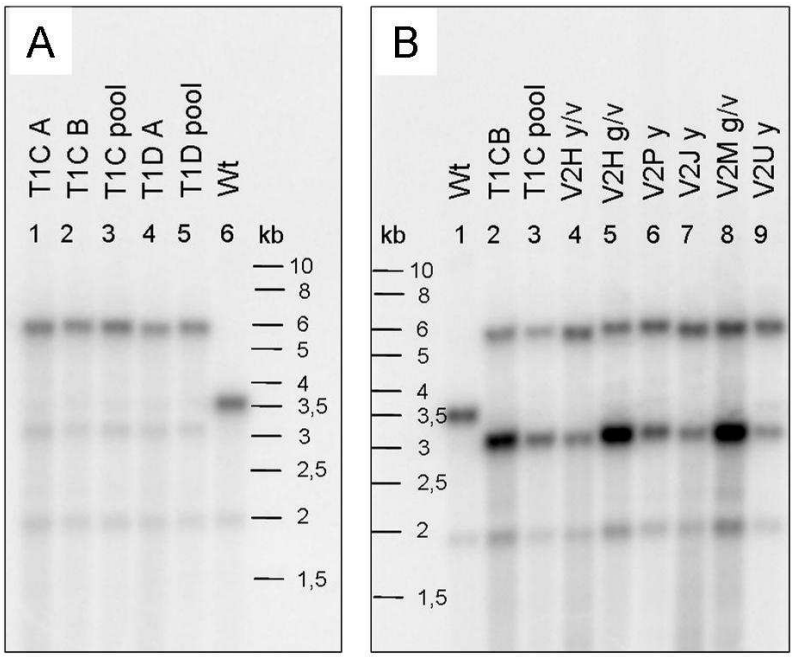

Figure 6: RFLP analysis assessing homoplasmy of transplastomic plants.

DNAs were digested with *Bgl*II and probed with a radiolabeled *psaB* fragment (II.2.1.11). Digestion with *Bgl*II produces fragments of approximately 3.5 kb in the wild type and approximately 6 kb in both murine and viral IL-10 transplastomic lines (see Figure 4). In all samples, the probe detects also a faint band at approximately 2 kb which comes from promiscuous DNA in the nucleus (Ruf et al., 2000; Wurbs et al., 2007). In all transplastomic lines, but not in the wild type, the probe detects a more or less intense band at approximately 3 kb, which most likely reflects recombination events involving the terminator region of the transgene (III.1.4.3). (**A**): Plants transformed with the murine IL-10 construct. The T_1 generation of two plants (C and D), which are derived form the same primary transformant (line #4), was analyzed individually and pooled. (**B**): plants transformed with the viral IL-10 construct. All plants derive from the same and only primary transformant obtained after particle bombardment (line #2). Representative plants from the T_1 (lanes 2 and 3) and T_0 generation (the rest), from the first (lanes 4, 5, 7) and the second regeneration round (lanes 6, 8, 9), from the soil (lanes 3-8) and the *in vitro* culture (lane 9) were analyzed. 'y' indicates a yellow plant, 'y/v' indicates a yellow sector from a variegated plant and 'g/v' a green sector from a variegated plant.

III.1.3 Phenotype of transplastomic lines

Regeneration of transplastomic plants after chloroplast transformation with the vector encoding the viral IL-10 was extremely difficult and time consuming, as the calli kept growing on the selective plates without generating shoots for months. Eventually, one slowly-growing pale-green transplastomic plant was obtained (Figure 7A) and was then subjected to an additional round of selection and regeneration giving rise to several clones. These plantlets also showed variable phenotypes and a slow growth rate, both in tissue culture and in soil. Most of the plantlets regenerated were yellow in the beginning, and developed later on green sectors that conferred a variegated phenotype to the leaves (Figure 7B). Some completely green plants were also obtained from the second regeneration round (Figure 7C), and had a normal development.

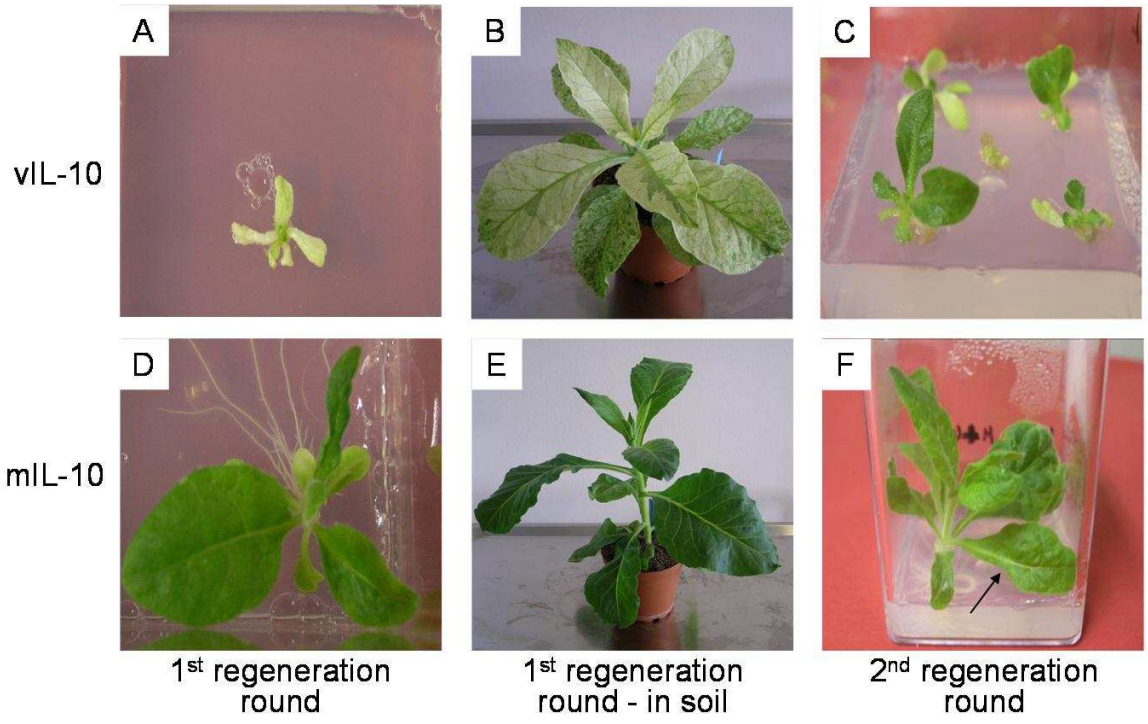

Figure 7: Phenotype of transplastomic plants.

Panels **A**, **B** and **C** show plants transformed with the construct for viral IL-10, while panels **D**, **E** and **F** represent transplastomic plants for the murine IL-10.

In transformants obtained with the construct encoding the murine IL-10, no obvious phenotype was observed in plants from the first regeneration round, neither in sterile culture

nor in soil (Figure 7D and E). However, from the second regeneration round, some plantlets showed slightly deformed and curled leaves (Figure 7F, indicated by the arrow).

For both constructs, all plants grown in the greenhouse flowered and, although most of them were male sterile and had to be hand-pollinated with wild-type pollen, produced viable seeds.

III.1.4 Characterization of homoplasmic plants

III.1.4.1 Immunoblot analysis

As the aim of this study was to obtain high accumulation levels of the recombinant cytokines in tobacco leaves, gene expression in the transplastomic plants was directly investigated at the protein level. It has already been reported that transplastomic plants accumulating extremely high amounts of recombinant proteins can have a mutant phenotype, as the result of the exhaustion of the gene expression capacity of the chloroplast by overuse of its ribosomes for the production of the recombinant protein (Oey et al., 2008). Considering this, the impaired growth and yellow phenotype of the vIL-10 transplastomic plants could foreshadow extremely high accumulation of the recombinant protein, at least of the viral version of the interleukin. Immunoblot analysis was performed on leaf extracts from (i) different transplastomic plants of both the T_0 and T_1 generations, (ii) tissue culture and greenhouse-grown plants and (iii) young and older leaves, to assess dependency of protein accumulation on leaf age (Birch-Machin et al., 2004; Zhou et al., 2008) (II.2.4.1, II.2.4.10).

Quite disappointingly, only a very faint band corresponding to the viral IL-10 was detectable only in the soluble extracts from plants or parts of leaves with a yellow phenotype (Figure 8). Even more surprisingly, no detection of a band corresponding to murine IL-10 was possible in any of the plant extracts analyzed (data not shown). IL-10 accumulation levels in the raw plant extract were then assessed by ELISA, and amounts up to 0.02 μg/ g FLW for the murine and 0.44 μg /g FLW for the viral IL-10, respectively, were determined.

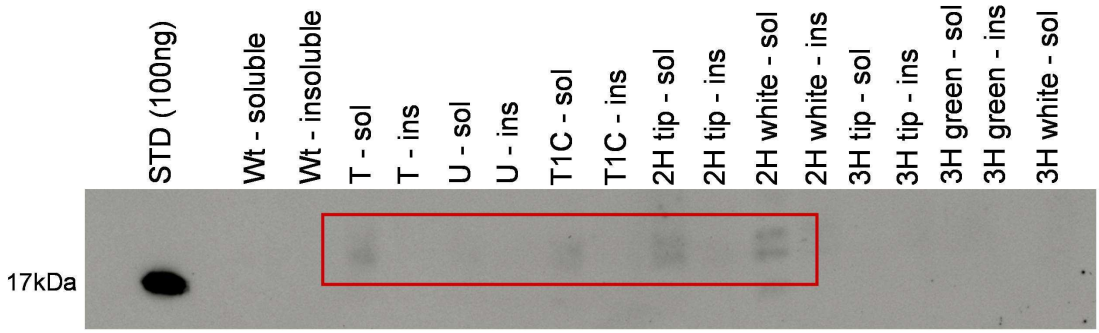

Figure 8: Immunodetection of viral IL-10 in leaf extracts of transplastomic plants.

40 µg of extracted total soluble proteins (II.2.4.1) or the equivalent amount of insoluble protein fractions were separated on a 15% (w/v) gel by SDS-PAGE (II.2.4.5), blotted to a PVDF membrane, and incubated with a monoclonal vIL-10-specific antibody (II.1.3). As control, a wild-type sample was included and as standard (STD), commercial recombinant vIL-10 was used. A faint signal was detectable in the soluble fraction of only a few samples (highlighted by the red box), which correspond to plants or part of leaves with a severe bleached phenotype. Note that the slightly higher molecular weight (approximately 18 kDa) of the plant-produced IL-10 compared to the standard is probably due to the presence of the 6xHis tag, and that a double band has been previously observed for both the commercial and the plant-produced IL-10 in immunoblots (III.4.1).

III.1.4.2 Northern blot analysis

Since for both viral and murine IL-10 transplastomic lines, extremely low to null recombinant protein levels could be detected by immunoblot (III.1.4.1), examination of transgene expression at the transcript level became necessary to unravel the causes of this unexpected result. Total RNA was extracted (II.2.1.12) from a few representative plants for each construct, and Northern blot analysis was performed (II.2.1.14) with transgene-specific probes in order to determine the presence of the viral and murine IL-10 transcript, respectively. For both transgenes, the presence of the transcript in the transplastomic lines was confirmed. Viral IL-10 mRNA accumulation was low in green sectors of somatically segregating plants (Figure 9A, sample ‘H green’) and undetectable in the green transplastomic plant analyzed (Figure 9A, ‘plant F’), although a very faint band could be detected upon overexposure of the blot (not shown). Interestingly, the tissues accumulating the highest levels of vIL-10 transcript coincided with those, in which at least a little bit of recombinant protein could be detected by immunoblot (Figure 8, sample ‘2H’). Nevertheless, the Northern blot analysis revealed the presence of stable mRNA of both transgenes and therefore does not explain the overall lack of accumulation of IL-10 protein.

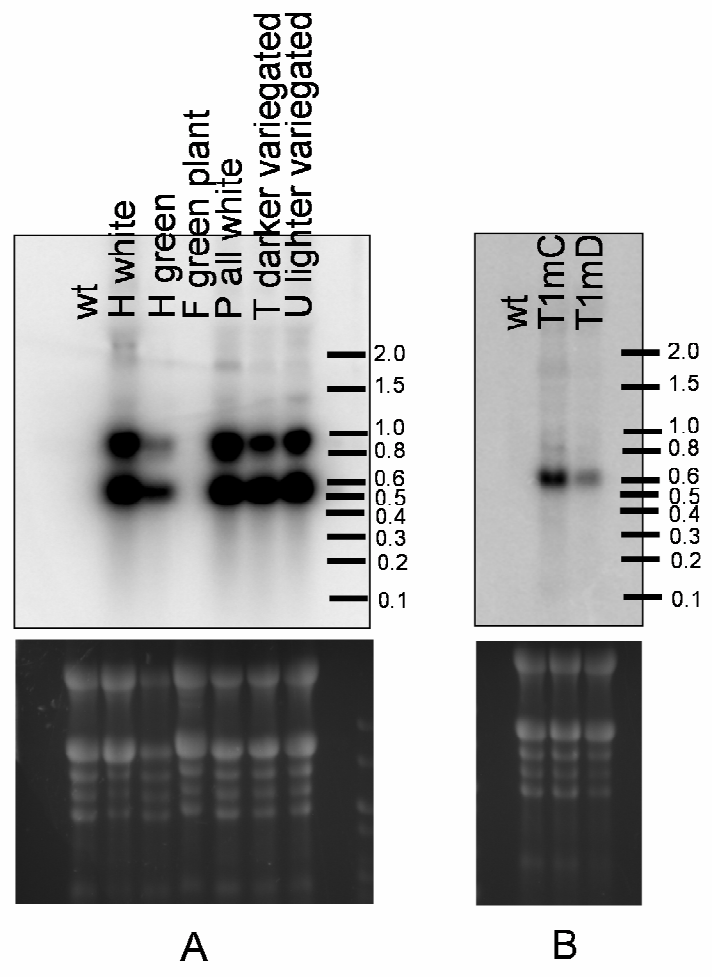

Figure 9: Northern blot analysis of transplastomic plants.

Ten µg of total RNA extracted from leaves (II.2.1.12) were loaded for each sample, and a radiolabeled PCR product specific for either the viral or the murine IL-10 transgene was used as probe (II.2.1.14). (**A**) Detection of the viral IL-10 transcript. Capital letters denote different plants. The phenotype of the analyzed material is also indicated. Note that the band at approximately 0.6 kb corresponds to the vIL-10 transcript, while the band at around 1 kb most likely represents a transcriptional read-through product (Zhou et al., 2007). (**B**) Detection of the murine IL-10 transcript in two T_1 generation plants. The band at approximately 0.6 kb corresponds to the mIL-10 mRNA. To confirm RNA integrity and equal loading, the ethidium bromide-stained agarose gel is also shown below each panel.

III.1.4.3 Investigation of recombination events in the transgene expression cassettes

The almost complete absence of recombinant protein from the transplastomic plants despite insertion of the transgene (III.1.2) and accumulation of the transcript (III.1.4.2), together with the fact that the pale phenotype observed for the transplastomic plants transformed with the viral IL-10 sequence showed somatic segregation (i.e. sectorial variegation, Figure 7B), prompted us to investigate in more detail the region of transgene integration in the chloroplast genome of these plants.

Somatic segregation is one of the hallmarks of cytoplasmic inheritance and usually indicates heteroplasmy of the plastid genome. Interestingly, green sectors and yellow sectors showed no presence of the wild type genome in RFLP analyses (Figure 6B), indicating that both green and yellow tissues were homoplasmic for the transgenes. However, the presence in the RFLP pattern of an unexpected band of molecular size smaller than the wt, suggested that some rearrangements had taken place within the plastid genome. Intriguingly, the intensity of this additional band was found to be much higher in the green sectors compared to the yellow ones in the plants transformed with the viral construct (Figure 6B, plant '2H'), but was uniformly much weaker across the green-looking plants transplastomic for the murine IL-10 sequence (Figure 6A). Molecular analysis of the plants transformed with either the viral or the murine IL-10 performed by PCR (not shown), indicated that for both lines homologous recombination between the Rubisco large subunit gene terminator region (TrbcL) used as 3'UTR of the transgene in the expression cassette and the endogenous copy of the terminator region present on the plastid genome had taken place. This recombination event had already been observed in transplastomic plants transformed with the same vector backbone (F. Zhou, Max Planck Institute, Golm, Germany, personal communication) and results in the excision of a circular DNA fragment which can be detected by amplification with outwardly oriented primers (Figure 10). This plastome rearrangement accounts for the unexpected band observed in the RFLP pattern of all transplastomic plants. Nevertheless, this recombination event should not affect transcription or translation of the transgene, and therefore does not explain the almost complete absence of recombinant IL-10 from the transplastomic plants.

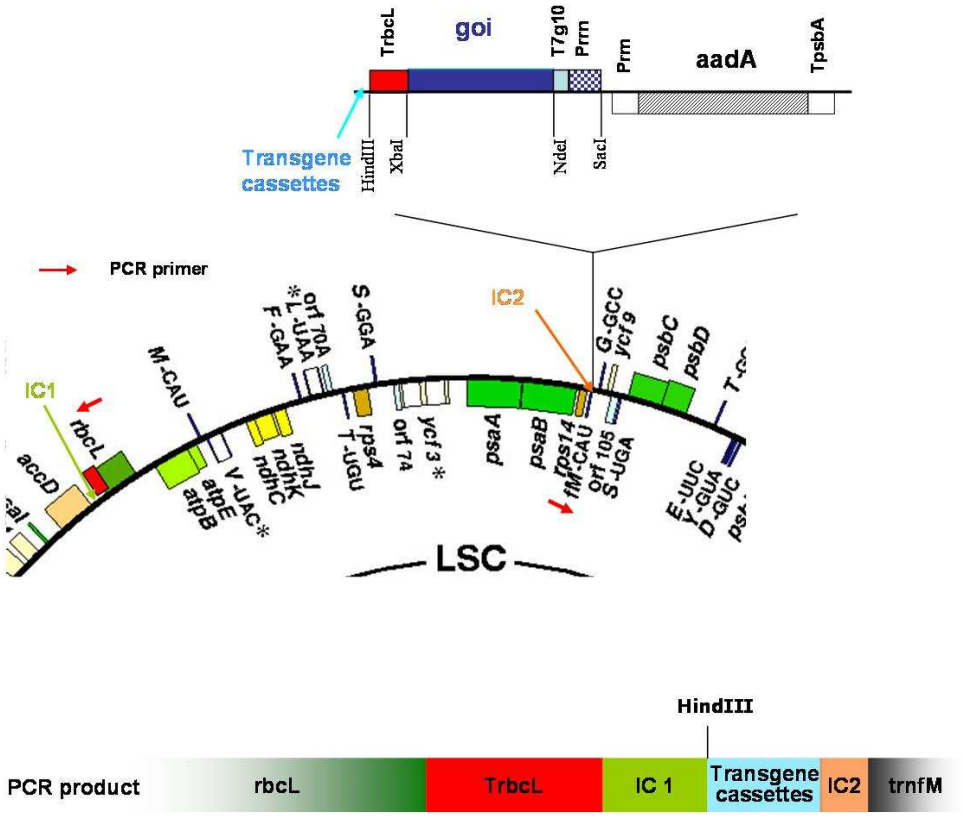

Figure 10: Detection of homologous recombination events between the TrbcL terminator regions of the transgene and the endogenous rbcL gene on the plastome.

A schematic representation of the transformation vector region that integrates into the tobacco plastome is shown, together with the position of insertion into the chloroplast genome (orange arrow). The terminator of the Rubisco large subunit gene (TrbcL) that undergoes homologous recombination is indicated by a red box on both the vector and the plastome, and the position of the endogenous copy present on the chloroplast genome is indicated by a green arrow. The annealing position of the primers oriented in opposite directions and used to detect the circular DNA molecule that is excised upon recombination of the TrbcL copies is indicated by red arrows. A schematic representation of the resulting PCR product is also given (courtesy of F. Zhou).

Therefore, the promoter and 5'UTR regions of the IL-10 transgenes in the transplastomic plants were examined. In the pRB95 chloroplast transformation vector, the *aadA* and the transgene are transcribed from divergent rRNA operon-derived promoters. The promoter driving the *aadA* had suffered a deletion of its 5' portion already in *E. coli*, presumably by microhomology-mediated illegitimate recombination at a directly repeated pentanucleotide sequence (CGAGC), resulting in a weaker 46-nucleotide shorter promoter version (Zhou et al., 2008). After introduction into the plastid genome, homologous recombination between the full-length *Prrn* promoter upstream of IL-10 (*Prrn-long* in Figure 11) and the shortened version (*Prrn-short* in Figure 11) can result in reciprocal exchange of the two promoter

versions by ‘flip-flop recombination’ (Rogalski et al., 2006) producing two isoforms of the plastid genome: one with the shorter P*rrn* version placed in front of *aadA* and the full-length version in front of the transgene, and the other with the shorter P*rrn* version in front of the transgene and the full-length version in front of *aadA* (Figure 11). This recombination event has already been described for expression of the recombinant protein Nef, whose accumulation to high levels in tobacco chloroplast caused a mutant phenotype almost identical to the variegated one observed for the viral IL-10 (Zhou et al., 2008). Surprisingly, sequencing of the promoter regions of *aadA* and the IL-10 transgene (amplified by PCR from total DNA isolated from one representative transplastomic plant each), revealed that rearrangements other than those already described for the *nef* transgene had occurred. In the case of the plant expressing the murine IL-10, the original sequence of the vector used for transformation could not be detected, and two different rearrangements had occurred (Figure 11). In one of these rearrangements, the flip-flop recombination had involved the two *Prrn* versions and the region in between, which was inverted compared to the original vector. In the other one, inversion of the intergenic sequence had also occurred along with exchange of the promoters, but additionally a portion of the 5’ sequence of the *aadA* gene had been duplicated and now replaced the T7 phage gene 10 translation control region (G10 in Figure 11) and part of the IL-10 sequence. The plant transformed with the construct for viral IL-10 expression, instead, harbored the initial conformation (*Prrn-long* driving IL-10, *Prrn-short* driving *aadA*) and a second conformation, in which the G10 sequence and the first 53 nucleotides of the murine IL-10 ORF had been replaced by part of the *Prrn-short* promoter and the *aadA* coding sequence.

These results indicate that, for both transgenes, recombination products that condition low IL-10 accumulation seem to be favoured over the original configuration, and that transcription of the viral IL-10 transgene from the stronger *Prrn-long* promoter probably accounts for detectability of viral IL-10 protein that, even though accumulating at extremely low levels, causes a severe pigment-deficient phenotype.

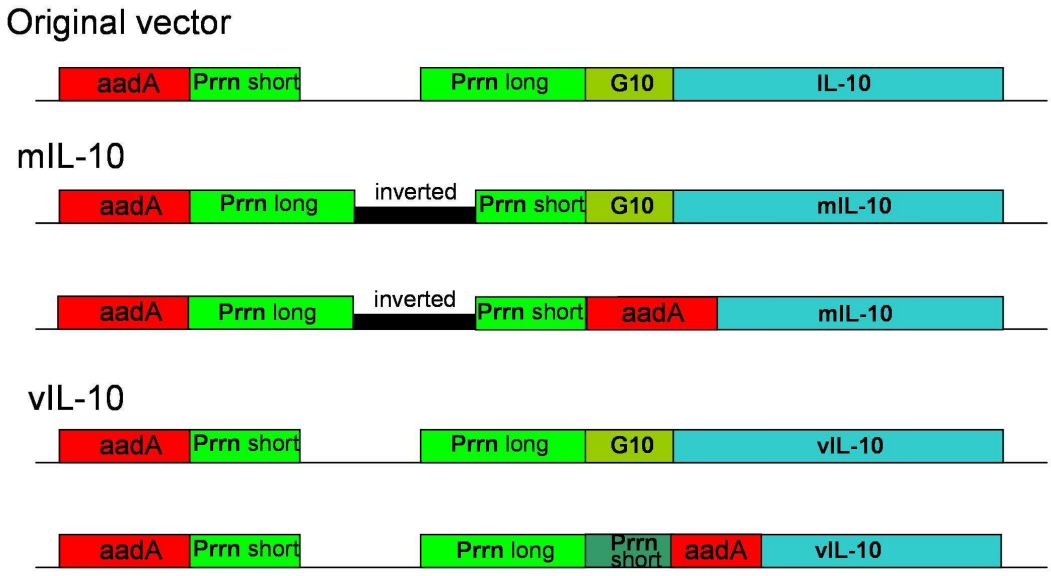

Figure 11: Recombination events in the promoter regions of the two transgene cassettes.

For both transgenes, the promoter region was amplified by PCR (II.2.1.1) from DNA extracted from one representative plant each (II.2.1.10), and the resulting fragment was sequenced. In both cases, a partial double sequence was obtained, and the two overlapping nucleotide sequences were determined by manually dissecting the chromatograms. The figure shows a schematic overview of the rearrangements identified. Note that, where a duplication of part of the *aadA* gene has occurred in front of the transgenes, the first 53 and 40 nucleotides are missing from the murine and viral IL-10 reading frames, respectively. *aadA*: aminoglycoside adenylyltransferase gene; Prrn short: short version of the rRNA promoter; Prrn long: long version of the rRNA promoter; G10: T7 phage gene 10 translation control region. Not drawn to scale.

III.1.4.4 Analysis of the total soluble protein pattern

Analysis of the total soluble proteins extracted from two representative transplastomic plants per construct, assayed by SDS-PAGE (II.2.4.6) and Coomassie Brilliant Blue staining (II.2.4.7), revealed reduced levels of the RuBisCo large subunit in those plants that were transformed with the construct for the viral IL-10 and displayed the yellow phenotype (Figure 12). In contrast, there was no appreciable difference between the TSP patterns of wild type plants and plants transformed with the construct for murine IL-10 (data not shown).

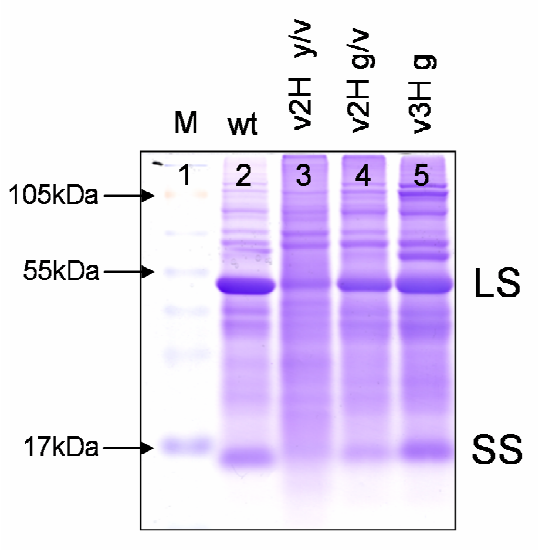

Figure 12: Analysis of the total soluble protein patterns of vIL-10 transplastomic plants.

Total soluble proteins (TSP) were extracted from either transplastomic or wild type leaf material (II.2.4.1). Samples of 30 µg TSP were separated on a 10% (w/v) Tris-Tricine gel by SDS-PAGE (II.2.4.6), and the gel was stained with the Coomassie Brilliant Blue dye (II.2.4.7). Lane 1: molecular weight marker; lane 2: wild type; lanes 3-5: different areas of the same leaf, the phenotype is indicated. Large (LS) and small (SS) subunits of RuBisCo are marked at the right. A clear reduction in LS and consequently SS amounts is observed in the transgenic plants in a manner that correlates with the bleached phenotype. 'y/v' indicates a yellow sector from a variegated plant, 'g/v' a green sector from a variegated plant and 'g' a green plant.

III.2 Nuclear expression of IL-10 in tobacco

III.2.1 Generation of the plant expression constructs for subcellular targeting

Three constructs each were designed for the mIL-10 and vIL-10 cDNAs, targeting the recombinant proteins to three different sub-cellular localizations: (i) the endoplasmic reticulum (ER), achieved by retaining the native N-terminal signal peptide and adding a C-terminal SEKDEL motif for ER retention (Figure 13, ER-m/vIL-10) (Mitoma and Ito, 1992); (ii) the plasma membrane (IL-10 facing the apoplast), achieved using the native signal peptide and adding the C-terminal hinge and transmembrane domain from the human T-cell receptor (Figure 13, Apo-m/vIL-10) (Schillberg et al., 2000); and (iii) the ER membrane (IL-10 facing the cytosol), achieved by deleting the native signal sequence and adding the C-terminal cytochrome *b5* (cyt*b5*) membrane anchor domain (Figure 13, Cyt-m/vIL-10) (Mitoma and Ito, 1992; Schouten et al., 1996; Zhao et al., 2003).

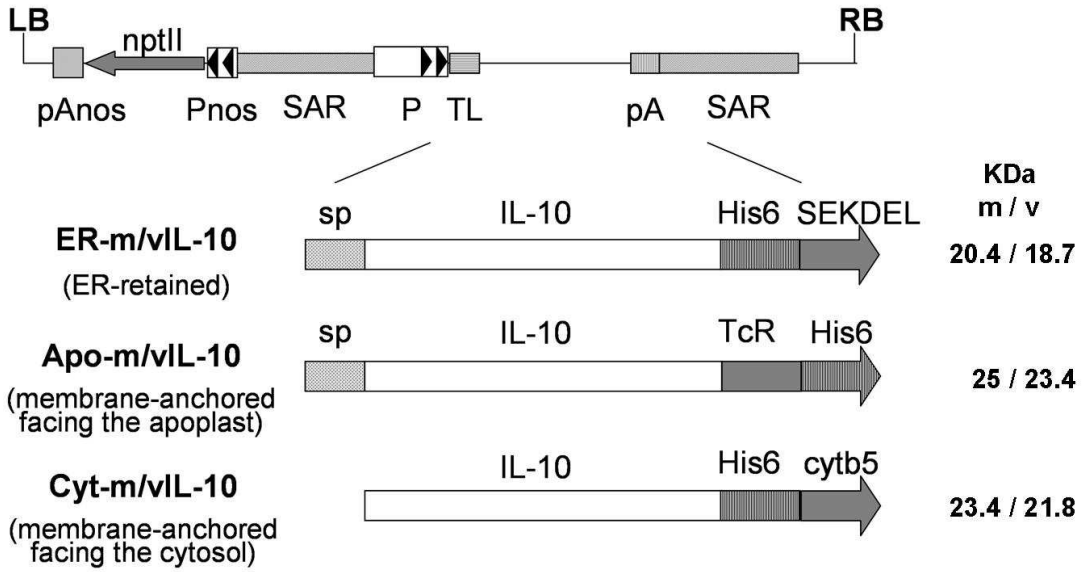

Figure 13: T-DNA region of the pTRAkt plant expression vector and gene cassettes targeting murine and viral IL-10 to different subcellular locations.

LB and RB, left and right border of the T-DNA; Pnos and pAnos, promoter and terminator of the nopaline synthase gene; nptII, coding sequence of the neomycin phosphotransferase gene; SAR, scaffold attachment region; P and pA, 35S promoter with duplicated enhancer and terminator of the cauliflower mosaic virus (CaMV) 35S gene; TL, 5' UTR of the tobacco etch virus (TEV); sp, native N-terminal signal peptide; IL-10, mature IL-10 sequence; His_6, histidine tag; SEKDEL, ER retention signal; TcR, C-terminal hinge and transmembrane domain of the human T-cell receptor; cytb5, transmembrane domain of the rat cytochrome-b5. On the right of each construct, the predicted molecular weight for the corresponding mature polypeptide is given. Not drawn to scale.

These constructs, all bearing a His_6-tag at the C-terminus to facilitate protein purification, were generated by subsequent PCR reactions (II.2.1.1) using up to three overlapping primer pairs (Table 2), designed to fuse the different localization sequences at the 5' of the transgene and to introduce the sequences for the appropriate restriction enzymes at the 3' and 5' ends (in case of the Cyt-vIL-10 construct it was necessary to fuse the TEV 5' UTR region (II.1.2.1) up to the *Xmn*I site directly to the IL-10 mature sequence, to avoid insertion of an additional amino acid at the 5' end). Each of the final fragments generated by PCR was gel purified (II.2.1.4), cloned into a pTOPO vector (II.1.2.1), transferred into *E. coli* DH5α competent cells (II.2.2.2) by heat shock (II.2.2.3), and its correctness was confirmed by sequencing. The inserts were then cut out of the pTOPO vector by restriction digest with the appropriate enzymes (II.2.1.5), ligated (II.2.1.7) into the digested and dephosphorylated (II.2.1.6) pTRAkt-gfp plant expression vector (II.1.2.1) and transformed into *E. coli* (II.2.2.3). For each transformation, a positive clone was selected upon plasmid restriction digestion (II.2.1.5), and the correct insertion into the vector was confirmed by sequencing

with primers designed on the vector backbone (pSS5', pSS3', II.1.2.2). All plasmids were transferred into *A. tumefaciens* strain GV3101 by electroporation (II.2.2.6), and glycerol stocks of a recombinant clone (II.2.2.7) were prepared (II.2.2.4).

Table 2: Primer pairs used to generate the different targeting constructs.

The m/v-IL-10 sequences were amplified from the respective plasmid containing the full-length cDNA (II.1.2.1) by PCR, performing up to three subsequent reactions to generate the final targeting constructs. The overlapping primer pairs used (II.1.2.2), designed to directly fuse the localization and His-6 sequences to the 5' end of the IL-10, are listed in the table and referred to each PCR step; the restriction sites introduced for cloning the fragments into the pTRAkt vector (II.1.2.1), are indicated in the right column.

Construct (m/v)	PCR reaction	Primer pair	Cloning enzymes (5'-3')
ER-IL-10	1/1	m/v-SP_f ; m/v-HisKDEL_r	*Nco*I-*Xba*I
Apo-IL-10	1/3	m/v-SP_f ; m/v-TcR_r1	
	2/3	m/v-SP_f ; m/v-TcR_r2	
	3/3	m/v-SP_f ; m/v-TcRHis_r3	*Nco*I-*Xba*I
Cyt-IL-10	1/2	m-cytb5_f ; m-Hiscytb5_r1	
		v-cytb5_f1 ; v-Hiscytb5_r1	
	2/2	m-cytb5_f ; m-cytb5_r2	*Bsp*HI -*Xba*I (mIL-10)
		v-cytb5_f2 ; v-cytb5_r2	*Xmn*I-*Xba*I (vIL-10)

III.2.2 *Agrobacterium*-mediated transient expression

III.2.2.1 Vacuum-infiltration of whole detached leaves

Transient expression in *Nicotiana tabacum* cv. Petit Havana SR1 leaves was carried out at least three and up to 5 times for each construct (III.2.1) by vacuum agroinfiltration of whole detached leaves (II.2.3.3). After 2-3 days of incubation, the infiltrated leaves sometimes appeared wilted, dried out and/or necrotic (not shown). This phenomenon was observed in most of the infiltrations performed, but not always, and the severity of the phenotype also varied between the experiments and, to some extent, between the constructs. However, due to the high variability of the leaf phenotype observed after vacuum agroinfiltration, it was difficult to attribute a specific phenotype to a specific construct.

Analysis of IL-10 accumulation levels in vacuum infiltrated leaves was performed using a sandwich ELISA (II.2.4.12) on the crude leaf extracts (II.2.4.1). Despite the high variation in the overall accumulation levels observed between experiments, the ratio between the

amount of IL-10 detected for each construct was always constant and reproducible within each experiment, and showed that both mIL-10 and vIL-10 accumulated to the highest levels in the ER (up to 10-16 μg/g fresh leaf weight (FLW), Figure 14).

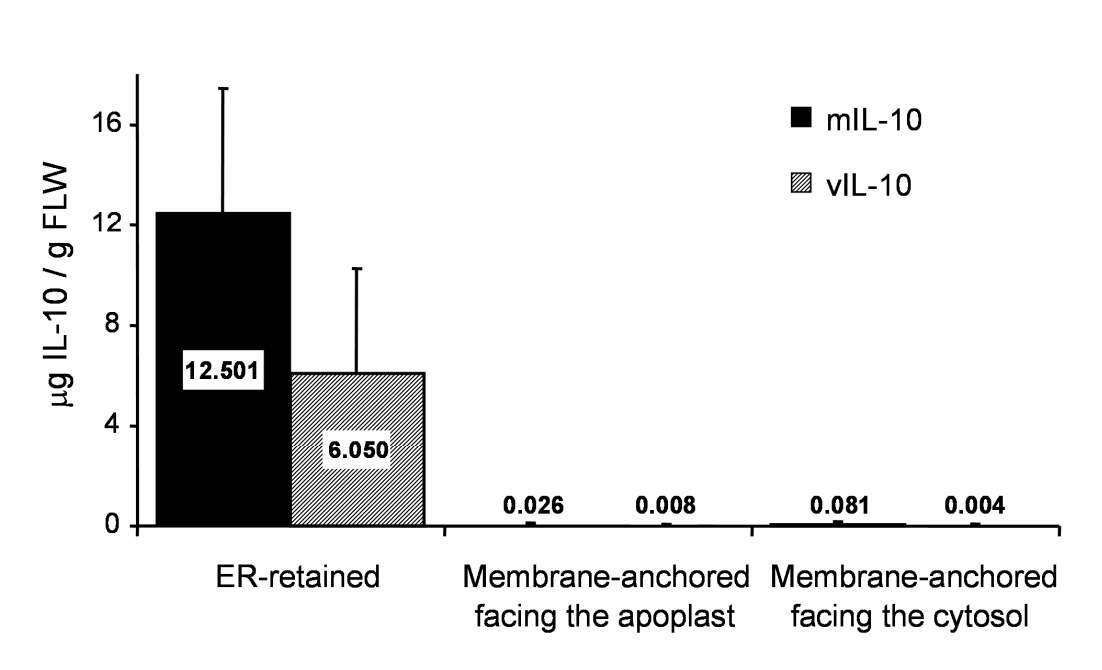

Figure 14: Comparison of IL-10 levels in leaves agroinfiltrated with the different targeting constructs.

N. tabacum cv. Petit Havana SR1 leaves were vacuum-infiltrated (II.2.3.3) with *A. tumefaciens* carrying the different plant expression constructs (III.2.1). For each construct, three to four leaves from different wild type plants were infiltrated; they were incubated on wet filter paper for 3 d, with a 16-h photoperiod at ~20°C. Quantification of IL-10 accumulation levels in the leaf extracts was performed by sandwich ELISA (II.2.4.12). The left and right bars represent the data for the viral and murine IL-10, respectively; the localizations reported on the x-axis refer to the constructs described in Figure 13. The data shown represent the mean ± SD of three independent experiments performed.

Immunoblot analysis of leaf extracts with IL-10-specific monoclonal antibodies (II.1.3) was also performed, to have a preliminary indication of correct processing of the recombinant proteins. The molecular weights of the detected proteins were consistent with those of the mature native polypeptides, taking into account the C-terminal His_6 and C-terminal localization tags (Figure 15), suggesting that they are properly synthesized and processed.

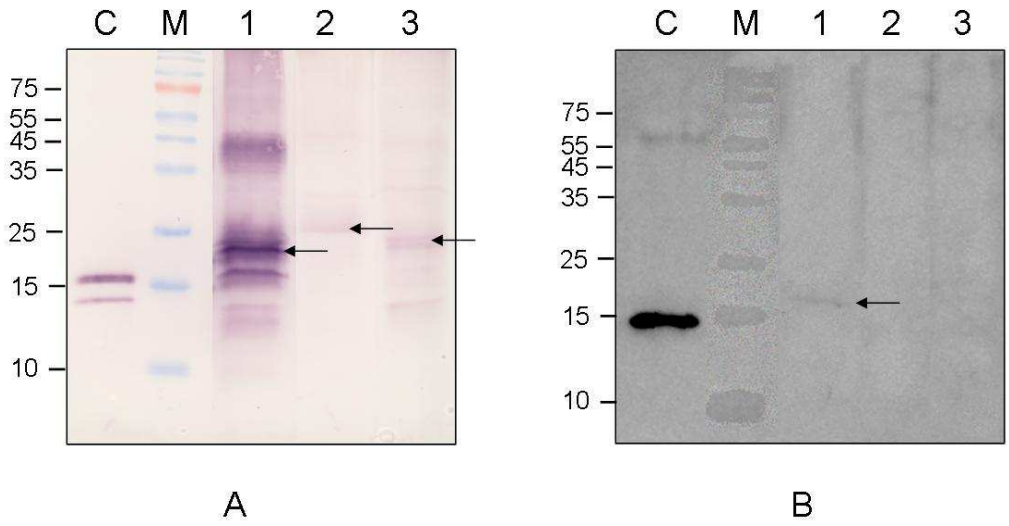

Figure 15: Immunoblot analysis of IL-10 transiently expressed in tobacco leaves by agroinfiltration.

Total soluble proteins were extracted grinding tobacco leaf tissue in two volumes extraction buffer (II.2.4.1), and separated by 17 % (w/v) SDS-PAGE. (**A**): murine IL-10 analysis. 65 µg TSP were blotted onto a nitrocellulose membrane and immuno detection was carried out with a monoclonal anti murine IL-10 (1:2000) followed by 1 h incubation with RAR^{AP} (1:5000) and NBT/BCIP detection at Rt (II.2.4.9). Commercial recombinant murine (20 ng, BD Pharmingen) was used as positive control. (**B**): viral IL-10 analysis. 50 µg TSP were blotted onto a PVDF membrane, immuno detection was carried out with a monoclonal anti viral IL-10 (1:1000) followed by 1 h incubation with RAR^{HRP} (1:5000), and the signal revealed with the ECL Plus Western Blotting Detection kit (GE Healthcare) (II.2.4.10II.2.4.9). Fifty ng of commercial recombinant viral IL-10 (R&D Systems) were used as positive control. C: recombinant IL-10 used as positive control; M: prestained protein marker; 1: extract from leaves infiltrated with the construct for ER-retained IL-10; 2: extract from leaves infiltrated with the construct for apoplastic IL-10; 3: extract from leaves infiltrated with the construct for cytosolic IL-10. Arrows indicate the IL-10 monomer.

III.2.2.2 Agroinjection in intact plants

To exclude that the variability in phenotype of the vacuum agroinfiltrated leaves was somehow influenced by the growth conditions and status of the wt plant/leaf used for infiltration, *in planta* agroinjection was performed with all the constructs on the same leaf in parallel. Additionally, the use of intact plants rather than detached leaves for agroinfiltration, allows to keep the leaf material under observation for longer times and to follow more carefully the evolvement of the eventual necrotic lesions. The experiment was repeated 4 times on two plants each, trying to minimize the position effect as much as possible within every experiment, injecting all constructs in three different leaves of the same plant, and in different sectors of the leaf. The phenotype observed after agroinjection of intact plants was more reproducible than the vacuum infiltration: injection with the constructs encoding the apoplastic versions of both murine and viral IL-10 (Apo-m/v-IL-10)

always caused necrosis and, in all cases, resulted in the fastest and most severe symptoms, when compared to the other constructs of the same IL-10 version (Figure 16A-B).

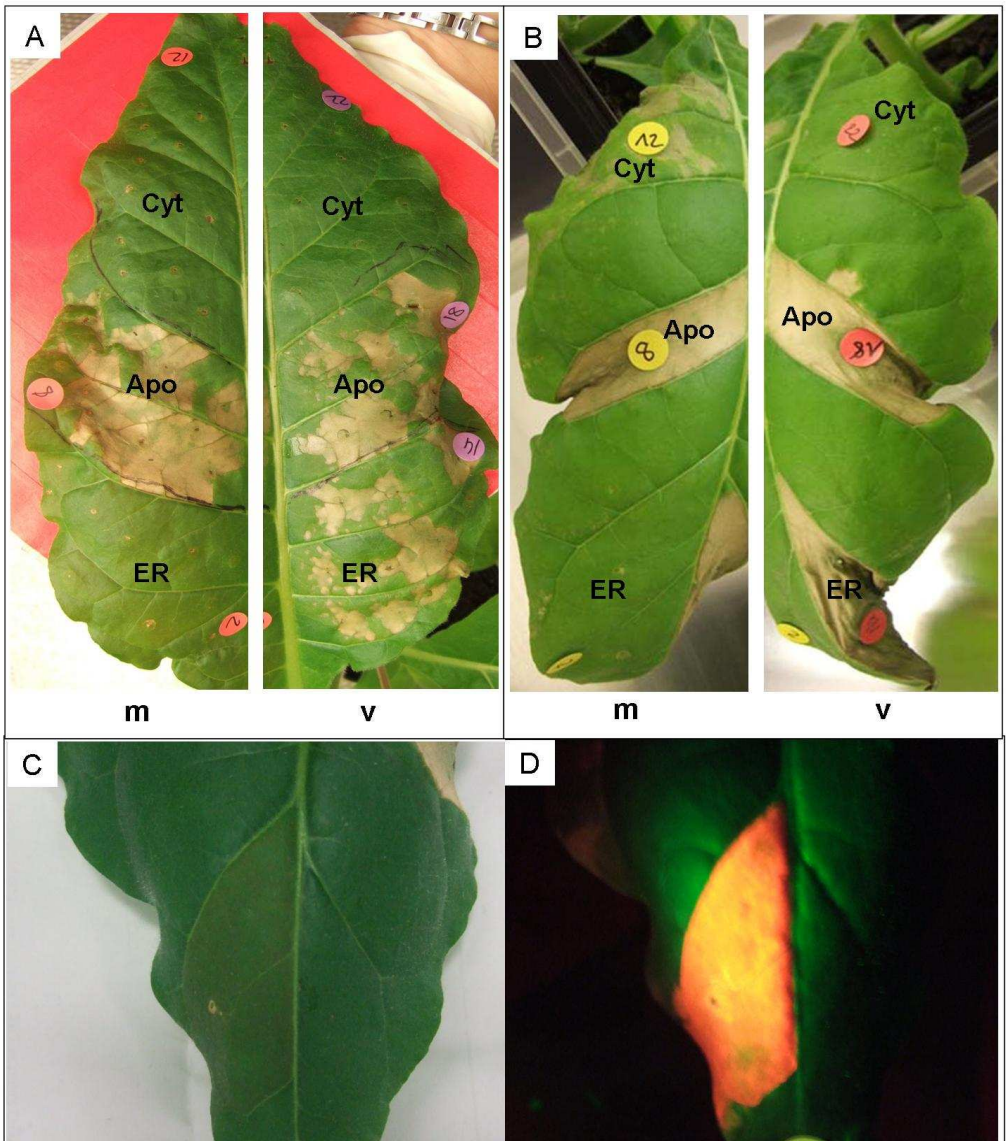

Figure 16: Symptoms caused by *in planta* agroinjection of the different IL-10 targeting constructs.

(**A-B**) Agrobacteria harbouring the pTRAkt vectors encoding the generated versions of murine and viral IL-10 (III.2.1) or the control vector TRAkc-rTPrfp (II.1.2.1) were injected into different sectors of the same leaf of intact *N. tabacum* cv. Petit Havana SR1 plants, and the infiltrated plants were grown at 20-25°C, 16 h photoperiod (7000 lux), for 3-5 days (II.2.3.4). The experiment was repeated 4 times, trying to randomize as much as possible the injection site for every construct. Partial (**A**) or complete (**B**) necrosis of the infiltrated areas developed 2-5 days after injection, in a construct-specific manner, and with the apoplastic version of both murine and viral IL-10 always causing the earliest and most severe symptoms. (**C-D**) Injection of agrobacteria carrying the pTRAkc-rTP-DsRed vector (II.1.2.1) was performed in parallel as negative control (**C**), and accumulation of DsRed (**D**) was visualized with an LCD lamp with glass fiber optic (Leica KL1500), an additional filter for green excitation (BP545/30) and a color foil (No. 182, light red).

Agroinjection of the construct for ER localization of the viral, but not the murine, IL-10 also constantly resulted in partial to complete necrosis of the infiltrated area, while the cytosolic version of murine IL-10 gave rise to necrotic lesions in two of the four experiments performed, and only in correspondence of those leaves that showed the most severe symptoms overall (Figure 16B). A culture of agrobacteria carrying a pTRAkc-rTPrfp plasmid encoding the fluorescent protein DsRed (II.1.2.1) was used both as visual positive control for the agroinfiltration procedure, and as negative control for the onset of the necrotic phenotype, as this construct has been extensively used in the laboratory and was never deleterious to the plants. As expected, the leaf sectors infiltrated with agrobacteria carrying the pTRAkc-rTPrfp plasmid showed DsRed fluorescence and no necrotic lesions (Figure 16C-D).

III.2.3 Stable expression in transgenic tobacco plants

Stable nuclear transformation of *N. tabacum* cv. Petit Havana SR1 was carried out according to the leaf disc method (II.2.3.2) using the most promising ER-m/vIL-10 encoding vectors (pTRAkt_ER-mIL-10 and pTRAkt_ER-vIL-10) that yielded the highest accumulation levels in the transient expression experiments (III.2.2).

III.2.3.1 Phenotype of stable transgenic plants

In vitro regeneration of plantlets from tobacco transformation with the construct encoding the murine IL-10 was straightforward, and also once transferred into soil, plants expressing mIL-10 did not display any mutant phenotype and grew as the wt (not shown).

Differently, transformation of *N. tabacum* Petit Havana SR1 with the construct encoding the ER-retarded version of the viral IL-10 gave rise to many normal looking plantlets, but also to a number of plantlets that appeared very pale in color and had a retarded growth (Figure 17A). Also after transfer into soil, these plants grew slowly, appeared lighter green, showed leaf thickening and more pronounced veining (Figure 17B); in some cases the flowers were impaired, and the plants had to be hand-pollinated because the stamens were shorter than the pistil (Figure 17C); some other plants never produced seeds because the flowers dried out and fell off the plant before opening (Figure 17D), and some very dwarf ones died without even developing flower buds (not shown).

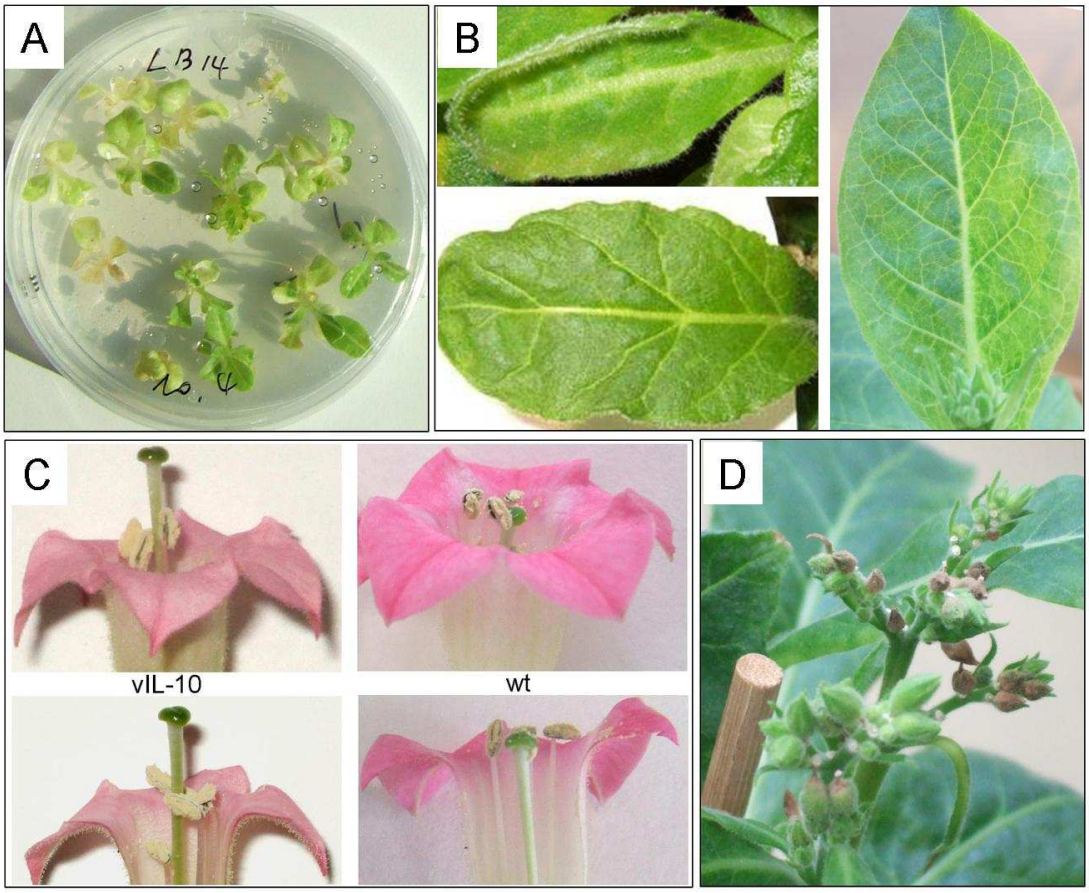

Figure 17: Phenotype of transgenic plants expressing vIL-10.

Transformation of *N. tabacum* cv. Petit Havana SR1 was performed by the leaf disc method (II.2.3.2) using agrobacteria carrying the plasmid encoding the ER-retarded version of viral IL-10 (III.2.1). Regeneration of transgenic plants on selective medium after transformation gave rise to many pale green – almost white – shoots, which had thicker leaves and grew more slowly compared to the green ones (**A**). Once moved from the sterile culture into soil, these shoots developed into slow growing, stunted plants that had more elongated leaves, thicker than wt plants, with unusually pronounced veining and sometimes a dark-light spotted appearance (**B**). Some of these plants developed abnormal flowers (**C**) which having the stamens shorter than the pistil had to be pollinated by hand, but eventually produced viable seeds. Instead, those plants showing the overall strongest phenotype, did not produce seeds because the floral buds dried out and fell off the plant before developing into mature flowers (**D**).

Despite the variety and multiplicity of phenotypic traits observed within the vIL-10 transgenic population (Figure 17), the degree of dwarfism was identified as a good indicator to summarize the overall severity of the symptoms. Interestingly, the pale green, stunted plantlets regenerated *in vitro* - which were initially regarded as unhealthy and discarded from the selection of 40 plants to constitute the starting T_0 population - turned out to be the plants accumulating the highest amounts of vIL-10, when later analyzed for recombinant protein levels by ELISA (II.2.4.12). As a matter of fact, a striking positive correlation was

always found between the vIL10 accumulation levels measured in the leaves and the size/phenotype of the transgenic plants (Figure 18).

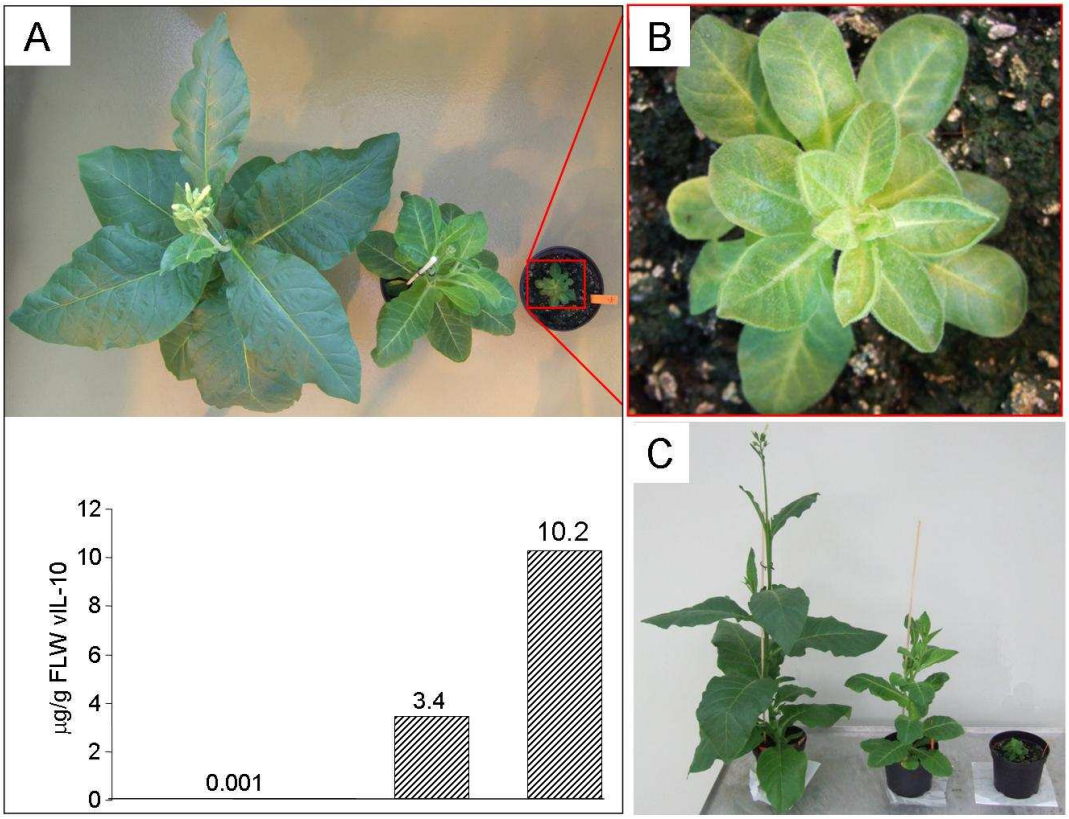

Figure 18: Phenotype of transgenic plants correlates with vIL-10 accumulation levels.

Analysis of vIL-10 accumulation levels in transgenic tobacco plants (II.2.4.12) revealed a strikingly correlation between the stunted phenotype and the amounts of recombinant protein detected in the leaf tissue. In this figure, three T_1 sister plants of the same age and grown under the same conditions, representative of the range of phenotypic alterations observed, are shown, and the corresponding accumulation levels of vIL-10 measured by ELISA in the leaf extract are reported below each plant (**A**). No differences could be detected regarding the appearance or the growth rate of the transgenic plant accumulating vIL-10 to the lowest level and the wt (not shown). (**B**) Enlargement of the dwarf plant in (A), which accumulates vIL-10 at the highest levels and displays the strongest phenotype observed. Note that, besides the stunted appearance, with shorter internodes and smaller leaves, this plant is still in a vegetative state, while the normal-looking sister is already flowering. (**C**) Side view of the same transgenic plants shown in (A), underlining the enormous difference in growth and development between the three expressors.

This same range of phenotypic characteristics, and their same correlation to the vIL-10 accumulation levels displayed by the tissue-culture derived plants, were also observed for the T_1 generation. Therefore, taking into consideration the high number of regenerated shoots displaying the phenotype (at least 20), the facts that also T_1 plants were affected, and the clear correlation between the severity of the symptoms and the vIL-10 accumulation levels, the abnormalities observed for the transgenics could not be adequately explained by position or tissue-culture effects. Rather, these observations strongly suggested that they

were most likely caused by the expression of the transgene/recombinant protein itself, rather than being the result of somaclonal variation induced by the *in vitro* tissue culture conditions.

III.2.3.2 Analysis of IL-10 accumulation levels in subsequent generations

For each construct, 40 transgenic plants were regenerated and the amount of IL-10 in the leaves of the hemizygous T_0 plants was estimated by ELISA (II.2.4.12). For mIL-10, the best yield was 21.3 µg/g FLW, whereas the best yield of vIL-10 was 8.9 µg/g FLW, mirroring the results of the transient expression assays (III.2.2).

Seeds from self-pollination of the six highest expressing plants for each construct were tested for germination on kanamycin-containing agar plates, and 20 resistant plants per line were transferred into soil and grown in the greenhouse (II.2.3.1). They were screened for IL-10 accumulation by immunodotblot (Figure 19, II.2.4.9), and the most promising ones were also analyzed by ELISA. In the T_1 generation, accumulation levels up to 37.0 µg/g FLW for mIL-10 and 10.8 µg/g FLW for vIL-10 were observed.

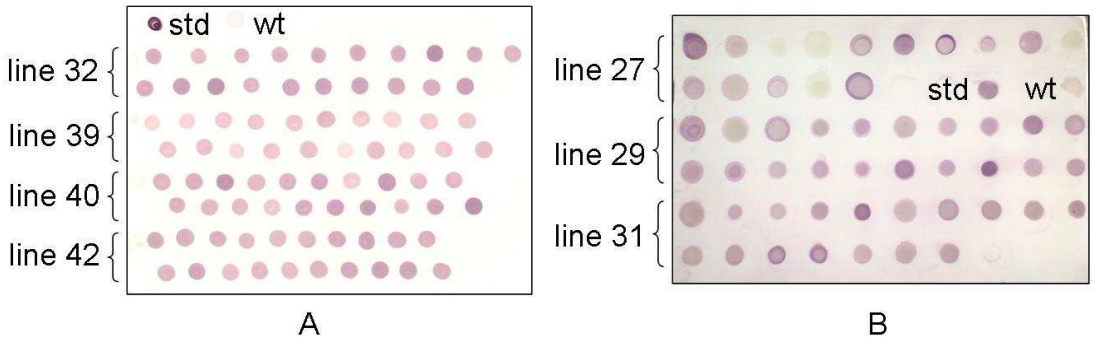

Figure 19: Dotblot screening of T_1 plants for IL-10 accumulation.

Total soluble proteins were extracted from leaf samples (II.2.4.1) and directly applied onto a nitrocellulose membrane (II.2.4.11). Protein extract from a wild type plant was used as negative control (wt), and either 20 or 100 ng of commercial murine or viral IL-10 were used as positive controls (STD), respectively. (**A**) Screening of T_1 plants for murine IL-10 accumulation. (**B**) Screening of T_1 plants for vIL-10 accumulation.

The same screening and analysis procedure was applied to the T_2 generation plants expressing mIL-10, and the highest accumulation level observed was 43.7 µg/g FLW, which is a further increase compared to the T_1 generation.

For the plants transformed with the construct for the expression of vIL-10, it was not possible to obtain seeds from the T1 generation plants, as they developed a severe phenotype (III.2.3.1) and never produced mature flowers (Figure 17F).

III.2.4 Immunolocalization of IL-10 in transgenic tobacco leaves

In order to confirm that, in the stable nuclear transformants, the IL-10 bearing the KDEL signal at the C-terminal was truly localized and accumulated in the ER, immunogold labelling and electron microscopy studies were performed. For both the murine and the viral IL-10 expressing plants of the T_1 generation, the localization studies confirmed that the recombinant proteins were retained and accumulated in the ER, as expected (Figure 20). No significant labeling was found in other cell compartments (data not shown).

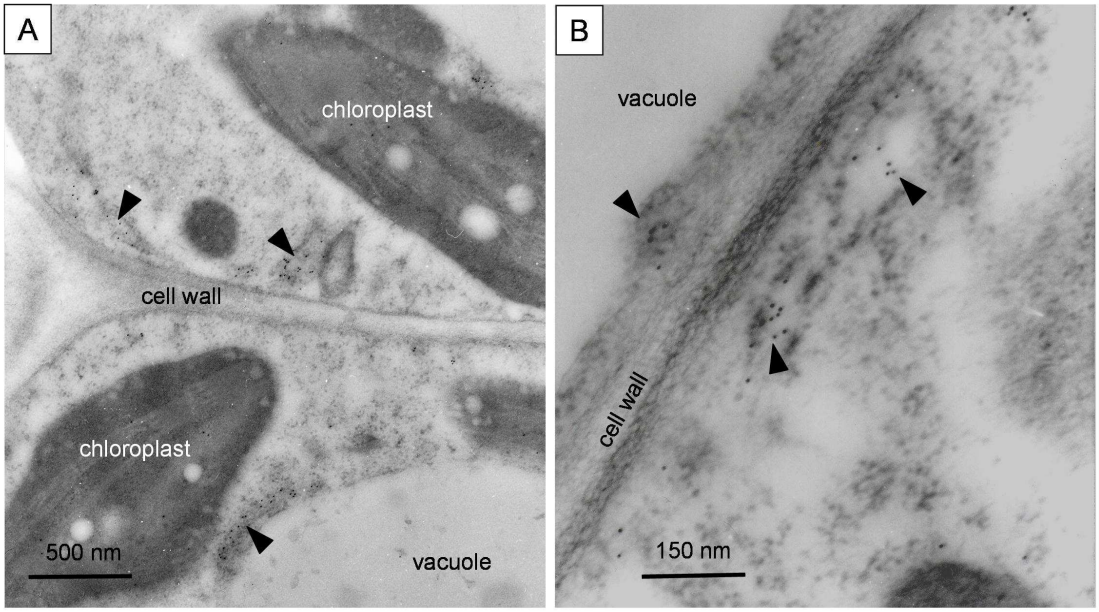

Figure 20: Immunolocalization of recombinant IL-10 in tobacco leaves.

Small squares of *N. tabacum* T_1 transgenic tobacco leaves expressing viral (**A**) or murine IL-10 (**B**) were fixed in 4% (w/v) formaldehyde, 0.2% (w/v) glutaraldehyde in 0.1 M phosphate buffer, pH 7.4 (II.2.5.2). Specimen were infiltrated and polymerized in LR White Resin. Ultra thin sections were obtained and incubated with either a goat anti-vIL-10 or a rabbit anti-mIL-10 as primary antibody, and with a secondary antibody conjugated to 10-nm gold particles (II.2.5.3). Gold labeling can be seen in the ER as indicated by arrowheads. Note that no labeling can be found in the cell wall and in the apoplast.

III.2.4.1 Ultrastructural analysis of transgenic leaves

Given the severe impact on plant development and the pale phenotype caused by expression of vIL-10, electron microscopy studies were performed on stable transgenic leaf material (T_1 generation), to investigate whether major alterations were also evident at the ultrastructural level. The differences noticed were related to the number of plastoglobules within the chloroplasts. Plastoglobules are low density lipoprotein particles attached to the

thylakoid membranes, and constitute an interior compartment of the chloroplast that functions for both lipid biosynthesis and storage. Figure 21 clearly shows that, while transgenic leaves expressing murine IL-10 had two to four small plastoglobules per chloroplast, like in wt leaves (not shown), the number of plastoglobules was considerably increased in chloroplasts from leaves expressing the viral variant of the cytokine, with up to 10-20 plastoglobules per chloroplast.

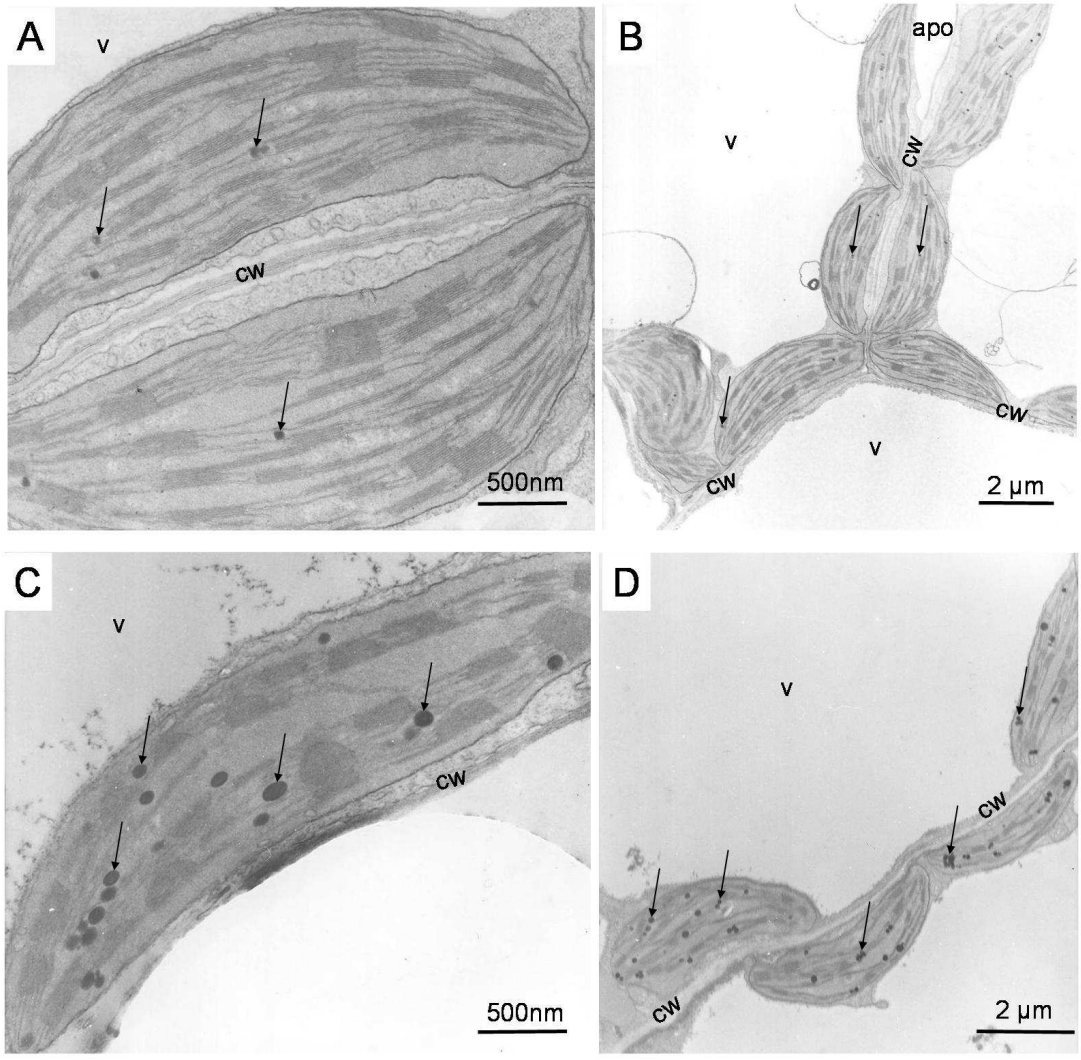

Figure 21: Ultrastructural details from chloroplasts of transgenic tobacco leaves expressing IL-10.

Small squares of *N. tabacum* T_1 transgenic tobacco leaves expressing murine (**A-B**) or viral IL-10 (**C-D**) were fixed in 2% (w/v) formaldehyde, 2.5% (w/v) glutaraldehyde in 0.1 M phosphate buffer, pH 7.4 (II.2.5.1). Specimen were first osmificated, then infiltrated and polymerized in Spurr resin. Ultra thin sections were obtained and analyzed with a transmission electron microscope. Some plastoglobules are indicated by arrows. apo, apoplast, cw, cell wall; v, vacuole.

III.3 Expression of IL-10 in BY-2 suspension cultures

III.3.1 Constitutive expression of murine and viral IL-10

Given the relatively low accumulation levels obtained for vIL-10, connected to the severe phenotype, in the stable nuclear transformants, tobacco BY-2 suspension cells were also transformed with the construct for ER-retention of vIL-10, in the attempt to reach higher vIL-10 accumulation levels without deleterious effects in this expression system. Transformation of BY-2 cells with the murine construct was also performed to have a mean of comparison with transgenic plants on the expression levels. From BY-2 transformation (II.2.3.7) with the pTRAkt_ER-vIL-10 and pTRAkt_ER-mIL-10 vectors (III.2.1), 25 calli per construct were analyzed. They were screened for recombinant protein production by immunodotblot analysis (II.2.4.9) of the protein extracts (II.2.4.2) and, for each construct, the seven most promising lines were tested in ELISA for IL-10 quantification (II.2.4.12). For the murine construct, the highest expression level observed was 18.1 μg/g FW, while for the viral one expression levels were up to 0.6 μg/g FW. For each construct, liquid suspension cultures of BY-2 cells from the highest expressing callus were established (II.2.3.6). IL-10 accumulation levels in the cell pellet were determined by ELISA at 3, 5 and 7 days after inoculation of the culture in fresh medium (dpi). These time-course measurements were repeated in three independent experiments, and the highest accumulation levels, observed for both lines at 5 dpi, were 9.3 ± 1.4 μg/g FW for the murine and 1.4 ± 0.4 μg/g FW for the viral IL-10 (Figure 22). Secretion of IL-10 in the culture medium was found to be less than 0.2% for both proteins (not shown). No obvious difference in the growth of the suspension cultures was observed, and the average weight of the cell pellet at 7 dpi was not substantially different for the two lines (Figure 22, upper right panel).

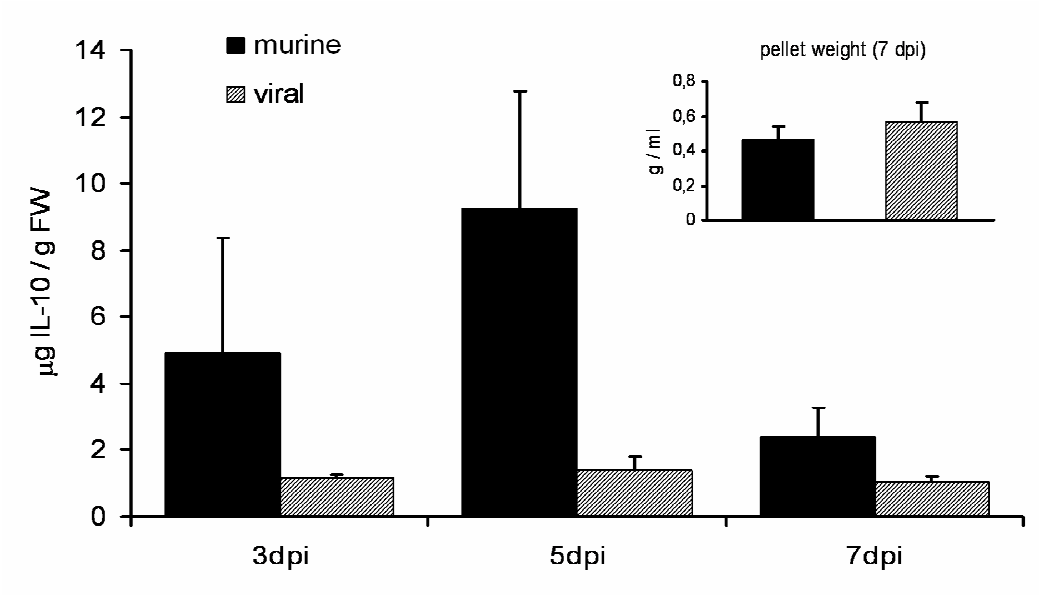

Figure 22: Accumulation of murine and viral IL-10 in BY2 suspension cultures.

Time course analysis of IL-10 accumulation levels in the cell pellet of BY-2 suspension cultures at 3, 5 and 7 days post inoculation (dpi) in fresh medium (II.2.3.6), assayed by ELISA, and expressed as µg/g fresh cell weight (FW); in the upper right panel, the average fresh pellet weight of the suspension cultures at 7 dpi is shown. Values are means ± SD of data from three independent time-course experiments with the highest producing line.

III.3.2 Inducible expression of vIL-10

A possible explanation for such low accumulation levels of the viral IL-10 compared to the murine IL-10 also in BY-2 cells, despite no obvious differences in the culture growth, was that if the viral IL-10 was indeed harmful to the plant cell in a concentration-dependant manner, we were actually selecting against high-expressing lines. It was therefore decided to use an inducible promoter, to assess whether induction of IL-10 expression at a defined time point of the cell culture growth could lead to higher accumulation levels of the recombinant protein. The tetracycline(Tet)-specific de-repressible expression system (Gatz and Quail, 1988) was chosen, which has already been successfully used in BY-2 cells (David and Perrot-Rechenmann, 2001). Initially, the construct for ER localization of vIL-10 was cloned as a *Kpn*I-*Xba*I fragment into the pBinHygTx vector (II.1.2.1), in which the transgene is under the transcriptional control of a modified 35S promoter ('Triple Op'), that contains three Tet-Repressor binding sites surrounding the TATA box (Figure 23). The plasmid was transferred into *A. tumefaciens* strain GV2260 by electroporation (II.2.2.6) and this was used to over-transform a BY-2 line stably transformed with the pBinTetR vector

(Gatz et al., 1992), which constitutively synthesizes the bacterial repressor protein TetR (kindly provided by Dr A. Schiermeyer, Fraunhofer IME, Aachen, Germany).

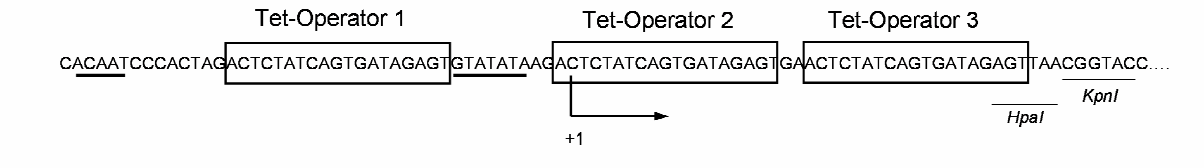

Figure 23: Tetracycline inducible 'Triple Op' promoter.

Sequence of the tetracycline inducible promoter region including one Tet-Operator (the 19 bp palindromic binding site for the Tet-Repressor) 1bp upstream of the TATA-box, a second operator 1bp downstream of the TATA-box and a third operator 23 bp downstream of the TATA-box of the normally constitutive CaMV 35S promoter. The CAAT-box and TATA-box are underlined.

However, the use of the pBinHygTX vector for tetracycline-specific de-repressible expression of vIL-10 in BY2 cells turned out to be more complicated than expected. In particular, setting up the induction conditions for transgene expression in the transformed calli to identify the transgenic clones was not straightforward.

Therefore, a vector containing an expression cassette with the Tet-inducible vIL-10 gene in tandem with the DsRed screenable marker gene under the control of a constitutive promoter was preferred. It was also decided to switch onto the pTRA vector backbone, which allows easier manipulation compared to the low-copy pBin-derived plasmids.

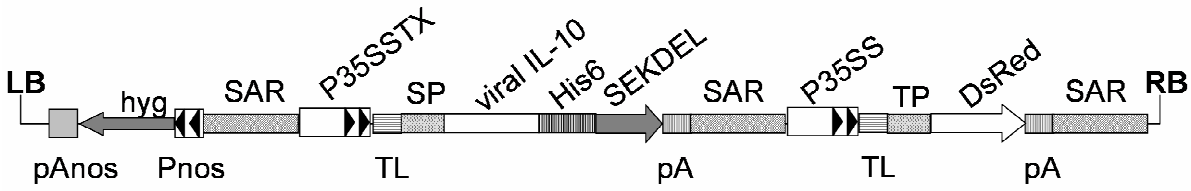

Figure 24: Schematic overview of the T-DNA region of the pTRA plant expression vector used for the tetracycline de-repressible expression of viral IL-10 in BY2 cells.

LB and RB, left and right border of the T-DNA; Pnos and pAnos, promoter and terminator of the nopaline synthase gene; hyg, coding sequence of the hygromycin phosphotransferase gene; SAR, scaffold attachment region; P35SSTX, 35S promoter of the cauliflower mosaic virus (CaMV) 35S gene with three Tet-Repressor binding sites surrounding the TATA box and duplicated enhancer; pA, terminator of CaMV 35S gene; TL, 5' UTR of the tobacco etch virus (TEV); SP, native vIL-10 signal peptide; viral IL-10, mature vIL-10 sequence; His6, histidine tag; SEKDEL, ER retention signal; P35SS, promoter of the 35S gene of CaMV with duplicated enhancer; TP, transit peptide of the barley granule bound starch synthase gene; DsRed, red fluorescent protein from *Discosoma* sp.. Not drawn to scale.

The TetR synthesizing BY2 transgenic line was over-transformed with this new pTRAhDsRed-eTXvIL-10 vector (Figure 24) (from Dr. T. Rademacher, RWTH Aachen University, Germany).

As DsRed accumulation is usually a good indicator of transgene expression levels when transformed in tandem with the target gene, only calli displaying the highest macroscopically visible DsRed fluorescence were selected, transferred to liquid culture and used for further analysis (Figure 25).

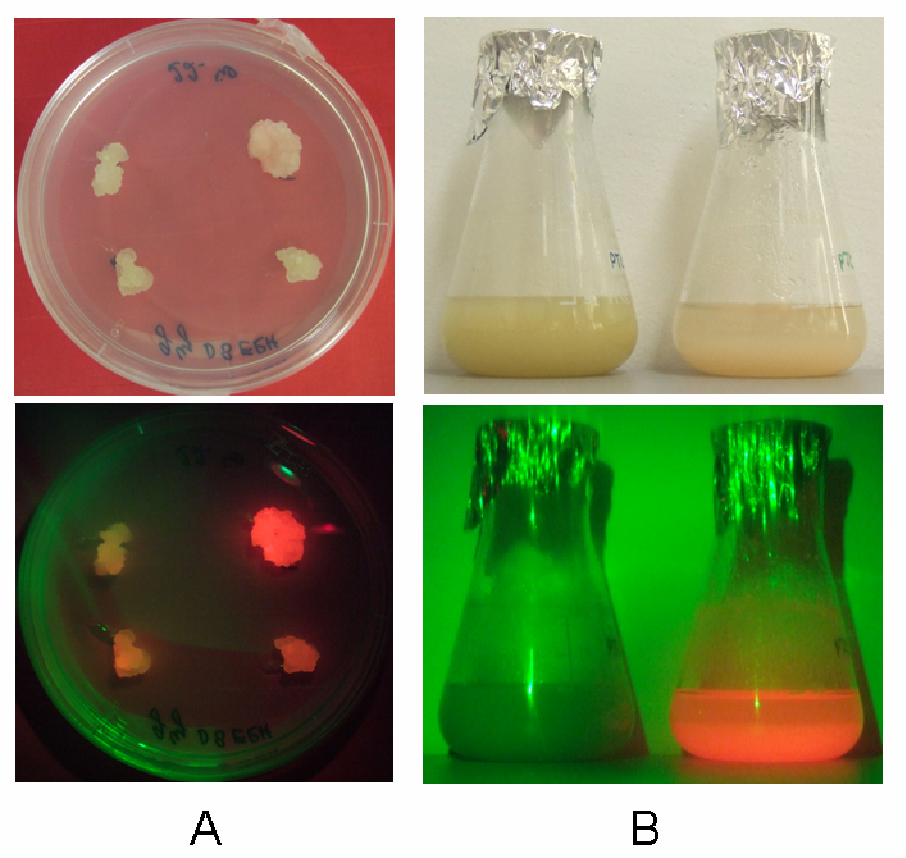

Figure 25: Selection of BY2 transgenic clones based on DsRed fluorescence.

Monitoring of *Discosoma* red fluorescent protein (DsRed) in transgenic BY-2 cells calli and suspension cultures transformed with the pTRAheTXvIL-10 vector. DsRed fluorescence was visualized with an LCD lamp with glass fiber optic (Leica KL1500), and additional filter for green excitation (BP545/30) and a colored foil (#182, light red). (**A**) Four transgenic BY-2 calli representing independent clones that show macroscopically different fluorescence intensity. (**B**) Liquid suspension cultures of BY-2 cells; wt cells on the left and transgenic on the right.

A preliminary evaluation of four clones showing the highest DsRed fluorescence was performed, inducing the BY-2 suspension cultures with tetracycline and monitoring vIL-10 accumulation in the cell pellets after 24, 48 and 72h. A clear correlation between the amount of recombinant protein and the macroscopic DsRed fluorescence intensity was observed. The conditions for induction -in terms of tetracycline concentration and time of induction- were optimized (10 µM Tet, directly after subculturing), and the highest producing clone was evaluated for vIL-10 accumulation by ELISA in three independent time-course experiments (Figure 26, striped bars). The results obtained were highly reproducible, and accumulation levels of vIL-10 up to 5.3 µg/g FW were reached. These levels are 3.5 times higher than those previously obtained in BY-2 suspension cultures which constitutively express the same transgene (1.5 µg/g FW) (Figure 26, solid bars). Negligible basal vIL-10 amounts were measured for the un-induced negative controls (< 0.055 µg/g FW), indicating a tight repression of transcription in the Tet-R expressing clone used for over-transformation (not shown).

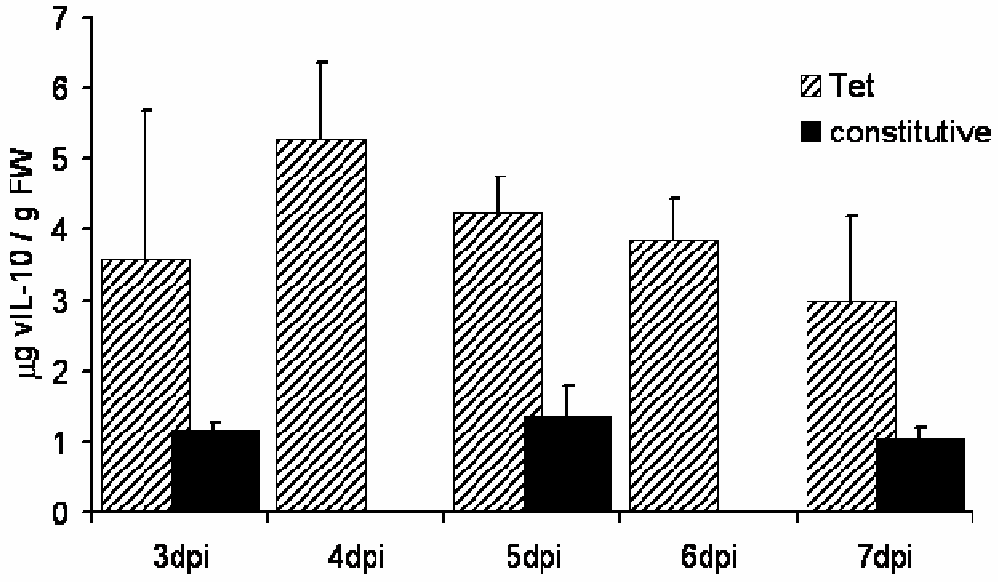

Figure 26: Improvement of viral IL-10 accumulation levels in BY2 suspension cultures upon expression of the transgene from a tetracycline inducible promoter.

Tet-R BY2 suspension cultures, over-transformed with the pTRAhDsRed-eTXvIL-10 vector carrying the vIL-10 gene under the control of the tetracycline-inducible promoter, were induced with 10 µM tetracycline when a saturated culture was transferred into 50 ml fresh medium at 2%(v/v) density (striped bars). Suspension cells were grown at 26°C, 180 rpm shaking, and 2ml aliquots were withdrawn daily from 3 to 7 days post induction (dpi) for analysis. Viral IL-10 accumulation was determined by ELISA on the cell pellet extracts. For comparison, the results obtained previously (III.3.1) with the constitutive expression of vIL-10 in BY2 cells at 3, 5 and 7 dpi are also shown (solid bars). The data reported are the means ± SD of the data from three independent experiments.

III.4 Characterization of plant-derived IL-10

III.4.1 Investigation of IL-10 dimeric state

The biological activity of IL-10 depends strictly on its dimeric state (Zdanov et al., 1995). In order to determine whether or not mIL-10 and vIL-10 were properly assembled into dimers, the His_6-tagged proteins were purified from stable T_1 transgenic tobacco leaves via immobilized-metal affinity chromatography (IMAC) on a nickel-nitrilotriacetic acid (Ni-NTA) column (II.2.4.13), concentrated, and fractionated by sodium dodecylsulfate polyacrylamide gel electrophoresis (SDS-PAGE) under either reducing or non-reducing conditions (II.2.4.5). Immunoblot analysis (II.2.4.9) confirmed the correct molecular weights of both proteins (19 and 21 kDa for the viral and murine IL-10, respectively; Figure 27A and B, right panels). When separated under non-reducing conditions, the plant-derived vIL-10 predominantly formed stable dimers (Figure 27A, left panel), whereas mIL-10 was partly dimeric and partly monomeric (Figure 27B, left panel). Since commercial mIL-10 also gives rise to a monomer band under these conditions, this is most likely an artifact of the SDS-PAGE method. This was confirmed by gel filtration analysis (II.2.4.14), which showed that the plant-derived mIL-10 eluted as a single peak with a profile corresponding to the size of the dimeric form (Figure 27C).

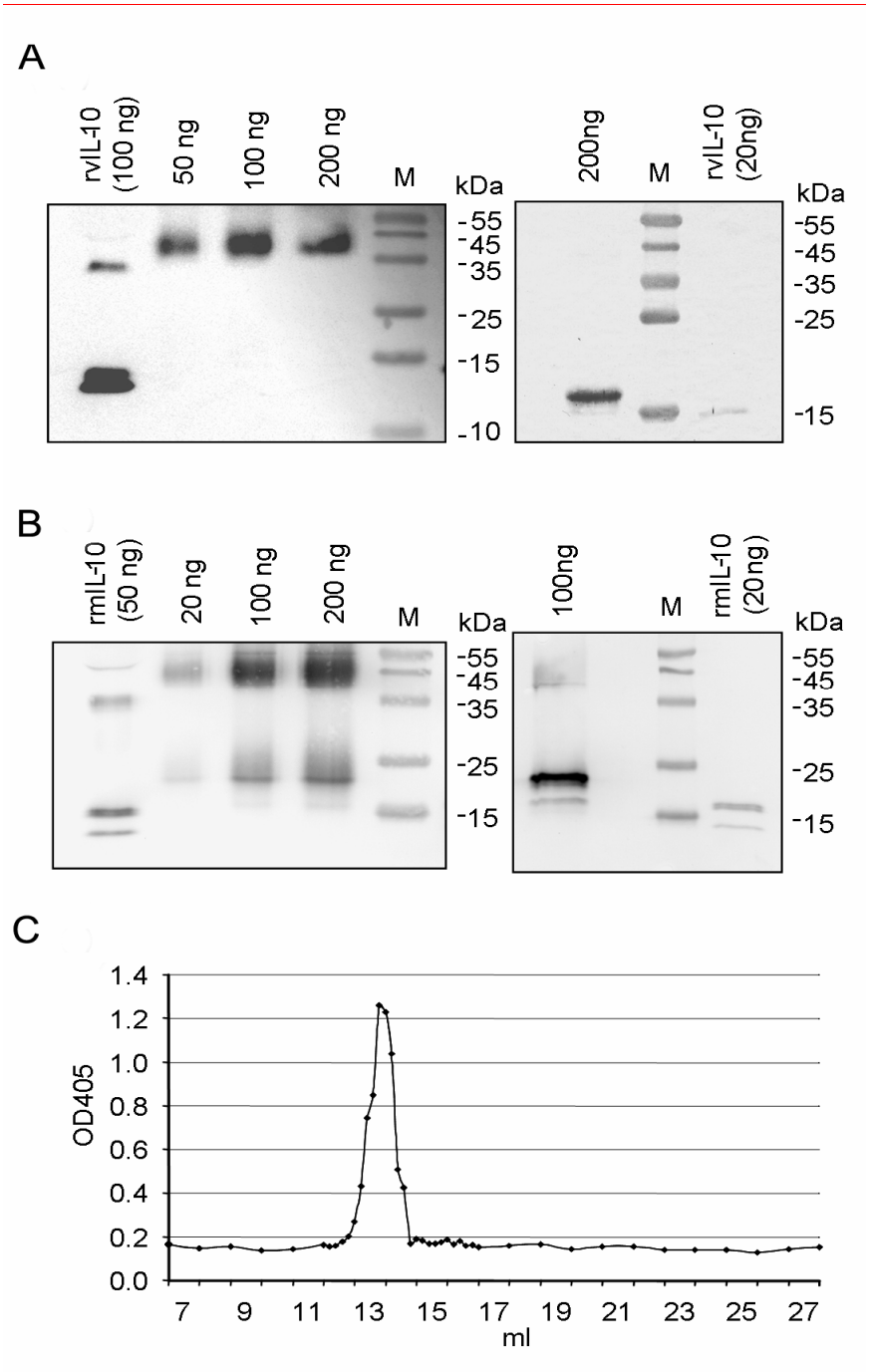

Figure 27: Assessment of IL-10 integrity and dimerization.

Viral (**A**) and murine (**B**) IL-10, purified from transgenic tobacco leaf extracts by IMAC, were analyzed by immunoblotting after separation by non-reducing (left panels) and reducing (right panels) SDS-PAGE. Commercial recombinant viral IL-10 produced in *E. coli* (rvIL-10) or murine IL-10 produced in insect cells (rmIL-10) were used as controls, and different amounts of plant-derived IL-10 were loaded, as indicated on top of each lane. (**C**) Elution profile of plant-derived mIL-10 from a Superdex 200 column showing a single peak which, compared to the elution volumes of standard reference molecules on the same columns (not shown), matches with the expected size of the dimer. Detection of IL-10 in the elution fractions was carried out by ELISA.

III.4.2 Analysis of *N*-glycans and N-terminus peptides

The mature mIL-10 polypeptide has two potential *N*-glycosylation acceptor sites, whereas vIL-10 has a single site. To determine the glycan composition, both plant-derived recombinant proteins were purified from transgenic tobacco leaves by affinity chromatography using a Ni-NTA column and separated by SDS-PAGE; the Coomassie Brilliant Blue stained bands were excised from the gel, digested with trypsin and analyzed by mass spectrometry (MS) (Dr. F. Altmann, J. Stadlmann, BoKu Vienna, Austria).

Despite the presence of a glycan acceptor site at Asn_{127}, the plant-derived vIL-10 was not glycosylated, as expected.

Murine IL-10 was glycosylated, but at only one of the two potential acceptor sites, as is the case for the native protein (Moore et al., 1990; Mosmann et al., 1990). Unexpectedly for a protein bearing a SEKDEL tag, oligo-mannose-type (OMT) *N*-glycans accounted for only 46% of the total *N*-glycan population, with Man_7 being the most abundant glycoform (not shown). Complex type *N*-glycans accounted for 44% of the total, with GnGnXF and GnGnX being the most prominent. GnMX was present at lower levels, while the other complex type *N*-glycans were found in only trace amounts (*N*-glycan abbreviations according to Proglycan). These results indicated that murine IL-10 was secreted instead of being retained in the ER, as most of these complex glycans carried terminal *N*-acetylglucosamine (Gn) residues, which is a typical feature of secreted proteins that pass through the *trans*-Golgi network on their way to the apoplast (Fitchette et al., 1994; Lerouge et al., 1998).

LC-MS analysis of plant-derived mIL-10 was performed on both the upper and lower bands in which the cytokine separates after SDS-PAGE (Figure 27B). No substantial differences in the MS spectra were found for the two proteins, indicating that the lower band does not represent a degradation product (not shown). Moreover, detailed analysis of the glycosylated peptide indicated that the protein in the two bands has the same *N*-glycosylation pattern (Figure 28A and B), suggesting that the difference in migration is probably the consequence of different conformations assumed by IL-10 during the SDS-PAGE. In support of this hypothesis is the fact that also the commercial mIL-10 –and even the non-glycosylated commercial vIL-10– show the same migrating behavior upon SDS-PAGE separation.

In contrast, when murine IL-10 purified from transgenic BY-2 cells was subjected to *N*-glycan analysis, the *N*-glycans found on the protein were only of the oligo-mannose-type, as expected for a protein retained in the ER (Figure 28C).

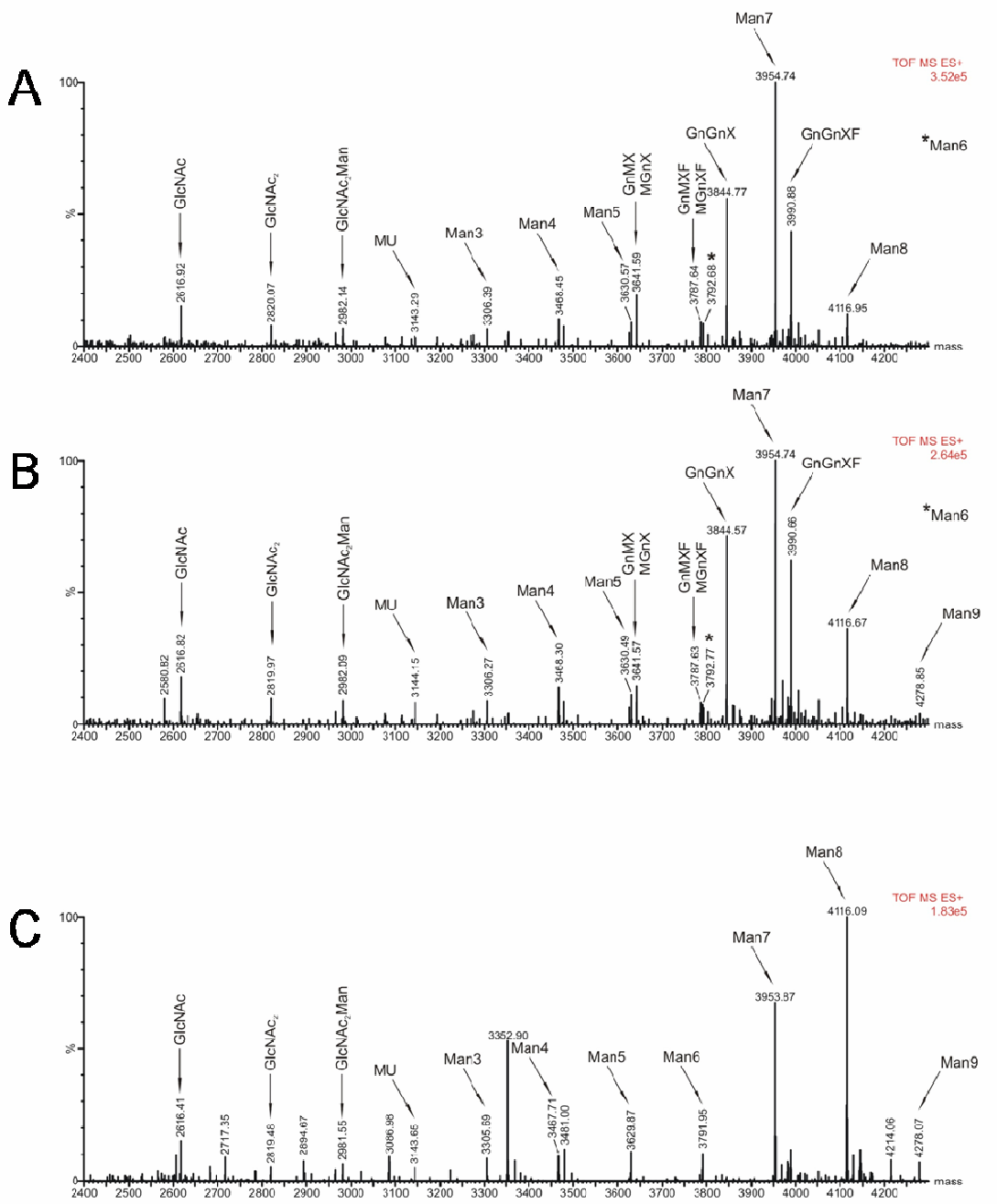

Figure 28: Liquid chromatography-mass spectrometry (LC-MS) of the glycosylated peptide EDNNCTHFPVGQSHMLLELR of murine IL-10.

Murine IL-10 purified by IMAC (II.2.4.13) and separated by SDS-PAGE (II.2.4.5) was digested with trypsin and the peptides subjected to LC-MS analysis (II.2.4.15). The spectrum of the glycosylated peptide is shown. (**A**) sample corresponding to the upper band of plant-derived mIL-10; (**B**) sample corresponding to the lower band of plant-derived mIL-10; (**C**) mIL-10 purified from transgenic BY-2 suspension cells (III.3.1). See http://www.proglycan.com for an explanation of *N*-glycan abbreviations.

However, it has to be pointed out that the recombinant protein had been purified from the cell pellet of a BY-2 suspension culture, therefore this result does not rule out the possibility that murine IL-10 is indeed secreted by the cells. As a matter of fact, the observation that the amount of mIL-10 secreted in the culture supernatant was lower than 0.2% (III.3.1) could be the consequence of a rapid degradation of the recombinant protein in the culture medium, rather than reflecting a tight ER retrieval of mIL-10. Actually, the results of the *N*-glycan analysis of the plant-purified mIL-10 combined with those obtained for the BY-2 derived cytokine, could be explained assuming that murine IL-10 is not efficiently retained in the ER and secreted in both expression systems, but is more rapidly degraded in the BY-2 supernatant than in the leaf apoplast.

Nevertheless, the high amount of complex type *N*-glycans found on the plant-purified mIL-10 contradicted the electron microscopy results, that had clearly localized the protein in the ER (Figure 20). As the only obvious difference between the leaf samples utilized for immunolocalization and for protein purification was the age of the plant material, mIL-10 was purified from young or old leaves of young and old plants and subjected to *N*-glycan analyses, to figure out if there was a correlation between the leaf or plant age and the intercellular fate of recombinant IL-10 in tobacco plants (Figure 29). The results of the *N*-glycan analysis confirmed that murine IL-10 in young leaves of young plants (4 weeks) bears mostly oligo-mannose type glycans (~93%) typical of a ER-retarded protein. The small amount of complex type glycans (<7%) is probably due to a minimal escape from the KDEL-mediated ER retrieval mechanism, which has been often observed for other recombinant proteins (Floss et al., 2008; Triguero et al., 2005). The *N*-glycan profile of mIL-10 purified from 6 weeks old plants, instead, showed around 50% of complex-type glycans on the protein, no matter if purified from young or old leaves (Figure 29). Additionally, the type of complex glycans found on these samples carried terminal *N*-acetylglucosamine (Gn) residues suggesting secretion of the recombinant protein from the plant cell (Fig. 4). This suggests that mIL-10 escaping the ER is secreted by the plant cell and not, for example, redirected to the lysosomal compartment. These results indicate that the increase in leakage of mIL-10 from the ER endomembrane system is dependent on the plant age rather than the leaf age.

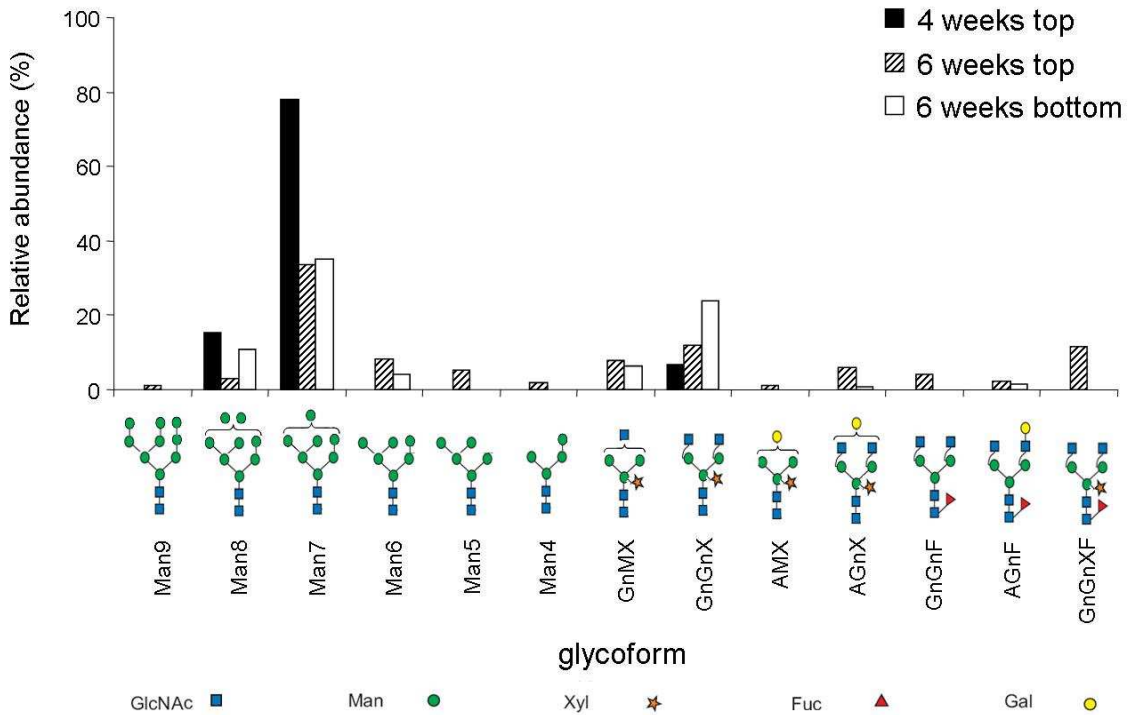

Figure 29: *N*-glycan analysis of plant produced murine IL-10 purified from leaf material of different age.

Murine IL-10 purified from stable transgenic leaf material of different age by IMAC (II.2.4.13) was digested with trypsin and the peptides subjected to liquid chromatography-mass spectrometry (LC-MS) analysis (II.2.4.15). The '4 week / top' sample corresponds to the material that was analyzed by immunolocalization and electron microscopy. The '6 weeks / bottom' sample corresponds to the plant material from which mIL-10 was purified for N-glycan analysis the first time. For each sample, the glycosylated peptide containing asparagine-30 of mIL-10 (EDNNCTHFPVGQSHMLLELR) was analyzed by mass spectrometry. The MS data from the tryptic peptides were compared with data sets generated by in silico tryptic digestion of the recombinant protein sequences using the PeptideMass program (http://www.expasy.org/tools/peptide-mass.html). See http://www.proglycan.com for an explanation of *N*-glycan abbreviations.

For both murine and viral IL-10, the identity of the N-terminal peptide was established by tandem MS analysis. The sequence of the mature mIL-10 polypeptide started with QYSRE while vIL-10 started with TDQCD (Figure 30), confirming co-translational ER translocation and correct cleavage of both signal peptides, as predicted by the SignalP 3.0 server (http://www.cbs.dtu.dk/services/SignalP/).

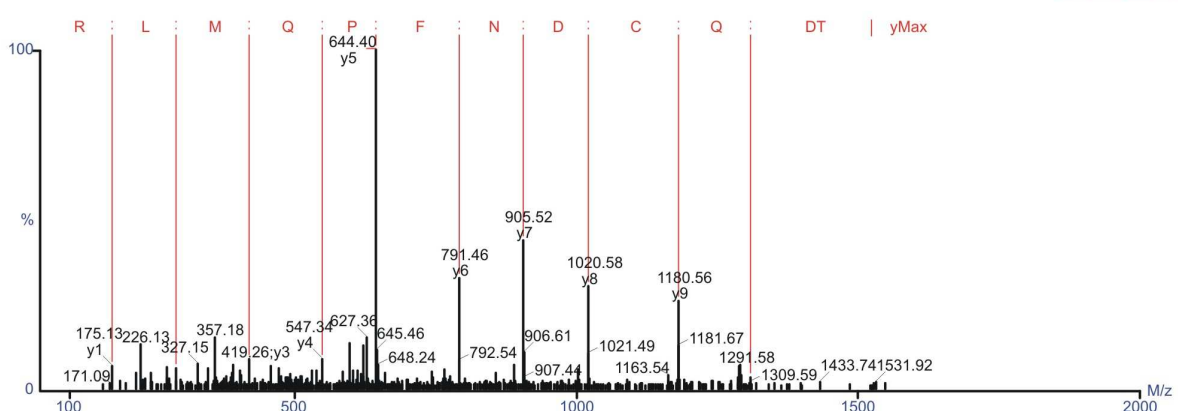

Figure 30: Liquid chromatography-tandem mass spectrometry (LC-MS/MS) profile of the viral IL-10 N-terminal tryptic peptide.

The Coomassie-stained band (II.2.4.7) of viral IL-10 purified from tobacco leaves (II.2.4.13) was digested with trypsin, extracted from gel pieces, and analyzed. First, the sample was analyzed in plain MS mode, and then the sequence of the N-terminal peptide was confirmed by tandem MS.

III.4.3 Detection of the KDEL-tag on mIL-10

A possible reason for the consistent mIL-10 escape from the ER, could be the loss of the KDEL tag upon cleavage by cell proteases, whose activity varies with the plant developmental stages (Stevens et al., 2000). Therefore mIL-10 purified form bottom leaves of 6-week-old plants was analyzed for presence of the KDEL-tag by immunoblot, and the analysis confirmed that the tag was still present on the protein (Figure 31).

As the recombinant protein still bears the KDEL tag, and the mIL-10 accumulation levels are not exceptionally high to suggest saturation of the KDEL retrieval machinery, the most likely explanation for the presence of complex type *N*-glycans on mIL-10 is that the tag is partially occluded following assembly of the IL-10 dimer, and is not completely accessible to the KDEL receptor.

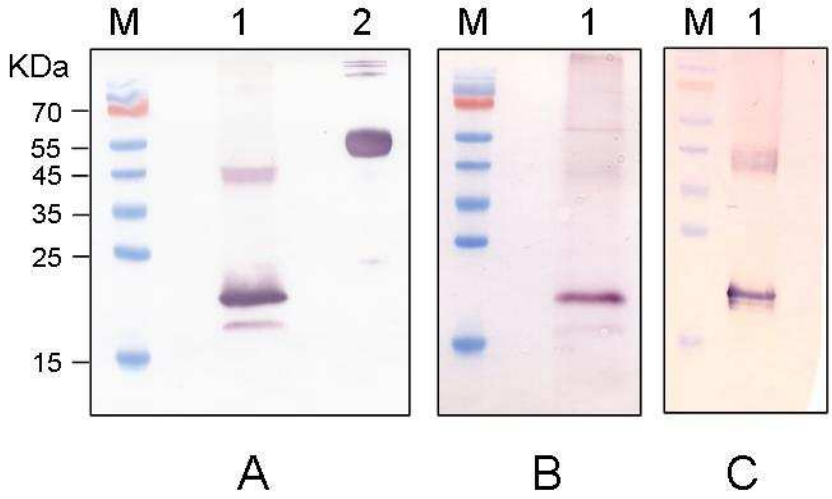

Figure 31: Confirmation of KDEL presence by immunoblot analysis.

To confirm the KDEL presence on the C-term of mIL-10, the plant purified recombinant protein was analyzed by immunoblot with antibodies against the KDEL, the 6xHIS tag, and the mIL-10 itself. (**A**) Five micrograms of mIL-10 purified from bottom leaves of 6 week old plants (lane 1) were separated on a 17% SDS gel, and the same amount of M12 antibody bearing a KDEL tag on the heavy chain was loaded as positive control (lane 2). Immunodetection was carried out with a mouse α KDEL antibody. (**B**) The same amount of mIL-10 as shown in panel A (lane 1) was analyzed in parallel with a rabbit anti 6xHIS antibody. Although the overall intensity of the signal is slightly lower, the results reflect precisely what obtained with the anti KDEL antibody. (**C**) As control, 100 ng of mIL-10 (lane1) were separated by SDS-PAGE and detected by a rat anti mIL-10 antibody.

III.5 Assessment of murine and viral IL-10 biological activity

III.5.1 STAT3 Phosphorylation assay

All the anti-inflammatory effects of IL-10 require the activation of signal transducer and activator of transcription 3 (STAT3), which acts downstream of the IL-10 receptor in both mouse and human cellular models (Moore et al., 2001). Therefore, the ability of plant-derived mIL-10 and vIL-10 to phosphorylate the Tyr_{705} residue of STAT3 was tested. To exclude possible interference from plant proteins co-purifying with the recombinant IL-10 molecules, equal amounts of wild type leaf material were subjected to the same purification procedure on a Ni-NTA column, and the eluate was used as a control in all biological activity assays. Stimulation of the mouse macrophage cell line J774 with different doses of plant-derived mIL-10 and vIL-10 triggered STAT3 tyrosine phosphorylation within 15 min and in a dose-dependent manner (Figure 32). The concentration of plant-derived

IL-10 required to elicit STAT3 tyrosine phosphorylation to a degree comparable to that observed in response to commercial mIL-10 (20 ng/ml) and vIL-10 (150 ng/ml) was 50 ng/ml for the murine protein (Figure 32A) and 500 ng/ml for the viral protein (Figure 32B). STAT3 phosphorylation resulted specifically from the presence of recombinant IL-10, since control eluate from wild type plant extracts had no detectable effect even at the highest dose tested.

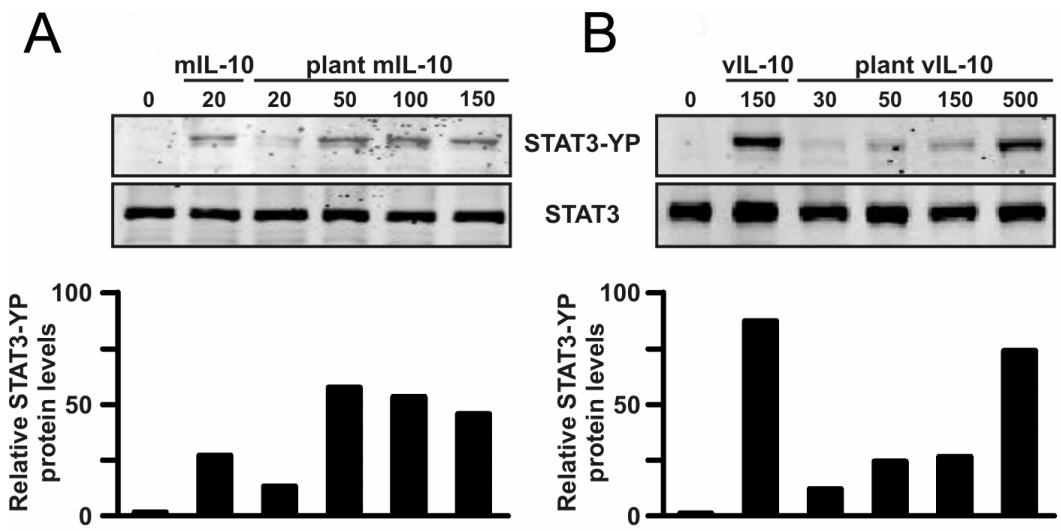

Figure 32: Activation of STAT3 phosphorylation by murine and viral IL-10 produced in tobacco plants.

STAT3 phosphorylation (STAT3-YP) was assessed by immunoblot analysis on protein extracts of macrophage cells treated with increasing doses of plant-derived IL-10 (II.2.6.2). (**A**) J774 cells were cultured for 15 min in the presence of eluate from wild type tobacco plants (lane 1; protein amount equivalent to the 150 ng/ml sample of the mIL-10-producing tobacco line), 20 ng/ml of commercial mIL-10 produced in insect cells (lane 2) or increasing concentrations of plant-derived mIL-10 (lanes 3-6). (**B**) J774 cells were cultured for 15 min in the presence of the eluate from purification of wild type tobacco plants (lane 1; protein amount equivalent to the 500 ng/ml sample of the vIL-10-producing tobacco line), 150 ng/ml of commercial vIL-10 (lane 2) or increasing concentration of plant vIL-10 (lanes 3-6). Total cell extracts (50 µg) were separated by SDS-PAGE and immunoblots were performed as described in the Materials and Methods section (II.2.6.2). One experiment representative of two is shown. The blots were scanned on the Odyssey Infrared Imaging System at 700 and 800 nm. The relative STAT3-YP levels, as quantified by the Odyssey software and normalized for the total STAT3, are reported below each panel.

III.5.2 Enhancement of LPS-induced SOCS3 modulation

It has been reported that suppressor of cytokine signaling 3 (SOCS3) is one of the targets of murine IL-10 (Cassatella et al., 1999; Ito et al., 1999). Indeed, *SOCS3* mRNA and SOCS3 protein expression in lipopolysaccharide (LPS)-stimulated J774 cells (II.2.6.4) is enhanced in the presence of commercial mIL-10 (Berlato et al., 2002). Similarly, purified

plant-derived mIL-10 increased the expression of LPS-induced *SOCS3* mRNA (Figure 33A) and SOCS3 protein (Figure 33B).

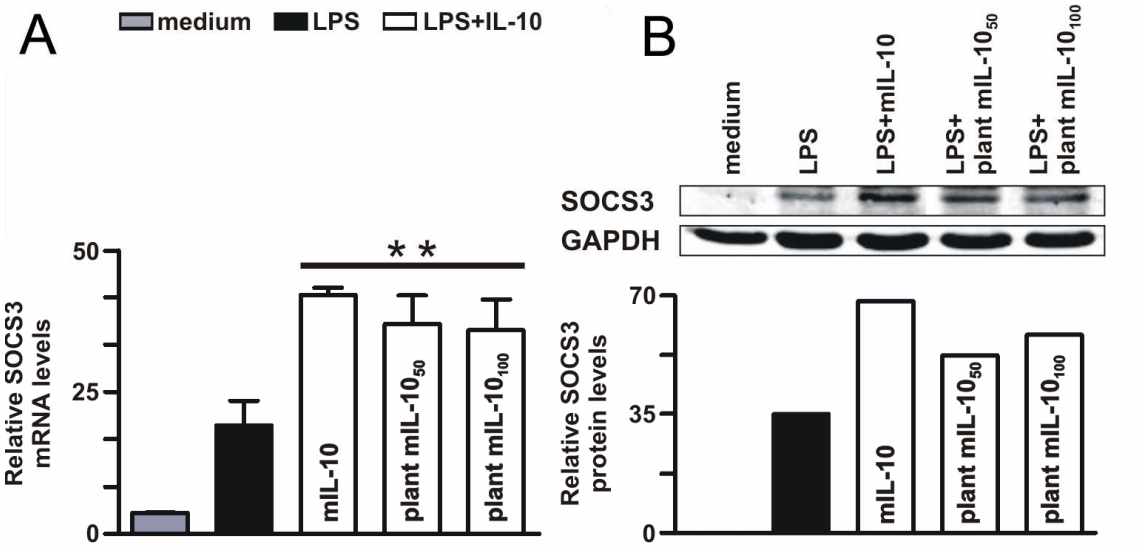

Figure 33: Effect of plant-derived murine IL-10 on LPS-induced *SOCS3* mRNA and SOCS3 protein expression.

(**A**): J774 cells were stimulated for 2 h with 100 ng/ml of LPS alone or in combination with commercial mIL-10 (20 ng/ml), or plant mIL-10 (50 and 100 ng/ml). Non stimulated cells ('medium') were included in the analysis to determine *SOCS3* basal expression levels. Total RNA was extracted (II.2.1.15) and then analyzed for *SOCS3* mRNA expression by real time RT-PCR (II.2.1.16). The graph shows the *SOCS3* mRNA levels (mean ± SD) assayed in triplicate and normalized to *GAPDH* expression. (**B**): J774 cells were incubated for 18 h in the presence of LPS alone (lane 2) or in combination with 20 ng/ml commercial IL-10 (lane 3) or 50 ng/ml (lane 4) or 100 ng/ml (lane 5) plant derived mIL-10. Non stimulated cells ('medium') were included in the analysis to determine SOCS3 basal expression levels. Whole cell extracts (50 µg) were immunoblotted using anti-NH_2 terminus SOCS3 antibody (*upper panel*) and antibodies specific for GAPDH (*lower panel*), followed by incubation with AlexaFluor 680 goat anti-rabbit and IRDye 800 goat anti-mouse antibody. The relative levels of SOCS3 protein, as quantified by the Odyssey software and normalized for the total GAPDH content, are reported at the bottom of each lane. The data shown in (**A**) and (**B**) are representative of two independent experiments. ** $p<0.001$.

III.5.3 Inhibition of LPS-induced TNFα production

The full functionality of plant-derived mIL-10 and vIL-10 was verified testing their inhibitory activity on the LPS-induced production of tumor necrosis factor alpha (TNFα). The amount of TNFα released into the culture supernatant of J774 cells stimulated with LPS for 18 h was reduced in the presence of plant-derived mIL-10 to the same extent observed with the commercial mIL-10 (Figure 34A). Similarly, the ability of plant-derived vIL-10 to inhibit LPS-induced TNFα production was equivalent to that of its commercial counterpart (Figure 34B). Addition of control eluate from wild type plants had no effect on the J774 response to LPS, or the suppressive activity of IL-10. These results confirmed that the

inhibition of TNFα production was dependent on the recombinant cytokines, and not on any co-purified plant proteins.

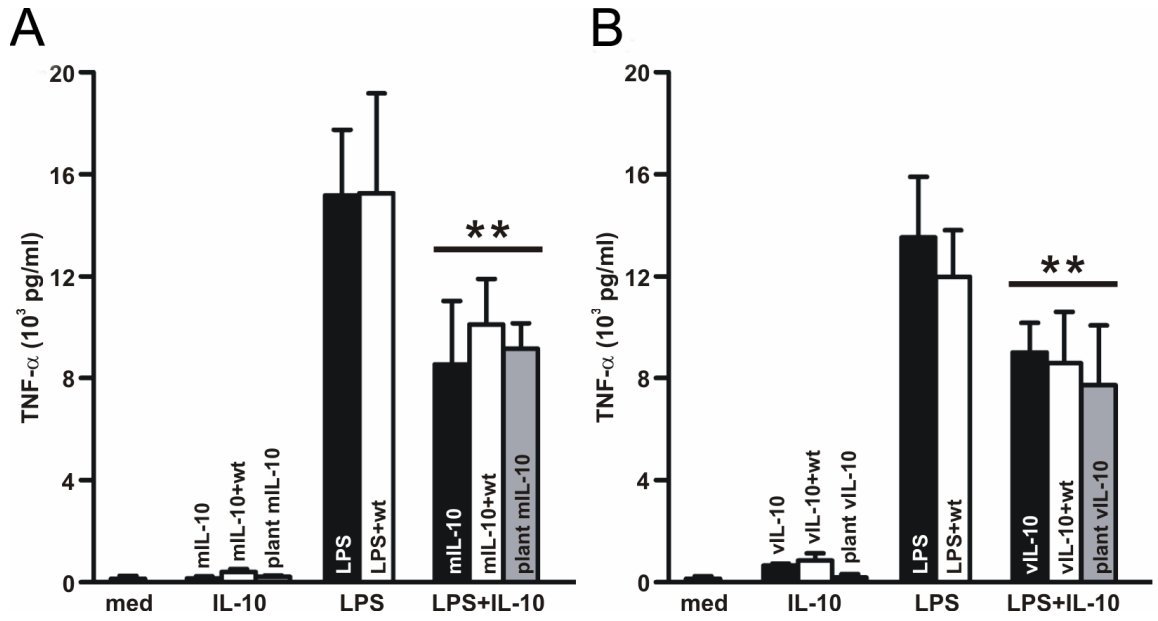

Figure 34: Inhibition of LPS-induced TNFα production by plant-derived murine and viral IL-10.

J774 cells were stimulated for 18 h with IL-10 alone, LPS alone, or LPS plus IL-10 (II.2.6.3). The eluate of the purification of wild type leaves (wt) was also included, alone or in combination with commercial IL-10, to exclude the interference of plant proteins with the assay. TNFα secretion in the culture medium (med) was quantified by ELISA and is reported as pg/ml supernatant. Values are the means ± SD of four independent experiments for the murine IL-10 (**A**) and three independent experiments for the viral IL-10 (**B**). ** $p<0.001$.

III.6 Stability studies

III.6.1 Investigation of different storage conditions and temperatures

In order to plan the feeding studies in the animal model, the stability of the recombinant proteins in different formulations and at different temperatures over three months was investigated. Transgenic leaf material was ground in liquid nitrogen and either stored frozen as a powder, lyophilized and stored at room temperature or directly used for protein extraction and the extract was then stored in the freezer. The amount of IL-10 in the samples was quantified by ELISA at every time point. Both murine and viral IL-10 behaved the same in terms of stability in the investigated conditions, and both resulted to be stable in the raw extract at -80°C or in the powder either at -20°C or -80°C over a three months period. In Figure 35 the results obtained for the murine IL-10 are reported as representative of both.

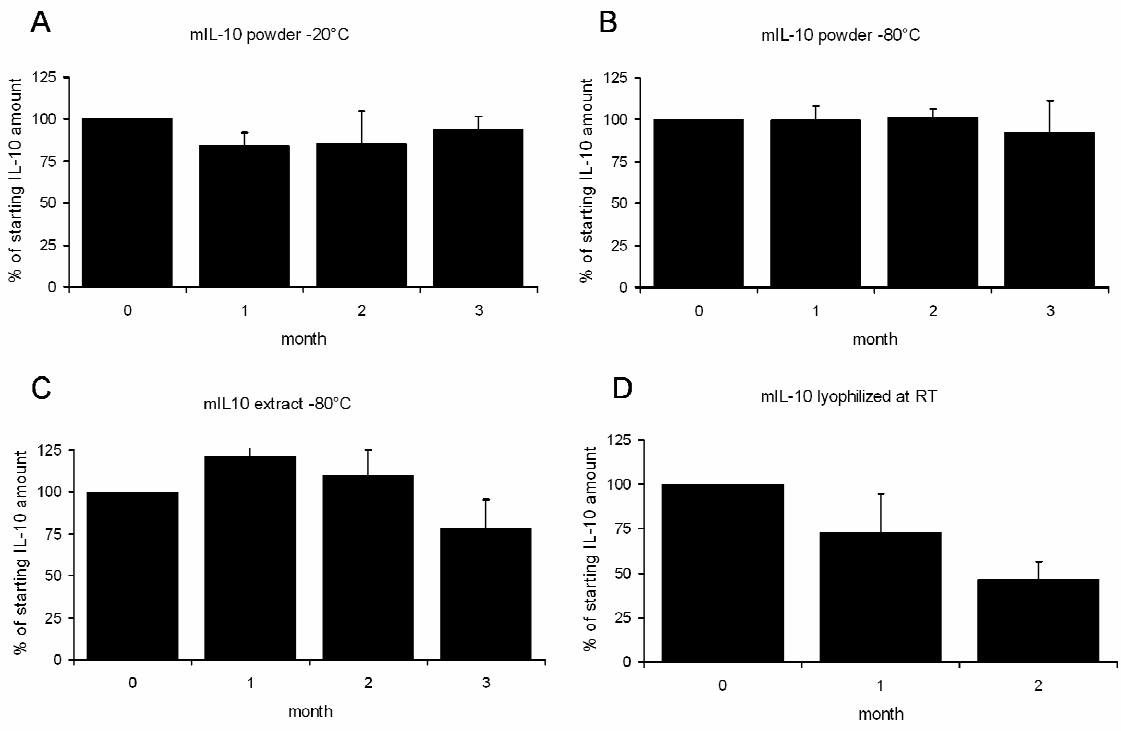

Figure 35: Stability studies of murine IL-10 in different storage conditions.

IL-10 levels were determined in the leaf extract at each time point by ELISA, and results are reported as % relative to the amount of IL-10 at time-point 0. (**A**): leaf powder stored at -20°C; (**B**): leaf powder stored at -80°C; (**C**): leaf extract stored at -80°C; (**D**): lyophilized leaf powder stored at room temperature.

III.6.2 Resistance of IL-10 to gastrointestinal degradation

The stability of murine and viral IL-10 produced in transgenic plants, either embedded in the lyophilized tobacco tissue or purified from the plant tissue, was compared using simulated gastric fluid (SGF, 3.2 g/L pepsin, pH 1.2) and simulated intestinal fluid (SIF, 10 g/L pancreatin, pH 6.8).

Both murine and viral plant-produced IL-10 resulted more resistant to gastric degradation when retained within the leaf tissue (Figure 36, upper panels), indicating that the plant matrix contributes to protect the recombinant proteins against proteolytic enzymes and low-pH conditions. This increased stability was especially relevant in the case of the viral IL-10, as after 30 s of digestion there was <4% of commercial IL-10, while in the lyophilized tissue >90% was still present.

Also in SIF digestion experiments, IL-10 embedded in the plant material turned out to be more resistant to degradation (Figure 36, lower panels). For both murine and viral IL-10,

>30% of the cytokine was still present after 30 min incubation, while the commercial counterparts were already undetectable.

In both digestion setups, the stability of plant purified IL-10 was comparable to, if not higher than, that of the respective commercial counterparts.

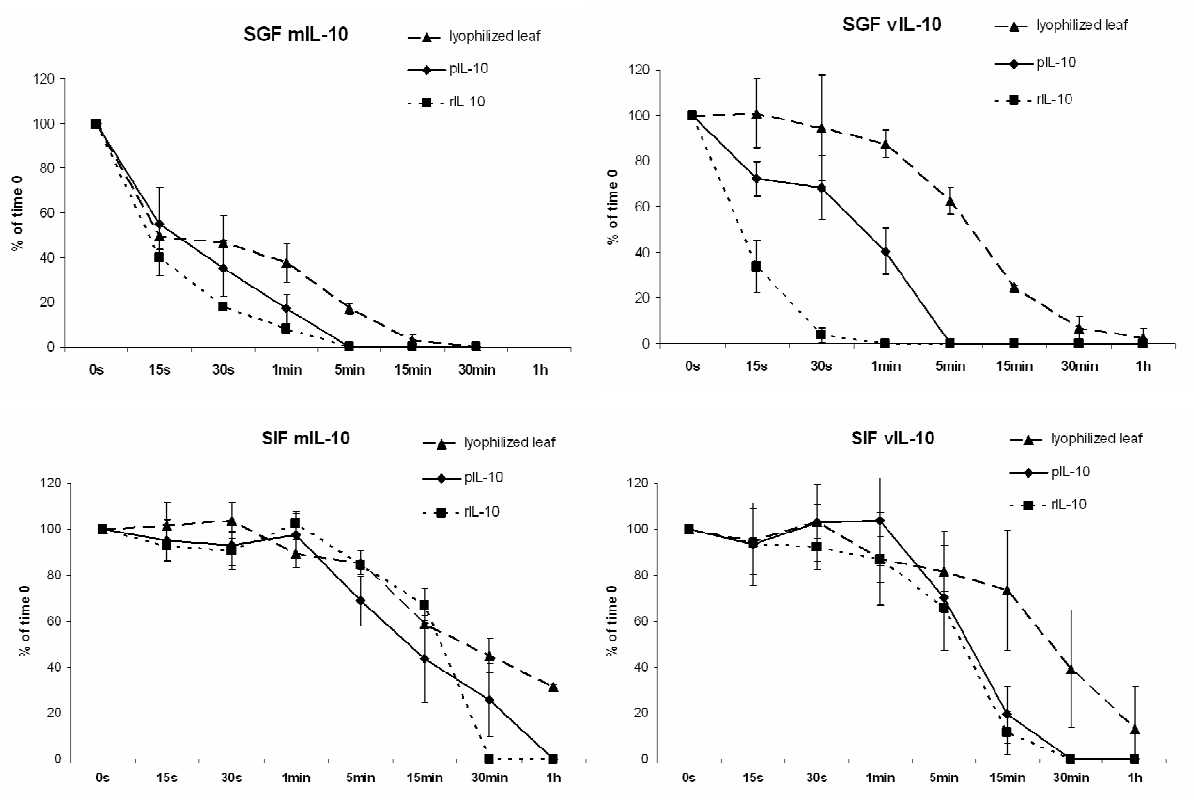

Figure 36: Stability of plant produced IL-10 in simulated gastrointestinal fluids.

The stability of plant-produced murine and viral IL-10, either embedded in the lyophilized tobacco tissue or purified from tobacco leaves, was compared, along with the commercial counterparts, in *in vitro* gastrointestinal simulation conditions (II.2.7). Purified IL-10 at a concentration of 1 ng/ml or 0.1g aliquots of lyophilized leaf tissue were digested in either simulated gastric fluid (SGF, 3.2 g/L pepsin, pH 1.2) or simulated intestinal fluid (SIF, 10 g/L pancreatin, pH 6.8) at 37°C. The digestion reactions were stopped with 45 mM Na_2CO_3 for SGF, or 10 mM EDTA for SIF, respectively. IL-10 content was determined by ELISA directly in the quenched digestion solution for the pure IL-10 samples, or in the plant extract for the lyophilized leaf material. The results shown are the mean of three independent experiments.

IV DISCUSSION

IV.1 Expression of IL-10 in the chloroplast of tobacco plants

Plastid transformation is a very attractive tool in molecular farming, due to the extremely high foreign protein accumulation levels that can be reached, compared to nuclear transformation (up to 100 times higher - De Cosa et al., 2001). This is most likely due to both higher stability of many foreign proteins inside the chloroplast than in the nucleo-cytoplasmic compartment, and to the high expression levels that result from the enormous numbers of genome copies and thus transgene copies per cell (Bock, 2001).

In the attempt to reach high IL-10 accumulation levels in plants, chloroplast transformation of *N. tabacum* cv. Petit Havana was performed using the pRB95 vector bearing the coding sequence of either the murine or the viral IL-10. However, quite disappointingly, chloroplast transformation turned out not to be a feasible approach for IL-10 production, as only unsatisfactory levels of recombinant protein could be obtained in the transplastomic plants generated.

The first hypothesis considered to explain the lack of recombinant protein accumulation, was protein degradation. Proteolytic degradation during plant development can be an important factor affecting yield and homogeneity of heterologous proteins produced by transgenic plants (Stevens et al., 2000) and, in particular, massive protein degradation is known to occur during tissue senescence. In the case of IL-10, however, the absence of recombinant protein did not seem to depend on leaf age (as observed in several earlier studies - Birch-Machin et al., 2004; Zhou et al., 2008), as both older and younger leaves were analyzed for IL-10 accumulation, and no obvious differences were observed between the samples.

Incorrect folding of IL-10 within the chloroplast, which would in turn lead to its rapid degradation, was also taken into consideration. The chloroplast stroma constitutes a reducing rather than oxidizing environment, and within each IL-10 monomer subunit there are two disulfide bonds which are susceptible to reduction (Zdanov et al., 1995). Several

examples in the literature suggest that disulfide bond formation in the chloroplast stroma may not be problematic: human somatotropin has been synthesized at high levels in chloroplasts in a biologically active form that depends on the formation of two disulfide bonds (Staub et al., 2000). The cholera toxin B pentamer with five disulfide bonds was also expressed in chloroplasts as functional oligomers up to 4.1% of TSP (Daniell et al., 2001). Nevertheless, this might be protein dependent, and it has to be considered that the redox state of the stroma is strongly influenced by the level of photosynthetic activity (Ruelland and Miginiac-Maslow, 1999) which, for example, was obviously impaired in the plants transformed with the viral IL-10 construct. Failure of IL-10 disulfide bonds formation in the chloroplasts of transplastomic plants could have possibly increased its susceptibility to proteolysis. Chloroplasts contain a range of proteolytic activities that target mis-folded, mis-targeted and damaged proteins for destruction (reviewed in Adam and Clarke, 2002), and proteolysis alone might account for the apparent lack of accumulation of IL-10. As a matter of fact, Menassa and colleagues have reported that the highly homologous human IL-10 protein targeted to the chloroplast of nuclear transgenic tobacco plants accumulated at extremely low levels (up to 0.0043 % TSP) and did not assemble into a homodimer, supporting the possibility of IL-10 protein instability inside the chloroplast environment (Menassa et al., 2004). Chloroplast proteases are indeed of prokaryotic type (e.g. Clp, Deg), and therefore have different substrate specificities compared to eukaryotic proteases (ubiquitin-proteasome system) which could be a reason for protein instability within the chloroplast.

However, the observations collected and the analyses performed on the transplastomic plants altogether, suggested that something more complex than simple protein degradation was taking place in IL-10 expressing plants. First of all, regeneration of transplastomic plants after biolistic bombardment was extremely difficult, as the callus tissue kept growing undifferentiated without producing shoots. Also, only five spectinomycin-resistant lines were eventually obtained for the murine construct and three for the viral one. Of these, only one line per construct turned out to be a true transplastomic line after the resistance test on double selective medium. This is an unusual and extremely low transformation efficiency, as upon one bombardment of tobacco leaves with the same vector backbone, usually around 10 independent transplastomic lines are obtained. Furthermore, plants derived from this only transplastomic line developed a yellow or variegated phenotype in the case of viral IL-10, and slightly deformed and curled leaves in the case of the murine transgene (Figure 7).

Interference of IL-10 with gene expression (e.g., at the level of codon usage) in the chloroplast was excluded in light of the fact that obvious toxicity problems, although with a different phenotype, arose also when the transgenes were expressed in the nucleus. This observation, together with the fact that the sequences of the murine and viral versions of IL-10 are highly homologous only at the amino acid level and retain an almost identical quaternary structure, strongly suggest that the IL-10 protein itself, and most probably its dimeric form, is responsible for the phenotypic alterations observed. The yellow phenotype could suggest a deleterious interaction of the recombinant protein with the plant photosynthetic apparatus. This has been seen before, for example, in a study where the outer surface protein A (OspA) produced in tobacco chloroplasts strongly affected the photosystem II in a concentration-dependent manner, rendering the plants unable to grow without exogenously supplied sugars (Hennig et al., 2007). However, in the case of IL-10, the impaired growth of transplastomic plants already on complex medium in the tissue culture led us to exclude that IL-10 interferes directly with photosynthesis, because the plantlets grew slowly and developed abnormalities despite the availability of nutrients, in particular sugars as carbon source. Interestingly, vIL-10 expression was accompanied by a sharp decline in the accumulation of plastid-encoded proteins, most notably Rubisco, by far the most abundant protein in plant cells (Figure 12). This observation raised the hypothesis that vIL-10 might interfere with the overall translation or protein folding processes, possibly by interacting with molecular chaperons or translation factors. However, to date, there is no published evidence or indication of such an interaction.

Sequencing of the promoter region of both transgenes indicated that the lack of IL-10 accumulation was a direct consequence of recombination events that had occurred within the plant, leading to either the deletion of the first 40-50 nucleotides of the IL-10 ORF or to the exchange of the transgene promoter (*Prrn*-long) with the weaker version (*Prrn*-short) (Figure 11). In fact, although the shorter *Prrn* promoter still contains the -35 consensus sequence and the -10 element, it is apparently much less active than the full length promoter (Zhou et al., 2008). Northern and western blot analyses indicated that the yellow phenotype observed for the viral IL-10 construct correlated with high mRNA and detectable foreign protein accumulation levels, indicating that even extremely low amounts of IL-10 are apparently detrimental to the plant. A yellow and variegated phenotype similar to the one observed for vIL-10, and an analogous correlation of high transgene mRNA accumulation levels with yellow and low transcript amounts with green plants or plant sectors, have been

recently described by Zhou *et al*. (2008). In that work, Nef-expressing transplastomic plants were generated by transformation of *N. tabacum* cv. Petit Havana with a plasmid based on the same pRB95 vector, and five out of 14 independently generated transplastomic lines displayed the altered phenotype. Analysis of the promoter region in those plants revealed an inverse relationship between expression and/or accumulation of AadA and Nef, and a positive correlation of the yellow phenotype with very high accumulation levels of the recombinant protein (~4 % TSP). As upon expression of Nef in the chloroplast as a fusion protein with p24, massive accumulation levels were reached without causing growth abnormalities (up to roughly 40% of TSP), the authors could exclude that the phenotypic alterations observed upon expression of Nef alone were the result of the exhaustion of the gene expression capacity of the chloroplast by overuse of its ribosomes for the production of the recombinant protein. They rather suggested a toxic effect of Nef, possibly caused by interference of the lipidated (Glenz et al., 2006) N-terminus of the recombinant protein with thylakoid structure and function which, in turn, would inhibit photosynthesis. Similarly, in the case of IL-10, the amount of the recombinant protein in transplastomic plants is so low that it is extremely improbable that such accumulation levels are exhausting the overall protein production capacity of the chloroplast. Instead, a more general harmful effect of the cytokine to the cell metabolism and/or development is more likely, also considering the plant's stunted phenotype and the cell death symptoms observed upon nuclear expression of the same proteins (III.2). The alterations of the original genome configuration leading to the exchange of the promoters between the transgene and *aadA* that were found for the only transplastomic line obtained, in the case of murine IL-10 (Figure 11), and in all lines generated, in the case of Nef (Zhou et al., 2008), indicate that there might be some selective pressure favouring the recombination product over the original configuration. This selective pressure could be either enhancement of the antibiotic resistance level, as achieved by combination of aadA with a stronger promoter which should confer a fitness advantage to the high selective pressure of spectinomycin, or a decrease in the expression level of the antigens, if high-level transgene expression is selected against. The antibiotic concentration that was used for transplastomic tissue selection in both studies is in accordance to the standard protocols for chloroplast transformation and it has never been reported as toxic, rendering the augmented antibiotic resistance level a weak explanation for the recombination events observed. Additionally, for the viral IL-10, the rearrangements occurred within the IL-10 expression cassette region and should not result in an increase in

AadA synthesis, because the *aadA* gene retained the short version of the promoter, but undoubtedly caused a reduced transgene expression and recombinant protein synthesis (Figure 11). Therefore, a high selective pressure against high-level IL-10 accumulation is definitely the most likely explanation for the results obtained upon chloroplast expression of IL-10.

If this is the case, it implies that even if the promoter rearrangements could be prevented by replacing the short *Prrn* promoter upstream the *aadA* gene with the strong version in the pRB95 vector, this would probably prevent the regeneration of any transplastomic plants, because high levels of toxic IL-10 would be lethal to the plant cells. Therefore, it becomes clear that a prerequisite to increase IL-10 accumulation levels in the chloroplast would be to understand the molecular basis of IL-10 interference with essential functions in this cell compartment, in order to generate truncated versions of IL-10 or design fusion proteins aimed at preventing the detrimental effects of IL-10 to the chloroplast. However, this is not a trivial task, especially considering that IL-10 has to be dimeric to retain its biological activity, and even little changes in the amino acid sequence of the protein might severely invalidate its conformation-dependent functionality, and tackling this problem was beyond the scope of this PhD work.

IV.2 Nuclear expression of IL-10 and subcellular targeting

The intracellular targeting of a recombinant protein often has a significant effect on its yield and, in some cases, also on its biological properties. In this work, targeting of both versions of IL-10 to three different subcellular compartments – the ER, cytosol and apoplast – was investigated in order to assess the impact on protein accumulation, and with the aim of exploiting the most promising strategy to generate stable transgenic tobacco plants. Preliminary studies of murine IL-10 transient expression driven by a PVX-based system in *N. benthamiana* (data not shown), had indicated that the ER was by far the most suitable compartment for mIL-10 accumulation compared to the cytosol and the apoplast, where IL-10 seemed to be extremely unstable (ER-retained reached around 10 μg/g FLW; cytosolic and apoplastic expression was nearly undetectable as determined by immunoblot analyses). A promising strategy to stabilize recombinant proteins which are otherwise

rapidly degraded in the cytosol or the apoplast, is to associate them with the plasma membrane (Vitale and Pedrazzini, 2005). Therefore, in the attempt to increase the overall IL-10 accumulation levels, new targeting constructs were generated to fuse the IL-10 sequence to membrane anchors that allow the recombinant proteins to be exposed to the apoplast or cytosol while retaining them in the membrane. To anchor IL-10 to the cytosolic side of the ER membrane, the mammalian ER isoform of cytochrome *b5* (cyt*b5*), a protein belonging to the type IV transmembrane polypeptides, also called tail-anchor (TA) proteins (Borgese et al., 2003), was exploited. Cyt*b5* does not have an N-terminal signal but holds a hydrophobic transmembrane domain (TDM), followed by a few polar luminal residues at the C-terminus, that allows spontaneous integration into the cytosolic face of the endoplasmic reticulum membrane post-translationally (D'Arrigo et al., 1993). To anchor IL-10 to the apoplastic side of the plasma membrane, instead, IL-10 was fused to the transmembrane domain of the human T cell receptor β chain, maintaining the native IL-10 signal peptide sequence to direct the recombinant protein into the secretion pathway. Both mammalian transmembrane domains have already been shown to be effective membrane anchors in plant cells, and to increase stability of the fused recombinant proteins (Schillberg et al., 2000; Barbante et al., 2008). For both murine and viral IL-10 these constructs, and the one for ER retention, were cloned into the pTRAkt binary vector for plant expression.

The three targeting strategies were evaluated by transient expression in tobacco leaves following agroinfiltration, since this provides a reliable indication of performance much more rapidly than the generation of stably transformed plants. Transient expression of the construct, by either vacuum-infiltration of detached leaves or by agroinjection on whole plants, showed a detrimental effect of both murine and viral IL-10, that was clear in its symptoms (dryness and necrosis of the infiltrated area) and dependent on the recombinant protein localization (apoplast and ER for the viral, apoplast and cytosol for the murine IL-10, respectively), but varied in intensity and reproducibility in between the experiments (Figure 16). Nevertheless, reliable recombinant protein quantification and comparison of all the constructs tested in parallel was possible, sampling the infiltrated leaf material before the onset of the cell death symptoms. Despite the addition of membrane anchors to stabilize the recombinant proteins in the cytosol and the apoplast, both versions of IL-10 accumulated to the highest levels in the ER, confirming the previous observation for mIL-10 with the PVX-mediated expression, and in line with what has been observed for hIL-10 stably expressed in tobacco (Menassa et al., 2004). An immunoblot evaluation of the

recombinant viral IL-10 bearing the membrane anchors transiently expressed in agroinfiltrated leaves was not possible, as the accumulation levels of the membrane-anchored versions of the viral interleukin were too low to be visualized by immunodetection on a western blot without prior protein purification or concentration (Figure 15). The absence of an immunoblot that, showing the size of the products, would ensure the authentic expression of the heterologous proteins, could rise some concerns on the real expression of the constructs, considering the extremely low IL-10 amounts measured by ELISA. However, it has to be pointed out that the ELISA setups that were used for quantification are extremely sensitive (down to ~10 pg/ml for the viral and to ~50 pg/ml for the murine IL-10, respectively) and highly specific (no cross-reactivity was observed with protein extracts of wt tobacco plants) ensuring a reliable determination of even very low amounts of recombinant protein in the crude leaf extracts. Additionally, considering that the sandwich ELISA for both murine and viral IL-10 were performed with two different monoclonal antibodies for coating and capturing, which recognize different epitopes on the molecules, it is very unlikely that the accumulation levels measured for the membrane-anchored IL-10 are artefacts. Moreover, as already mentioned, the accumulation levels measured, as well as the increased stability of IL-10 in the ER, are in line with the results reported by Menassa and colleagues for the highly homologous human IL-10 (Menassa et al., 2001; Menassa et al., 2004), suggesting that the extremely low amounts of IL-10 facing the cytosol and the apoplast are the results of the protein instability and/or susceptibility to degradation, rather than the impaired expression of the targeting constructs. Many other recombinant proteins have also accumulated to the highest levels in the ER when different targeting strategies were compared (Conrad and Fiedler, 1998; Twyman et al., 2005; Petruccelli et al., 2006). The data obtained in this work confirm the beneficial environment within the ER, favoring correct protein folding and assembly, and high protein stability.

Stable transgenic tobacco plants were therefore generated with the constructs that yielded the highest accumulation levels by targeting the recombinant proteins to the endoplasmic reticulum. In T_1 transgenic plants, the highest level of mIL-10 accumulation was 37.0 µg/g FLW (0.6% total soluble protein (TSP)) and the highest level of vIL-10 accumulation was 10.8 µg/g FLW (0.1% TSP). These yields fall into the 0.1-1.0% TSP range typically observed for pharmaceutical proteins produced in nuclear transgenic plants (Twyman et al., 2003) and are much higher than the 0.0055% TSP previously reported for the ER-targeted

hIL-10, which is very similar in structure to the murine and viral orthologs (Menassa et al., 2001). The accumulation of murine IL-10 increased between the T_0 and T_1 generations (form 21.3 to 37.0 μg/g FLW), indicating that recombinant protein yields are partly dependent on the transgene copy number and/or zygosity. Differently, for vIL-10 an improvement in protein accumulation levels between the T_0 and T_1 generations could not be observed (8.9 and 10.8 μg/g FLW, respectively), most likely because expression of the viral cytokine caused a phenotype, whose severity correlated with the level of protein accumulation, and the highest vIL-10 accumulating T_0 plants did not produce seeds.

In addition to the macroscopic phenotypic alterations observed, ultrastructural analysis of transgenic leaves expressing high levels of vIL-10 revealed an increased number of plastoglobules within the chloroplasts. Plastoglobules are lipid bodies produced by plastids which constitute a distinct structural and functional sub-compartment of thylakoids, and contain both lipid binding proteins and enzymes involved in lipid biosynthesis and metabolism. Plastoglobule numbers increase in plants subjected to environmental conditions that increase oxidative stress on the photosynthetic apparatus. These include high concentrations of CO_2 (Sallas et al., 2003), drought (Munne-Bosch and Alegre, 2001), high saline concentration (Sam et al., 2003) and viral infection (Hernandez et al., 2004). In fact, it has been shown that plastoglobules contain the enzyme tocopherol cyclase, whose increased activity during oxidative stress protects the thylakoid membranes and photosynthetic proteins form oxidative damage caused by activated oxygen species (Austin et al., 2006). The increased number of plastoglobules within the chloroplasts of transgenic tobacco leaves accumulating high levels of viral IL-10, therefore, most likely represents a sign of cellular stress associated with the expression of the viral cytokine.

Excluded that the phenotypic abnormalities observed for the vIL-10 transgenic plants could be the result of transgene position effects – as they were observed for many independent transgenic lines – or somehow related to the *in vitro* tissue culture conditions – as they persisted also in the T_1 generation – they were most likely caused by the expression of the recombinant protein itself. Therefore, expression of the recombinant protein in BY2 cells was also investigated, hoping that viral IL-10, whatever the cause of its harmfulness might be, would not be detrimental to the plant cell in this expression system and could reach higher yields. However, in tobacco cell suspension cultures, accumulation levels of murine IL-10 were almost one order of magnitude higher than those reached for the viral cytokine,

despite no obvious phenotype of the transgenic cells expressing vIL-10 (Figure 22). Interestingly, inducible expression of the viral transgene driven by a tetracycline inducible promoter, led to an increase in vIL-10 accumulation levels of 3.5 fold compared to those reached using a constitutive promoter in the same expression platform (Figure 26). These results show that vIL-10 accumulation levels can be improved upon usage of an inducible transgene expression system, may possibly be further increased with additional optimization of the induction conditions, and indirectly confirm that, at least to some extent, vIL-10 is harmful to plant cells above a certain threshold. Likewise, inducible expression of vIL-10 should also lead to higher accumulation levels in whole plants, and generation of stable transgenic tobacco lines exploiting a regulatory system that allows transgene expression at a defined time point is a promising strategy that remains to be explored.

IV.3 Characterization of plant-derived IL-10

The expression of a recombinant protein containing a native signal peptide requires the signal peptide to be correctly interpreted by the heterologous host cell, otherwise the protein could be improperly cleaved or not cleaved at all. This is especially relevant for pharmaceutical proteins, where imprecise cleavage could affect the biological activity of the protein and might raise safety concerns (Streatfield, 2007). The mIL-10 signal peptide was correctly processed in tobacco, as shown by sequencing the N-terminal peptide of the mature protein, which had the same QYSRE N-terminus previously reported for native mIL-10 (Moore et al., 1993). There are at least two different N-terminal sequence reported for vIL-10: QCDNF and TDQCD. The former is claimed in several publications (Zdanov et al., 1997; Ding et al., 2000; Yoon et al., 2005) and is most likely based on the prediction first reported by Moore and colleagues (Moore et al., 1990). The latter is predicted by the latest version of the widely-used SignalP 3.0 Server (Bendtsen et al., 2004; Emanuelsson et al., 2007), and is reported in at least one publication (Salek-Ardakani et al., 2002). Tandem MS analysis of the N-terminal peptide of the purified vIL-10 produced in tobacco showed the N-terminal sequence to be TDQCD, in line with the prediction of the SignalP 3.0 Server (Figure 30). To our knowledge, this is the first time that the N-terminal amino acidic sequence of mature vIL-10 determined by bioinformatic tools, has been experimentally confirmed following expression in a eukaryotic cell.

Although vIL-10 is not glycosylated (Hsu et al., 1990), both the native and recombinant mIL-10 are heterogeneously *N*-glycosylated at an acceptor site near the N-terminus (Moore et al., 1990). This glycosylation has no known influence on mIL-10 activity (Moore et al., 2001), but the presence of plant complex type *N*-glycans on therapeutic glycoproteins renders them potentially immunogenic and thus raises safety concerns, particularly in the case of parenteral administration. Even so the potential immunogenicity of plant glycans may also be important for orally administered proteins, especially in patients with severe food allergies. The glycan modifications that occur in the ER produce high-mannose-type *N*-glycans that are conserved between mammals and plants, so the use of a KDEL signal for ER retention not only increases protein yields, but also prevents the addition of plant complex type glycans. *N*-glycan analysis (Figure 29) indicated that mIL-10 bears only ER-specific glycans in young plants, while in mature plants, although carrying a SEKDEL tag, is not efficiently retrieved to the ER, and is modified by enzymes located in the *trans*-Golgi network (Fitchette et al., 1994; Pagny et al., 2000). In addition, the presence of terminal GlcNAc residues on the complex glycan structures would suggest that mIL-10 escaping the ER is secreted by the plant cell and not, for example, directed to the vacuole (Lerouge et al., 1998). The high efficiency of ER retrieval has been documented for a number of recombinant proteins produced in plants (Gomord et al., 1997; Frigerio et al., 2001; Sriraman et al., 2004), but there are also several examples of KDEL-tagged recombinant proteins containing complex type glycans, indicating that the retrieval system can be leaky and must be evaluated on a case-by-case basis (Triguero et al., 2005; Floss et al., 2008). As immunoblot analysis of the purified protein confirmed that the KDEL-tag is still present (Figure 31) and IL-10 yields are not high enough to suggest saturation of the KDEL retrieval machinery (Crofts et al., 1999), the most likely explanation for the presence of complex type *N*-glycans on mIL-10 is that the tag is partially occluded following assembly of the IL-10 dimer, and is not completely accessible to the KDEL receptor. As a matter of fact, limited exposure of the KDEL sequence has previously been discussed as a potential explanation for differences in retrieval efficiency for different recombinant proteins (Sriraman et al., 2004).

Non-reducing SDS-PAGE followed by immunoblot analysis and (for mIL-10) gel filtration analysis confirmed that both vIL-10 and mIL-10 assemble into dimers in tobacco leaves. Moreover, it appears that the dimerization of both plant-derived versions of IL-10 is more efficient than that of their commercially produced counterparts (Figure 27). Since the higher

dimer/monomer ratio is consistent regardless of the total amount of protein loaded onto the gel, the possibility that this is an artifact caused by high protein concentration can be ruled out. It is also unlikely that the presence of plant glycans is responsible, since vIL-10 is not glycosylated. The most probable explanation is that the presence of the C-terminal SEKDEL and His_6 tags may enhance the stability of the dimers. However, to confirm this assumption, it would be necessary to express non-tagged versions of the proteins and compare the dimer/monomer ratios. Increased stability of plant-derived IL-10 dimers was also observed for hIL-10 by Menassa and colleagues (Menassa et al., 2001). Interestingly, hIL-10 is not glycosylated and the C-terminal tags had been cleaved from the plant-derived hIL-10 by thrombin digestion, which should remove all additional amino acids except a lysine and a valine. This would suggest that as little as two additional amino acids are sufficient to increase the stability of the IL-10 dimer; however, the authors did not comment on this.

The ability of both vIL-10 and mIL-10 to form dimers indicated that the recombinant proteins were likely to retain their biological activity, a hypothesis that was tested by exposing LPS-stimulated J774 mouse macrophage cells to different amounts of recombinant IL-10 and assaying the effect on downstream components of the signaling pathway. A clear dose-dependent effect on STAT3 phosphorylation after treatment with both variants of IL-10 was observed, indicating that the plant-derived proteins properly interacted with the IL-10 receptor and initiated the signal transduction cascade. Moreover, mIL-10 was able to upregulate the expression of the intracellular negative regulator of cytokine responses, SOCS3. Most importantly, given that IL-10 is best known for its ability to inhibit pro-inflammatory cytokine and chemokine expression in LPS-stimulated macrophages, it was demonstrated that both mIL-10 and vIL-10 are able to inhibit the LPS-induced production of TNFα. Higher doses of the plant-derived proteins as compared to the corresponding commercial IL-10 products were required. As put forward also in the discussion of the increased stability of the plant-produced IL-10 dimers compared to the commercial counterparts, it seems very unlikely that plant glycans are responsible for the higher doses of plant-derived IL-10 required to elicit the same biological response in *in vitro* assays, because the viral variant of this cytokine is not glycosylated. Therefore, the most plausible difference that could account for this discrepancy is the presence of the KDEL and His_6 tag sequences at the C-terminus of the plant-produced proteins. As a matter of fact, preliminary results from the laboratory showed that murine IL-10 bearing the KDEL tag (without the His_6 tag), expressed in *Arabidopsis thaliana* seeds, is able to induce STAT3

phosphorylation and to inhibit LPS-induced TNFα secretion to the same extent of the commercial mIL-10 in *in vitro* assays using the same J774 macrophage cell line (Francesca Morandini 2009, PhD thesis). This observation strongly suggests that the presence of the His_6 tag at the C-terminus of the protein is responsible for the slightly lower biological activity of the murine IL-10 purified from tobacco leaves. This could be due to little modifications of the IL-10 dimer structure, possibly caused by repulsion between the two charged histidine tails brought in proximity upon formation of the dimer. To confirm this assumption, however, the viral version of the cytokine bearing only the KDEL tag should also be generated and tested *in vitro* for its biological activity. Additionally, structural analyses of the IL-10 dimers with or without His-tag could also be performed to verify eventual conformational modifications between the different variants. Nevertheless, it is important to point out that this slightly lower biological activity of plant-derived IL-10 compared to the commercial counterparts will have no impact on the planning of feeding studies since the dose of IL-10 necessary to enhance oral tolerance needs to be determined empirically by administering different amounts of transgenic plant material to the mice.

As the future goal is to deliver IL-10 expressed within the plant tissue as a dietary supplement to NOD mice, it was critical to determine whether plant-produced IL-10 was resistant to gastrointestinal degradation, and whether the plant cellular matrix contributed to any protection against enzymes and low-pH conditions. *In vitro* studies with simulated digestive solutions are widely used as models of animal digestion to investigate the controlled release of experimental pharmaceuticals (Doherty et al., 1991), as well as the digestibility of plant and animal proteins and food additives (Zikakis et al., 1977; Tilch and Elias, 1984). The stability of murine and viral IL-10 produced in transgenic plants, either embedded in the lyophilized tobacco tissue or purified form the plant tissue, was compared using simulated gastric fluid (SGF) to model stomach conditions, and simulated intestinal fluid (SIF) for proximal small bowel conditions. Both variants of the cytokine resulted more resistant to gastric degradation when retained within the leaf tissue in both simulated fluids, indicating that the plant matrix indeed contributes to protect the recombinant proteins against proteolytic enzymes (Figure 36). Moreover, a slightly increased resistance to simulated gastrointestinal degradation was observed also for plant produced IL-10s compared to the commercial counterparts, which, once again, may be a result of the increased stability of the dimer produced in plants. In SGF experiments, the increased stability of IL-10 embedded in leaf tissue was especially relevant in the case of the viral

IL-10. Perhaps this is due to the fact that transgenic plants expressing this cytokine, but not the murine one, have thicker and harder leaves, among the other phenotypic abnormalities, which render them more resistant to degradation. Taken together, these results indicate that murine and viral IL-10 are protected in plant tissue. This enhanced resistance to degradation within the gut represents and advantage for transgenic plant delivery of IL-10 and supports the concept of edible vaccines, as biologically relevant amounts of recombinant protein could be directly delivered to the GALT using the oral administration of minimally processed plant material.

IV.4 Deleterious effects of heterologous IL-10 expression

Leaving untouched the promising results achieved in this thesis, it seems important to make a conclusive remark and overview of the problems associated with the expression of these recombinant proteins in plants. In fact, in order to succeed in establishing plants as a competitive platform for production of high amounts of IL-10, it is a fundamental prerequisite to overcome or avoid the detrimental effects caused by high accumulation levels of the recombinant protein.

In this PhD work, IL-10 - be it murine or viral - has shown to be harmful, at least to some extent, in all subcellular compartments investigated, and the amount of recombinant protein sufficient to cause cell death seemed to depend on the protein localization (i.e. the different accumulation levels, but same phenotype, observed upon transient expression of the targeting constructs by agroinfiltration). Expression of IL-10 in the chloroplast was also not tolerated by the plant. Unfortunately, as already mentioned, it was not possible to find in the available literature or in the existing protein databases any evidence or indication of a possible interaction of neither murine nor viral IL-10 with any plant cell components.

The highly homologous human IL-10 has been expressed in nuclear transformed tobacco plants (Menassa et al., 2001; Menassa et al., 2004; Patel et al., 2007). As a matter of fact, in their works Menassa and colleagues report extremely low accumulation levels in all the subcellular compartments investigated (ER, cytosol, chloroplast, mitochondrion; at the most 0.0055% TSP in the ER) and unusually low numbers of transgenic plants regenerated and analyzed for each construct (from 16 to 22). In the light of the results obtained in this PhD work, these observations raise the doubt that high hIL-10 expressing lines could not be

regenerated from the *in vitro* cultures or that high expressing shoots have been discarded as unhealthy during the experimental work, transferring only the good looking – but low expressing – ones into soil. However, the authors deny any regeneration problems or altered phenotype encountered upon human IL-10 expression in tobacco (Rima Menassa, personal communication), and are focusing their research on proving mistargeting of the recombinant protein into the vacuole and its consequent degradation therein (R. Menassa *et al,*. PBVA conference 2006, poster presentation).

Conversely, a research group at the Arkansas State University that has also performed nuclear stable transformation of tobacco with the sequence encoding human IL-10, encountered major difficulties in regenerating transgenic plants, observed a stunted phenotype with thick, curled leaves very similar to the one here reported for nuclear expression of the viral IL-10, and extremely low accumulation levels that induced them to abandon the project without further investigating the causes of such abnormalities (Maureen Dolan, personal communication).

Intriguingly, Lothar Steidler and co-workers at the University of Cork, Ireland, who successfully expressed human IL-10 in *Lactococcus lactis* (Schotte et al., 2000; Steidler et al., 2000), refer that in all the other bacterial species they tested hIL-10 expression was lethal (Bradbury, 2003).

The results on murine and viral IL-10 expression, together with these information on the human one, prompt to think that IL-10 harmfulness is indeed related to the protein itself, and most probably to its quaternary structure, which is highly conserved among the three cytokine variants. Moreover, it seems clear that IL-10 must interfere with some molecule or structure which is conserved among plant cells, chloroplasts and bacteria.

To prove whether the protein itself was responsible for the observed detrimental effects, either the plant-derived or the commercial IL-10 were injected into tobacco leaves, but no alterations or necrosis of the infiltrated area could be detected (not shown). This could be due to the inadequate amount of protein used, or simply reflect the fact that IL-10 is only deleterious within the plant cell and could not enter the plasma membrane upon injection into the apoplast. This experiment, therefore, does not allow clear conclusions. Attempts to isolate a putative binding partner of IL-10 within the plant cell, performing *in vivo* cross-linking by formaldehyde infiltration of transgenic leaves and subsequently purifying the his-tagged IL-10 by IMAC, were also not successful (not shown). Immunoprecipitation

of the recombinant protein from stable transgenic or agroinfiltrated leaf extracts is another possibility that could be considered in the future to identify possible interacting molecules.

Unraveling the molecular mechanisms underlying the serious adverse effects of IL-10 seems to be the basic requirement to develop future strategies to achieve satisfactory accumulation levels of IL-10 in various expression systems.

V CONCLUSIONS AND FUTURE PERSPECTIVES

Taken together, the results presented in this thesis clearly demonstrate that tobacco plants can express the viral and murine IL-10 genes, and correctly process and assemble the corresponding proteins into functional, biologically-active dimers.

Further strategies could be employed to boost accumulation of mIL-10 avoiding its detrimental effects, e.g. exploiting sequences for the accumulation and sequestration in oil or protein bodies, or through the co-expression of shielding molecules (Patel et al., 2007). In the case of vIL-10, as already mentioned, generation of stable transgenic plants with the transgene under the control of inducible promoters would allow expression in a target tissue only following a specific treatment, such as chemical spraying, restricting recombinant protein accumulation to a fine timeframe to limit detrimental effects on plant growth and perhaps leading to higher vIL-10 yields (Streatfield, 2007). Nevertheless, it has to be pointed out that the yields of both recombinant proteins in tobacco plants generated during this work are already high enough to allow delivery to mice of an immunologically relevant dose of IL-10 in a reasonable amount of leaf material, without the need of extensive purification. In fact, on the basis of comparable feeding experiments (Ma et al., 2004), 2-10 μg of IL-10 per day should be sufficient to elicit immunomodulatory effects; this would require the administration of a few milligrams of lyophilized plant tissue, which could be ingested by a mouse without substantially interfering with its dietary needs and should be well tolerated by the animals (Menassa et al., 2007). Additionally, in simulated digestion experiments, it was demonstrated that IL-10 is protected in the plant tissue, as the plant cellular matrix confers resistance to degradation within the gut. This represents a great advantage for transgenic plant delivery of IL-10, and underlines the suitability of exploiting tobacco as production platform for IL-10 aimed at oral administration.

The use of tobacco as expression system for heterologous proteins aimed at oral administration may raise concerns related to the fact that it is not an edible plant. As a matter of fact, the common practice for oral delivery of recombinant antigens produced in tobacco is their purification and administration by gastric intubation. Certainly, if the proof-of-concept in the NOD mice will be demonstrated and oral delivery of IL-10 will be

confirmed as a promising strategy to enhance oral tolerance to co-fed antigens, it will be necessary to consider edible plants as expression systems for the production of this cytokine in order to further proceed with the studies and, eventually, with the clinical trials. However, for our purposes, delivery of unprocessed tobacco leaf material to mice does not represent a limitation.

Therefore, this work paves the way to performing feeding studies in animal models of autoimmune diseases to comparatively evaluate the effectiveness of the viral and murine IL-10 as immunomodulators. In particular, it will allow to determine whether simultaneous feeding of NOD mice with plant material containing GAD65 and IL-10 could reduce the amount of auto-antigen necessary to prevent the onset of T1DM.

VI SUMMARY

Interleukin-10 (IL-10) is a potent anti-inflammatory cytokine, with therapeutic applications in several autoimmune and inflammatory diseases. Oral administration of this cytokine, alone or in combination with disease-associated autoantigens, could confer protection form the onset of a specific autoimmune disease through the induction of oral tolerance.

Transgenic plants are attractive systems for production of therapeutic proteins because of the ability to do large scale-up at low cost, and the low maintenance requirements. They are highly amenable to oral administration and could become effective delivery systems without extensive protein purification.

The ability of tobacco plants to produce high levels of biologically-active viral and murine IL-10 was investigated. To reach high accumulation levels of the transgenes, plastid transformation of the IL-10 genes as well as different targeting strategies of the nuclear encoded recombinant proteins were investigated. Chloroplast transformation turned out not to be a feasible approach for the recombinant production of IL-10, as unsatisfactory accumulation levels were obtained upon expression of both transgenes.

For tobacco nuclear transformation, three different subcellular targeting strategies, directing the recombinant protein into the endoplasmic reticulum (ER), cytosol and apoplast, were first assessed in transient expression experiments, and stable transgenic plants were then generated with the constructs that yielded the highest accumulation levels by targeting the recombinant proteins to the ER. The recombinant proteins were purified from transgenic leaf material and characterized in terms of their *N*-glycan composition, dimerization, stability and biological activity in *in vitro* assays. Both molecules formed stable dimers, were able to activate the IL-10 signaling pathway and to induce specific anti-inflammatory responses in mouse J774 macrophage cells.

It was therefore demonstrated that tobacco plants are able to correctly process viral and murine IL-10 into biologically active dimers, representing a suitable platform for the production for these cytokines. The accumulation levels obtained are high enough to allow delivery of an immunologically relevant dose of IL-10 in a reasonable amount of leaf material, without extensive purification. This study paves the way to performing feeding

studies in mouse models of autoimmune diseases, that will allow evaluation of the immunomodulatory properties and effectiveness of the viral and murine IL-10 in inducing oral tolerance.

RIASSUNTO

L'interleuchina-10 (IL-10) e' una citochina immunosoppressiva con potenziale applicazione terapeutica in diverse malattie autoimmuni e infiammatorie. La somministrazione orale di questa citochina, da sola o in combinazione con autoantigeni associati alla malattia, potrebbe conferire protezione dall'insorgenza di specifiche malattie autoimmuni attraverso l'induzione di tolleranza orale.

Un valido sistema alternativo per la produzione di proteine ricombinanti di interesse farmaceutico è rappresentato dalle piante transgeniche, data la possibilità di estendere la produzione su larga scala a bassi costi, e i minimi requisiti che richiedono per il loro mantenimento. Le piante, inoltre, possono essere assunte direttamente come alimento e potrebbero diventare esse stesse veicoli per la somministrazione delle proteine ricombinanti eliminando la necessità di purificarle.

Ci si è proposti di valutare se le piante di tabacco fossero in grado di produrre alti livelli di IL-10 virale e murina biologicamente attiva. Per ottenere alti livelli di espressione dei transgeni, sono state effettuate sia la trasformazione dei plastidi, sia la trasformazione nucleare, valutando diverse strategie di localizzazione delle proteine ricombinanti. La trasformazione dei cloroplasti è risultato un approccio non attuabile per la produzione di IL-10 virale o murina ricombinante, in quanto i livelli di accumulo sono risultati decisamente insoddisfacenti per entrambi i transgeni.

Invece, per quanto riguarda la trasformazione nucleare, sono state valutate tre diverse strategie di localizzazione sub-cellulare, per dirigere la proteina ricombinante nel reticolo endoplasmico (RE), nel citosol e nell'apoplasto, dapprima in esperimenti di espressione transiente e, successivamente, sono state generate piante transgeniche stabili con il costrutto che aveva fornito i più alti livelli di accumulo indirizzando la proteina nel RE. Le proteine ricombinanti sono state purificate da materiale fogliare transgenico e sono state caratterizzate rispetto alla composizione degli *N*-glicani, alla dimerizzazione, alla loro stabilità e attività biologica in saggi *in vitro*. Entrambe le molecole prodotte in pianta formano dimeri stabili, e sono in grado di attivare la cascata di trasduzione del segnale di IL-10 e di indurre risposte anti-infiammatorie specifiche nella linea cellulare di macrofagi murini J774.

E’ stato dimostrato che le piante di tabacco sono in grado di processare correttamente l’IL-10 virale e murina in dimeri biologicamente attivi, e che quindi rappresentano una valida piattaforma per la produzione di queste citochine. Inoltre, i livelli di accumulo ottenuti sono sufficientemente elevati da permettere di somministrare una dose immunologicamente rilevante di IL-10 in una ragionevole quantità di materiale fogliare, senza richiedere laboriose purificazioni.

Questo lavoro apre la strada alla realizzazione di studi di somministrazione orale in modelli murini di malattie autoimmuni, che permetteranno di effettuare una valutazione comparativa delle proprietà immunomodulatorie nonché dell’efficacia delle IL-10 virale e murina nell’indurre tolleranza orale.

VII REFERENCES

Adam, Z. and Clarke, A.K. (2002) Cutting edge of chloroplast proteolysis. *Trends Plant Sci*, **7**, 451-456.

Adang, M.J., Brody, M.S., Cardineau, G., Eagan, N., Roush, R.T., Shewmaker, C.K., Jones, A., Oakes, J.V. and McBride, K.E. (1993) The reconstruction and expression of a Bacillus thuringiensis cryIIIA gene in protoplasts and potato plants. *Plant Mol Biol*, **21**, 1131-1145.

Anandalakshmi, R., Pruss, G.J., Ge, X., Marathe, R., Mallory, A.C., Smith, T.H. and Vance, V.B. (1998) A viral suppressor of gene silencing in plants. *Proc Natl Acad Sci U S A*, **95**, 13079-13084.

Asadullah, K., Friedrich, M., Hanneken, S., Rohrbach, C., Audring, H., Vergopoulos, A., Ebeling, M., Docke, W.D., Volk, H.D. and Sterry, W. (2001) Effects of systemic interleukin-10 therapy on psoriatic skin lesions: histologic, immunohistologic, and molecular biology findings. *J Invest Dermatol*, **116**, 721-727.

Asadullah, K., Sterry, W. and Volk, H.D. (2003) Interleukin-10 therapy--review of a new approach. *Pharmacol Rev*, **55**, 241-269.

Austin, J.R., 2nd, Frost, E., Vidi, P.A., Kessler, F. and Staehelin, L.A. (2006) Plastoglobules are lipoprotein subcompartments of the chloroplast that are permanently coupled to thylakoid membranes and contain biosynthetic enzymes. *Plant Cell*, **18**, 1693-1703.

Ausubel, F., Brent, R. and Kingston, R. (1994). Wiley, Interscience, New York.

Ausubel, F., Brent, R. and Kingston, R. (1998) *Current Protocols in Molecular Cloning*. Wiley, Interscience, New York.

Avesani, L., Falorni, A., Tornielli, G.B., Marusic, C., Porceddu, A., Polverari, A., Faleri, C., Calcinaro, F. and Pezzotti, M. (2003) Improved in planta expression of the human islet autoantigen glutamic acid decarboxylase (GAD65). *Transgenic Res*, **12**, 203-212.

Balasa, B., La Cava, A., Van Gunst, K., Mocnik, L., Balakrishna, D., Nguyen, N., Tucker, L. and Sarvetnick, N. (2000) A mechanism for IL-10-mediated diabetes in the nonobese diabetic (NOD) mouse: ICAM-1 deficiency blocks accelerated diabetes. *J Immunol*, **165**, 7330-7337.

Barbante, A., Irons, S., Hawes, C., Frigerio, L., Vitale, A. and Pedrazzini, E. (2008) Anchorage to the cytosolic face of the endoplasmic reticulum membrane: a new strategy to stabilize a cytosolic recombinant antigen in plants. *Plant Biotechnol J*, DOI: 10.1111/j.1467-7652.2008.00342.x.

Bartlett, J.G., Alves, S.C., Smedley, M., Snape, J.W. and Harwood, W.A. (2008) High-throughput Agrobacterium-mediated barley transformation. *Plant Methods*, **4**, 22.

Battaglia, M. and Roncarolo, M.G. (2004) The role of cytokines (and not only) in inducing and expanding T regulatory type 1 cells. *Transplantation*, **77**, S16-18.

Becker, D. (1990) Binary vectors which allow the exchange of plant selectable markers and reporter genes. *Nucleic Acids Res*, **18**, 203.

Bendtsen, J.D., Nielsen, H., von Heijne, G. and Brunak, S. (2004) Improved prediction of signal peptides: SignalP 3.0. *J Mol Biol*, **340**, 783-795.

Berlato, C., Cassatella, M.A., Kinjyo, I., Gatto, L., Yoshimura, A. and Bazzoni, F. (2002) Involvement of suppressor of cytokine signaling-3 as a mediator of the inhibitory

effects of IL-10 on lipopolysaccharide-induced macrophage activation. *J Immunol*, **168**, 6404-6411.

Birch-Machin, I., Newell, C.A., Hibberd, J.M. and Gray, J.C. (2004) Accumulation of rotavirus VP6 protein in chloroplasts of transplastomic tobacco is limited by protein stability. *Plant Biotechnol J*, **2**, 261-270.

Bock, R. (2001) Transgenic plastids in basic research and plant biotechnology. *J Mol Biol*, **312**, 425-438.

Bock, R. (2007) Plastid biotechnology: prospects for herbicide and insect resistance, metabolic engineering and molecular farming. *Curr Opin Biotechnol*, **18**, 100-106.

Boehm, R. (2007) Bioproduction of therapeutic proteins in the 21st century and the role of plants and plant cells as production platforms. *Ann N Y Acad Sci*, **1102**, 121-134.

Borgese, N., Colombo, S. and Pedrazzini, E. (2003) The tale of tail-anchored proteins: coming from the cytosol and looking for a membrane. *J Cell Biol*, **161**, 1013-1019.

Bradbury, J. (2003) Designing bacteria and white cells to deliver drugs to the gut. *The Lancet*, **362**, 964-965.

Bradford, M.M. (1976) A rapid and sensitive method for the quantitation of microgram quantities of protein utilizing the principle of protein-dye binding. *Anal Biochem*, **72**, 248-254.

Brennan, F.R., Jones, T.D., Gilleland, L.B., Bellaby, T., Xu, F., North, P.C., Thompson, A., Staczek, J., Lin, T., Johnson, J.E., Hamilton, W.D. and Gilleland, H.E., Jr. (1999) Pseudomonas aeruginosa outer-membrane protein F epitopes are highly immunogenic in mice when expressed on a plant virus. *Microbiology*, **145 (Pt 1)**, 211-220.

Breyne, P., van Montagu, M., Depicker, A. and Gheysen, G. (1992) Characterization of a plant scaffold attachment region in a DNA fragment that normalizes transgene expression in tobacco. *Plant Cell*, **4**, 463-471.

Butaye, K.M., Goderis, I.J., Wouters, P.F., Pues, J.M., Delaure, S.L., Broekaert, W.F., Depicker, A., Cammue, B.P. and De Bolle, M.F. (2004) Stable high-level transgene expression in Arabidopsis thaliana using gene silencing mutants and matrix attachment regions. *Plant J*, **39**, 440-449.

Cassatella, M.A., Gasperini, S., Bovolenta, C., Calzetti, F., Vollebregt, M., Scapini, P., Marchi, M., Suzuki, R., Suzuki, A. and Yoshimura, A. (1999) Interleukin-10 (IL-10) selectively enhances CIS3/SOCS3 mRNA expression in human neutrophils: evidence for an IL-10-induced pathway that is independent of STAT protein activation. *Blood*, **94**, 2880-2889.

Christensen, A.H. and Quail, P.H. (1996) Ubiquitin promoter-based vectors for high-level expression of selectable and/or screenable marker genes in monocotyledonous plants. *Transgenic Res*, **5**, 213-218.

Christou, P. (1997) Rice transformation: bombardment. *Plant Mol Biol*, **35**, 197-203.

Commandeur, U., Twyman, R.M. and Fischer, R. (2003) The biosafety of molecular farming in plants. *AgBiotechNet*, **30**, 109-112.

Conrad, U. and Fiedler, U. (1998) Compartment-specific accumulation of recombinant immunoglobulins in plant cells: an essential tool for antibody production and immunomodulation of physiological functions and pathogen activity. *Plant Mol Biol*, **38**, 101-109.

Cramer, C.L., Boothe, J.G. and Oishi, K.K. (1999) Transgenic plants for therapeutic proteins: linking upstream and downstream strategies. *Curr Top Microbiol Immunol*, **240**, 95-118.

Crofts, A.J., Leborgne-Castel, N., Hillmer, S., Robinson, D.G., Phillipson, B., Carlsson, L.E., Ashford, D.A. and Denecke, J. (1999) Saturation of the endoplasmic reticulum retention machinery reveals anterograde bulk flow. *Plant Cell*, **11**, 2233-2248.

D'Arrigo, A., Manera, E., Longhi, R. and Borgese, N. (1993) The specific subcellular localization of two isoforms of cytochrome b5 suggests novel targeting pathways. *J Biol Chem*, **268**, 2802-2808.

Daniell, H. (2006) Production of biopharmaceuticals and vaccines in plants via the chloroplast genome. *Biotechnol J*, **1**, 1071-1079.

Daniell, H., Lee, S.B., Panchal, T. and Wiebe, P.O. (2001) Expression of the native cholera toxin B subunit gene and assembly as functional oligomers in transgenic tobacco chloroplasts. *J Mol Biol*, **311**, 1001-1009.

Davey, M.R., Rech, E.L. and Mulligan, B.J. (1989) Direct DNA transfer to plant cells. *Plant Mol Biol*, **13**, 273-285.

David, K.M. and Perrot-Rechenmann, C. (2001) Characterization of a tobacco Bright Yellow 2 cell line expressing the tetracycline repressor at a high level for strict regulation of transgene expression. *Plant Physiol*, **125**, 1548-1553.

De Cosa, B., Moar, W., Lee, S.B., Miller, M. and Daniell, H. (2001) Overexpression of the Bt cry2Aa2 operon in chloroplasts leads to formation of insecticidal crystals. *Nat Biotechnol*, **19**, 71-74.

de Waal Malefyt, R., Haanen, J., Spits, H., Roncarolo, M.G., te Velde, A., Figdor, C., Johnson, K., Kastelein, R., Yssel, H. and de Vries, J.E. (1991) Interleukin 10 (IL-10) and viral IL-10 strongly reduce antigen-specific human T cell proliferation by diminishing the antigen-presenting capacity of monocytes via downregulation of class II major histocompatibility complex expression. *J Exp Med*, **174**, 915-924.

Deblaere, R., Bytebier, B., De Greve, H., Deboeck, F., Schell, J., Van Montagu, M. and Leemans, J. (1985) Efficient octopine Ti plasmid-derived vectors for Agrobacterium-mediated gene transfer to plants. *Nucleic Acids Res*, **13**, 4777-4788.

Ding, Y., Qin, L., Kotenko, S.V., Pestka, S. and Bromberg, J.S. (2000) A single amino acid determines the immunostimulatory activity of interleukin 10. *J Exp Med*, **191**, 213-224.

Doherty, A.M., Kaltenbronn, J.S., Hudspeth, J.P., Repine, J.T., Roark, W.H., Sircar, I., Tinney, F.J., Connolly, C.J., Hodges, J.C., Taylor, M.D. and et al. (1991) New inhibitors of human renin that contain novel replacements at the P2 site. *J Med Chem*, **34**, 1258-1271.

Emanuelsson, O., Brunak, S., von Heijne, G. and Nielsen, H. (2007) Locating proteins in the cell using TargetP, SignalP and related tools. *Nat Protoc*, **2**, 953-971.

Fairbanks, G., Steck, T.L. and Wallach, D.F. (1971) Electrophoretic analysis of the major polypeptides of the human erythrocyte membrane. *Biochemistry*, **10**, 2606-2617.

Finer, J.J., Finer, K.R. and Ponappa, T. (1999) Particle bombardment mediated transformation. *Curr Top Microbiol Immunol*, **240**, 59-80.

Fiorentino, D.F., Zlotnik, A., Mosmann, T.R., Howard, M. and O'Garra, A. (1991) IL-10 inhibits cytokine production by activated macrophages. *J Immunol*, **147**, 3815-3822.

Fischer, R. and Emans, N. (2000) Molecular farming of pharmaceutical proteins. *Transgenic Res*, **9**, 279-299.

Fischer, R., Schumann, D., Zimmermann, S., Drossard, J., Sack, M. and Schillberg, S. (1999) Expression and characterization of bispecific single-chain Fv fragments produced in transgenic plants. *Eur J Biochem*, **262**, 810-816.

Fitchen, J., Beachy, R.N. and Hein, M.B. (1995) Plant virus expressing hybrid coat protein with added murine epitope elicits autoantibody response. *Vaccine*, **13**, 1051-1057.

Fitchette, A., Gomord, V., A, C. and Faye, L. (1994) Distribution of xylosylation and fucosylation in the plant Golgi-apparatus. *Plant J*, **5**, 673-682.

Floss, D.M., Sack, M., Stadlmann, J., Rademacher, T., Scheller, J., Stoger, E., Fischer, R. and Conrad, U. (2008) Biochemical and functional characterization of anti-HIV antibody-ELP fusion proteins from transgenic plants. *Plant Biotechnol J*, **6**, 379-391.

Fraley, R.T., Rogers, S.G., Horsch, R.B., Sanders, P.R., Flick, J.S., Adams, S.P., Bittner, M.L., Brand, L.A., Fink, C.L., Fry, J.S., Galluppi, G.R., Goldberg, S.B., Hoffmann, N.L. and Woo, S.C. (1983) Expression of bacterial genes in plant cells. *Proc Natl Acad Sci U S A*, **80**, 4803-4807.

Franken, E., Teuschel, U. and Hain, R. (1997) Recombinant proteins from transgenic plants. *Curr Opin Biotechnol*, **8**, 411-416.

Frigerio, L., Pastres, A., Prada, A. and Vitale, A. (2001) Influence of KDEL on the fate of trimeric or assembly-defective phaseolin: selective use of an alternative route to vacuoles. *Plant Cell*, **13**, 1109-1126.

Frutos, R., Denise, H., Vivares, C., Neuhaus, J.M., Vitale, S., Pedrazzini, E., Ma, J., Dix, P., Gray, J., Pezzotti, M., Conrad, U. and Robinson, D. (2008) Pharmaceutical proteins in plants. A strategic genetic engineering approach for the production of tuberculosis antigens. *Ann N Y Acad Sci*, **1149**, 275-280.

Garside, P., Mowat, A.M. and Khoruts, A. (1999) Oral tolerance in disease. *Gut*, **44**, 137-142.

Gasparis, S., Bregier, C., Orczyk, W. and Nadolska-Orczyk, A. (2008) Agrobacterium-mediated transformation of oat (Avena sativa L.) cultivars via immature embryo and leaf explants. *Plant Cell Rep*, **27**, 1721-1729.

Gatz, C., Frohberg, C. and Wendenburg, R. (1992) Stringent repression and homogeneous de-repression by tetracycline of a modified CaMV 35S promoter in intact transgenic tobacco plants. *Plant J*, **2**, 397-404.

Gatz, C. and Quail, P.H. (1988) Tn10-encoded tet repressor can regulate an operator-containing plant promoter. *Proc Natl Acad Sci U S A*, **85**, 1394-1397.

Gelvin, S.B. (2003) Agrobacterium-mediated plant transformation: the biology behind the "gene-jockeying" tool. *Microbiol Mol Biol Rev*, **67**, 16-37.

Giddings, G., Allison, G., Brooks, D. and Carter, A. (2000) Transgenic plants as factories for biopharmaceuticals. *Nat Biotechnol*, **18**, 1151-1155.

Giritch, A., Marillonnet, S., Engler, C., van Eldik, G., Botterman, J., Klimyuk, V. and Gleba, Y. (2006) Rapid high-yield expression of full-size IgG antibodies in plants coinfected with noncompeting viral vectors. *Proc Natl Acad Sci U S A*, **103**, 14701-14706.

Gleba, Y., Klimyuk, V. and Marillonnet, S. (2007) Viral vectors for the expression of proteins in plants. *Curr Opin Biotechnol*, **18**, 134-141.

Glenz, K., Bouchon, B., Stehle, T., Wallich, R., Simon, M.M. and Warzecha, H. (2006) Production of a recombinant bacterial lipoprotein in higher plant chloroplasts. *Nat Biotechnol*, **24**, 76-77.

Gomord, V., Denmat, L.A., Fitchette-Laine, A.C., Satiat-Jeunemaitre, B., Hawes, C. and Faye, L. (1997) The C-terminal HDEL sequence is sufficient for retention of secretory proteins in the endoplasmic reticulum (ER) but promotes vacuolar targeting of proteins that escape the ER. *Plant J*, **11**, 313-325.

Groux, H., Bigler, M., de Vries, J.E. and Roncarolo, M.G. (1996) Interleukin-10 induces a long-term antigen-specific anergic state in human CD4+ T cells. *J Exp Med*, **184**, 19-29.

Gurel, S., Gurel, E., Kaur, R., Wong, J., Meng, L., Tan, H.Q. and Lemaux, P.G. (2009) Efficient, reproducible Agrobacterium-mediated transformation of sorghum using heat treatment of immature embryos. *Plant Cell Rep*, **28**, 429-444.

Hanninen, A. (2000) Prevention of autoimmune type 1 diabetes via mucosal tolerance: is mucosal autoantigen administration as safe and effective as it should be? *Scand J Immunol*, **52**, 217-225.

Harwood, W.A., Bartlett, J.G., Alves, S.C., Perry, M., Smedley, M.A., Leyland, N. and Snape, J.W. (2009) Barley transformation using Agrobacterium-mediated techniques. *Methods Mol Biol*, **478**, 137-147.

Hellwig, S., Drossard, J., Twyman, R.M. and Fischer, R. (2004) Plant cell cultures for the production of recombinant proteins. *Nat Biotechnol*, **22**, 1415-1422.

Hennig, A., Bonfig, K., Roitsch, T. and Warzecha, H. (2007) Expression of the recombinant bacterial outer surface protein A in tobacco chloroplasts leads to thylakoid localization and loss of photosynthesis. *Febs J*, **274**, 5749-5758.

Hernandez, J., Rubio, M., Olmos, E., Ros-Barcelo, A. and Martinez-Gomez, P. (2004) Oxidative stress induced by long-term plum pox virus infection in peach (*Prunus persica*). *Physiol. Plant.*, **122**, 486-495.

Hiei, Y. and Komari, T. (2008) Agrobacterium-mediated transformation of rice using immature embryos or calli induced from mature seed. *Nat Protoc*, **3**, 824-834.

Holmes, D.S. and Quigley, M. (1981) A rapid boiling method for the preparation of bacterial plasmids. *Anal Biochem*, **114**, 193-197.

Horsch, R.B., Rogers, S.G. and Fraley, R.T. (1985) Transgenic plants. *Cold Spring Harb Symp Quant Biol*, **50**, 433-437.

Howe, A., Sato, S., Dweikat, I., Fromm, M. and Clemente, T. (2006) Rapid and reproducible Agrobacterium-mediated transformation of sorghum. *Plant Cell Rep*, **25**, 784-791.

Hsu, D.H., de Waal Malefyt, R., Fiorentino, D.F., Dang, M.N., Vieira, P., de Vries, J., Spits, H., Mosmann, T.R. and Moore, K.W. (1990) Expression of interleukin-10 activity by Epstein-Barr virus protein BCRF1. *Science*, **250**, 830-832.

Ito, S., Ansari, P., Sakatsume, M., Dickensheets, H., Vazquez, N., Donnelly, R.P., Larner, A.C. and Finbloom, D.S. (1999) Interleukin-10 inhibits expression of both interferon alpha- and interferon gamma- induced genes by suppressing tyrosine phosphorylation of STAT1. *Blood*, **93**, 1456-1463.

Jach, G., Binot, E., Frings, S., Luxa, K. and Schell, J. (2001) Use of red fluorescent protein from Discosoma sp. (dsRED) as a reporter for plant gene expression. *Plant J*, **28**, 483-491.

Jefferson, R.A., Kavanagh, T.A. and Bevan, M.W. (1987) GUS fusions: beta-glucuronidase as a sensitive and versatile gene fusion marker in higher plants. *Embo J*, **6**, 3901-3907.

Kanamoto, H., Yamashita, A., Asao, H., Okumura, S., Takase, H., Hattori, M., Yokota, A. and Tomizawa, K. (2006) Efficient and stable transformation of Lactuca sativa L. cv. Cisco (lettuce) plastids. *Transgenic Res*, **15**, 205-217.

Kapila, J., De Rycke, R., Van Montagu, M. and Angenon, G. (1997) An Agrobacterium-mediated transient gene expression system for intact leaves. *Plant Science*, **122**, 101-108.

Kay, R., Chan, A., Daly, M. and McPherson, J. (1987) Duplication of CaMV 35S Promoter Sequences Creates a Strong Enhancer for Plant Genes. *Science*, **236**, 1299-1302.

Kidambi, S. and Patel, S.B. (2008) Diabetes mellitus: considerations for dentistry. *J Am Dent Assoc*, **139 Suppl**, 8S-18S.

Kim, T.G., Kim, M.Y., Kim, B.G., Kang, T.J., Kim, Y.S., Jang, Y.S., Arntzen, C.J. and Yang, M.S. (2007) Synthesis and assembly of Escherichia coli heat-labile enterotoxin B subunit in transgenic lettuce (Lactuca sativa). *Protein Expr Purif*, **51**, 22-27.

Kimball, A.B., Kawamura, T., Tejura, K., Boss, C., Hancox, A.R., Vogel, J.C., Steinberg, S.M., Turner, M.L. and Blauvelt, A. (2002) Clinical and immunologic assessment of patients with psoriasis in a randomized, double-blind, placebo-controlled trial using recombinant human interleukin 10. *Arch Dermatol*, **138**, 1341-1346.

Kolarich, D. and Altmann, F. (2000) N-glycan analysis by matrix-assisted laser desorption/ionization mass spectrometry of electrophoretically separated nonmammalian proteins: application to peanut allergen Ara h 1 and olive pollen allergen Ole e 1. *Anal Biochem*, **285**, 64-75.

Kolarich, D., Altmann, F. and Sunderasan, E. (2006) Structural analysis of the glycoprotein allergen Hev b 4 from natural rubber latex by mass spectrometry. *Biochim Biophys Acta*, **1760**, 715-720.

Koncz, C. and Schell, J. (1986) The promoter of TL-DNA gene 5 controls the tissue-specific expression of chimeric genes carried by a novel type of Agrobacterium binary vector. *Mol Gen Genet*, **204**, 383-396.

Kong, Q., Richter, L., Yang, Y.F., Arntzen, C.J., Mason, H.S. and Thanavala, Y. (2001) Oral immunization with hepatitis B surface antigen expressed in transgenic plants. *Proc Natl Acad Sci U S A*, **98**, 11539-11544.

Kumar, S., Dhingra, A. and Daniell, H. (2004) Plastid-expressed betaine aldehyde dehydrogenase gene in carrot cultured cells, roots, and leaves confers enhanced salt tolerance. *Plant Physiol*, **136**, 2843-2854.

Kuroda, H. and Maliga, P. (2001) Complementarity of the 16S rRNA penultimate stem with sequences downstream of the AUG destabilizes the plastid mRNAs. *Nucleic Acids Res*, **29**, 970-975.

Laemmli, U.K. (1970) Cleavage of structural proteins during the assembly of the head of bacteriophage T4. *Nature*, **227**, 680-685.

Lal, P., Ramachandran, V.G., Goyal, R. and Sharma, R. (2007) Edible vaccines: current status and future. *Indian J Med Microbiol*, **25**, 93-102.

Larche, M. and Wraith, D.C. (2005) Peptide-based therapeutic vaccines for allergic and autoimmune diseases. *Nat Med*, **11**, S69-76.

Lelivelt, C.L., McCabe, M.S., Newell, C.A., Desnoo, C.B., van Dun, K.M., Birch-Machin, I., Gray, J.C., Mills, K.H. and Nugent, J.M. (2005) Stable plastid transformation in lettuce (Lactuca sativa L.). *Plant Mol Biol*, **58**, 763-774.

Lerouge, P., Cabanes-Macheteau, M., Rayon, C., Fischette-Laine, A.C., Gomord, V. and Faye, L. (1998) N-glycoprotein biosynthesis in plants: recent developments and future trends. *Plant Mol Biol*, **38**, 31-48.

Lienard, D., Sourrouille, C., Gomord, V. and Faye, L. (2007) Pharming and transgenic plants. *Biotechnol Annu Rev*, **13**, 115-147.

Lindbo, J.A. (2007) TRBO: a high-efficiency tobacco mosaic virus RNA-based overexpression vector. *Plant Physiol*, **145**, 1232-1240.

Lou, X.M., Yao, Q.H., Zhang, Z., Peng, R.H., Xiong, A.S. and Wang, H.K. (2007) Expression of the human hepatitis B virus large surface antigen gene in transgenic tomato plants. *Clin Vaccine Immunol*, **14**, 464-469.

Lucas, A. and McFadden, G. (2004) Secreted immunomodulatory viral proteins as novel biotherapeutics. *J Immunol*, **173**, 4765-4774.

Ma, J.K., Barros, E., Bock, R., Christou, P., Dale, P.J., Dix, P.J., Fischer, R., Irwin, J., Mahoney, R., Pezzotti, M., Schillberg, S., Sparrow, P., Stoger, E. and Twyman, R.M. (2005) Molecular farming for new drugs and vaccines. Current perspectives on the production of pharmaceuticals in transgenic plants. *EMBO Rep*, **6**, 593-599.

Ma, J.K., Drake, P.M. and Christou, P. (2003) The production of recombinant pharmaceutical proteins in plants. *Nat Rev Genet*, **4**, 794-805.

Ma, J.K., Hiatt, A., Hein, M., Vine, N.D., Wang, F., Stabila, P., van Dolleweerd, C., Mostov, K. and Lehner, T. (1995) Generation and assembly of secretory antibodies in plants. *Science*, **268**, 716-719.

Ma, S., Huang, Y., Yin, Z., Menassa, R., Brandle, J.E. and Jevnikar, A.M. (2004) Induction of oral tolerance to prevent diabetes with transgenic plants requires glutamic acid decarboxylase (GAD) and IL-4. *Proc Natl Acad Sci U S A*, **101**, 5680-5685.

Marillonnet, S., Giritch, A., Gils, M., Kandzia, R., Klimyuk, V. and Gleba, Y. (2004) In planta engineering of viral RNA replicons: efficient assembly by recombination of DNA modules delivered by Agrobacterium. *Proc Natl Acad Sci U S A*, **101**, 6852-6857.

Mason, H.S., Ball, J.M., Shi, J.J., Jiang, X., Estes, M.K. and Arntzen, C.J. (1996) Expression of Norwalk virus capsid protein in transgenic tobacco and potato and its oral immunogenicity in mice. *Proc Natl Acad Sci U S A*, **93**, 5335-5340.

Mason, H.S., Haq, T.A., Clements, J.D. and Arntzen, C.J. (1998) Edible vaccine protects mice against Escherichia coli heat-labile enterotoxin (LT): potatoes expressing a synthetic LT-B gene. *Vaccine*, **16**, 1336-1343.

Mason, H.S., Lam, D.M. and Arntzen, C.J. (1992) Expression of hepatitis B surface antigen in transgenic plants. *Proc Natl Acad Sci U S A*, **89**, 11745-11749.

Mayer, L. and Shao, L. (2004) Therapeutic potential of oral tolerance. *Nat Rev Immunol*, **4**, 407-419.

McBride, K.E., Svab, Z., Schaaf, D.J., Hogan, P.S., Stalker, D.M. and Maliga, P. (1995) Amplification of a chimeric Bacillus gene in chloroplasts leads to an extraordinary level of an insecticidal protein in tobacco. *Biotechnology (N Y)*, **13**, 362-365.

Menassa, R., Du, C., Yin, Z.Q., Ma, S., Poussier, P., Brandle, J. and Jevnikar, A.M. (2007) Therapeutic effectiveness of orally administered transgenic low-alkaloid tobacco expressing human interleukin-10 in a mouse model of colitis. *Plant Biotechnol J*, **5**, 50-59.

Menassa, R., Kennette, W., Nguyen, V., Rymerson, R., Jevnikar, A. and Brandle, J. (2004) Subcellular targeting of human interleukin-10 in plants. *J Biotechnol*, **108**, 179-183.

Menassa, R., Nguyen, V., Jevnikar, A. and Brandle, J. (2001) A self-contained system for the field production of plant recombinant interleukin-10. *Molecular Breeding*, **8**, 177-185.

Meyers, A., Chakauya, E., Shephard, E., Tanzer, F.L., Maclean, J., Lynch, A., Williamson, A.L. and Rybicki, E.P. (2008) Expression of HIV-1 antigens in plants as potential subunit vaccines. *BMC Biotechnol*, **8**, 53.

Mitoma, J. and Ito, A. (1992) The carboxy-terminal 10 amino acid residues of cytochrome b5 are necessary for its targeting to the endoplasmic reticulum. *Embo J*, **11**, 4197-4203.

Moore, K.W., de Waal Malefyt, R., Coffman, R.L. and O'Garra, A. (2001) Interleukin-10 and the interleukin-10 receptor. *Annu Rev Immunol*, **19**, 683-765.

Moore, K.W., O'Garra, A., De Waal Malefyt, R., Vieira, P. and Mosmann, T.R. (1993) Interleukin-10. *Annu Rev Immunol*, **11**, 165-190.

Moore, K.W., Vieira, P., Fiorentino, D.F., Trounstine, M.L., Khan, T.A. and Mosmann, T.R. (1990) Homology of cytokine synthesis inhibitory factor (IL-10) to the Epstein-Barr virus gene BCRFI. *Science*, **248**, 1230-1234.

Mosmann, T.R., Schumacher, J.H., Fiorentino, D.F., Leverah, J., Moore, K.W. and Bond, M.W. (1990) Isolation of monoclonal antibodies specific for IL-4, IL-5, IL-6, and a new Th2-specific cytokine (IL-10), cytokine synthesis inhibitory factor, by using a solid phase radioimmunoadsorbent assay. *J Immunol*, **145**, 2938-2945.

Munne-Bosch, S. and Alegre, L. (2001) Subcellular compartmentation of the diterpene carnosic acid and its derivatives in the leaves of rosemary. *Plant Physiol*, **125**, 1094-1102.

Nochi, T., Takagi, H., Yuki, Y., Yang, L., Masumura, T., Mejima, M., Nakanishi, U., Matsumura, A., Uozumi, A., Hiroi, T., Morita, S., Tanaka, K., Takaiwa, F. and Kiyono, H. (2007) Rice-based mucosal vaccine as a global strategy for cold-chain- and needle-free vaccination. *Proc Natl Acad Sci U S A*, **104**, 10986-10991.

Oey, M., Lohse, M., Kreikemeyer, B. and Bock, R. (2008) Exhaustion of the chloroplast protein synthesis capacity by massive expression of a highly stable protein antibiotic. *Plant J*, **57**, 436-445.

Pagny, S., Cabanes-Macheteau, M., Gillikin, J.W., Leborgne-Castel, N., Lerouge, P., Boston, R.S., Faye, L. and Gomord, V. (2000) Protein recycling from the Golgi apparatus to the endoplasmic reticulum in plants and its minor contribution to calreticulin retention. *Plant Cell*, **12**, 739-756.

Patel, J., Zhu, H., Menassa, R., Gyenis, L., Richman, A. and Brandle, J. (2007) Elastin-like polypeptide fusions enhance the accumulation of recombinant proteins in tobacco leaves. *Transgenic Res*, **16**, 239-249.

Petruccelli, S., Otegui, M.S., Lareu, F., Tran Dinh, O., Fitchette, A.C., Circosta, A., Rumbo, M., Bardor, M., Carcamo, R., Gomord, V. and Beachy, R.N. (2006) A KDEL-tagged monoclonal antibody is efficiently retained in the endoplasmic reticulum in leaves, but is both partially secreted and sorted to protein storage vacuoles in seeds. *Plant Biotechnol J*, **4**, 511-527.

Pogue, G.P., Lindbo, J.A., Garger, S.J. and Fitzmaurice, W.P. (2002) Making an ally from an enemy: plant virology and the new agriculture. *Annu Rev Phytopathol*, **40**, 45-74.

Rigano, M.M., Sala, F., Arntzen, C.J. and Walmsley, A.M. (2003) Targeting of plant-derived vaccine antigens to immunoresponsive mucosal sites. *Vaccine*, **21**, 809-811.

Rigano, M.M. and Walmsley, A.M. (2005) Expression systems and developments in plant-made vaccines. *Immunol Cell Biol*, **83**, 271-277.

Risacher, T., Craze, M., Bowden, S., Paul, W. and Barsby, T. (2009) Highly efficient Agrobacterium-mediated transformation of wheat via in planta inoculation. *Methods Mol Biol*, **478**, 115-124.

Rogalski, M., Ruf, S. and Bock, R. (2006) Tobacco plastid ribosomal protein S18 is essential for cell survival. *Nucleic Acids Res*, **34**, 4537-4545.

Ruelland, E. and Miginiac-Maslow, M. (1999) Regulation of chloroplast enzyme activities by thioredoxins: activation or relief from inhibition? *Trends Plant Sci*, **4**, 136-141.

Ruf, S., Biehler, K. and Bock, R. (2000) A small chloroplast-encoded protein as a novel architectural component of the light-harvesting antenna. *J Cell Biol*, **149**, 369-378.

Ruf, S., Hermann, M., Berger, I.J., Carrer, H. and Bock, R. (2001) Stable genetic transformation of tomato plastids and expression of a foreign protein in fruit. *Nat Biotechnol*, **19**, 870-875.

Ruf, S., Karcher, D. and Bock, R. (2007) Determining the transgene containment level provided by chloroplast transformation. *Proc Natl Acad Sci U S A*, **104**, 6998-7002.

Sainsbury, F. and Lomonossoff, G.P. (2008) Extremely high-level and rapid transient protein production in plants without the use of viral replication. *Plant Physiol*, **148**, 1212-1218.

Salek-Ardakani, S., Stuart, A.D., Arrand, J.E., Lyons, S., Arrand, J.R. and Mackett, M. (2002) High level expression and purification of the Epstein-Barr virus encoded cytokine viral interleukin 10: efficient removal of endotoxin. *Cytokine*, **17**, 1-13.

Sallas, L., Luomala, E.M., Ultriainen, J., Kainulainen, P. and Holopainen, J.K. (2003) Contrasting effects of elevated carbon dioxide concentration and temperature on Rubisco activity, chlorophyll fluorescence, needle ultrastructure and secondary metabolites in conifer seedlings. *Tree Physiol*, **23**, 97-108.

Sam, O., Ramirez, C., Coronado, M., Testillano, P. and Risueno, M. (2003) Changes in tomato leaves induced by NaCl stress: leaf organization and cell ultrastructure. *Biol Plant*, **47**, 361-366.

Sambrook, J., Fritsch, E.F. and Maniatis, T. (1996) *Molecular Cloning - A Laboratory Manual*.

Sambrook, J. and Russel, D. (2001) *Molecular Cloning - A Laboratory Manual*.

Santi, L., Batchelor, L., Huang, Z., Hjelm, B., Kilbourne, J., Arntzen, C.J., Chen, Q. and Mason, H.S. (2008) An efficient plant viral expression system generating orally immunogenic Norwalk virus-like particles. *Vaccine*, **26**, 1846-1854.

Schagger, H. and von Jagow, G. (1987) Tricine-sodium dodecyl sulfate-polyacrylamide gel electrophoresis for the separation of proteins in the range from 1 to 100 kDa. *Anal Biochem*, **166**, 368-379.

Schillberg, S., Zimmermann, S., Findlay, K. and Fischer, R. (2000) Plasma membrane display of anti-viral single chain Fv fragments confers resistance to tobacco mosaic virus. *Molecular Breeding*, **6**, 317-326.

Schillberg, S., Zimmermann, S., Voss, A. and Fischer, R. (1999) Apoplastic and cytosolic expression of full-size antibodies and antibody fragments in *Nicotiana tabacum*. *Transgenic Res*, **8**, 255-263.

Schotte, L., Steidler, L., Vandekerckhove, J. and Remaut, E. (2000) Secretion of biologically active murine interleukin-10 by Lactococcus lactis. *Enzyme Microb Technol*, **27**, 761-765.

Schouten, A., Roosien, J., van Engelen, F.A., de Jong, G.A., Borst-Vrenssen, A.W., Zilverentant, J.F., Bosch, D., Stiekema, W.J., Gommers, F.J., Schots, A. and Bakker, J. (1996) The C-terminal KDEL sequence increases the expression level of a single-chain antibody designed to be targeted to both the cytosol and the secretory pathway in transgenic tobacco. *Plant Mol Biol*, **30**, 781-793.

Schuster, D.P. and Duvuuri, V. (2002) Diabetes mellitus. *Clin Podiatr Med Surg*, **19**, 79-107.

Seki, M., Iida, A. and Morikawa, H. (1999) Transient expression of the beta-glucuronidase gene in tissues of Arabidopsis thaliana by bombardment-mediated transformation. *Mol Biotechnol*, **11**, 251-255.

Sheludko, Y.V. (2008) Agrobacterium-mediated transient expression as an approach to production of recombinant proteins in plants. *Recent Pat Biotechnol*, **2**, 198-208.

Shevchenko, A., Wilm, M., Vorm, O. and Mann, M. (1996) Mass spectrometric sequencing of proteins silver-stained polyacrylamide gels. *Anal Chem*, **68**, 850-858.

Smith, N., Kilpatrick, J. and Whitelam, G. (2001) Superfluous transgene integration in plants. *Crit Rev Plant Sci*, **20**, 215-249.

Sorrentino, A., Schillberg, S., Fischer, R., Porta, R. and Mariniello, L. (2008) Molecular farming of human tissue transglutaminase in tobacco plants. *Amino Acids*.

Sprang, S. and Bazan, J. (1993) Cytokine structural taxonomy and mechanisms of receptor engagement. *Curr Opin Struct Biol*, **3**, 815-827.

Sripriya, R., Raghupathy, V. and Veluthambi, K. (2008) Generation of selectable marker-free sheath blight resistant transgenic rice plants by efficient co-transformation of a cointegrate vector T-DNA and a binary vector T-DNA in one Agrobacterium tumefaciens strain. *Plant Cell Rep*, **27**, 1635-1644.

Sriraman, R., Bardor, M., Sack, M., Vaquero, C., Faye, L., Fischer, R., Finnern, R. and Lerouge, P. (2004) Recombinant anti-hCG antibodies retained in the endoplasmic reticulum of transformed plants lack core-xylose and core-alpha(1,3)-fucose residues. *Plant Biotechnol J*, **2**, 279-287.

Staub, J.M., Garcia, B., Graves, J., Hajdukiewicz, P.T., Hunter, P., Nehra, N., Paradkar, V., Schlittler, M., Carroll, J.A., Spatola, L., Ward, D., Ye, G. and Russell, D.A. (2000) High-yield production of a human therapeutic protein in tobacco chloroplasts. *Nat Biotechnol*, **18**, 333-338.

Steidler, L., Hans, W., Schotte, L., Neirynck, S., Obermeier, F., Falk, W., Fiers, W. and Remaut, E. (2000) Treatment of murine colitis by Lactococcus lactis secreting interleukin-10. *Science*, **289**, 1352-1355.

Stevens, L., Stoopen, G., Elbers, I., Molthoff, J., Bakker, H., Lommen, A., Bosch, D. and Jordi, W. (2000) Effect of climate conditions and plant developmental stage on the stability of antibodies expressed in transgenic tobacco. *Plant Physiol*, **124**, 173-182.

Stoger, E., Sack, M., Perrin, Y., Vaquero, C., Torres, E., Twyman, R.M., Christou, P. and Fischer, R. (2002) Practical considerations for pharmaceutical antibody production in different crop systems. *Mol Breeding*, **9**, 149-158.

Stoger, E., Vaquero, C., Torres, E., Sack, M., Nicholson, L., Drossard, J., Williams, S., Keen, D., Perrin, Y., Christou, P. and Fischer, R. (2000) Cereal crops as viable production and storage systems for pharmaceutical scFv antibodies. *Plant Mol Biol*, **42**, 583-590.

Streatfield, S.J. (2006) Mucosal immunization using recombinant plant-based oral vaccines. *Methods*, **38**, 150-157.

Streatfield, S.J. (2007) Approaches to achieve high-level heterologous protein production in plants. *Plant Biotechnol J*, **5**, 2-15.

Sun, J.B., Rask, C., Olsson, T., Holmgren, J. and Czerkinsky, C. (1996) Treatment of experimental autoimmune encephalomyelitis by feeding myelin basic protein conjugated to cholera toxin B subunit. *Proc Natl Acad Sci U S A*, **93**, 7196-7201.

Svab, Z. and Maliga, P. (1991) Mutation proximal to the tRNA binding region of the Nicotiana plastid 16S rRNA confers resistance to spectinomycin. *Mol Gen Genet*, **228**, 316-319.

Tacket, C.O. (2005) Plant-derived vaccines against diarrheal diseases. *Vaccine*, **23**, 1866-1869.

Tacket, C.O., Mason, H.S., Losonsky, G., Estes, M.K., Levine, M.M. and Arntzen, C.J. (2000) Human immune responses to a novel norwalk virus vaccine delivered in transgenic potatoes. *J Infect Dis*, **182**, 302-305.

Taylor, N.J. and Fauquet, C.M. (2002) Microparticle bombardment as a tool in plant science and agricultural biotechnology. *DNA Cell Biol*, **21**, 963-977.

Tilch, C. and Elias, P.S. (1984) Investigation of the mutagenicity of ethylphenylglycidate. *Mutat Res*, **138**, 1-8.

To, K.Y., Cheng, M.C., Chen, L.F. and Chen, S.C. (1996) Introduction and expression of foreign DNA in isolated spinach chloroplasts by electroporation. *Plant J*, **10**, 737-743.

Torres, E., Vaquero, C., Nicholson, L., Sack, M., Stoger, E., Drossard, J., Christou, P., Fischer, R. and Perrin, Y. (1999) Rice cell culture as an alternative production system for functional diagnostic and therapeutic antibodies. *Transgenic Res*, **8**, 441-449.

Tregoning, J.S., Clare, S., Bowe, F., Edwards, L., Fairweather, N., Qazi, O., Nixon, P.J., Maliga, P., Dougan, G. and Hussell, T. (2005) Protection against tetanus toxin using a plant-based vaccine. *Eur J Immunol*, **35**, 1320-1326.

Triguero, A., Cabrera, G., Cremata, J.A., Yuen, C.T., Wheeler, J. and Ramirez, N.I. (2005) Plant-derived mouse IgG monoclonal antibody fused to KDEL endoplasmic reticulum-retention signal is N-glycosylated homogeneously throughout the plant with mostly high-mannose-type N-glycans. *Plant Biotechnol J*, **3**, 449-457.

Twyman, R.M., Schillberg, S. and Fischer, R. (2005) Transgenic plants in the biopharmaceutical market. *Expert Opin Emerg Drugs*, **10**, 185-218.

Twyman, R.M., Stoger, E., Schillberg, S., Christou, P. and Fischer, R. (2003) Molecular farming in plants: host systems and expression technology. *Trends Biotechnol*, **21**, 570-578.

Van Droogenbroeck, B., Cao, J., Stadlmann, J., Altmann, F., Colanesi, S., Hillmer, S., Robinson, D.G., Van Lerberge, E., Terryn, N., Van Montagu, M., Liang, M., Depicker, A. and De Jaeger, G. (2007) Aberrant localization and underglycosylation of highly accumulating single-chain Fv-Fc antibodies in transgenic Arabidopsis seeds. *Proc Natl Acad Sci U S A*, **104**, 1430-1435.

Vaquero, C., Sack, M., Chandler, J., Drossard, J., Schuster, F., Monecke, M., Schillberg, S. and Fischer, R. (1999) Transient expression of a tumor-specific single-chain fragment and a chimeric antibody in tobacco leaves. *Proc Natl Acad Sci U S A*, **96**, 11128-11133.

Vega, J.M., Yu, W., Kennon, A.R., Chen, X. and Zhang, Z.J. (2008) Improvement of Agrobacterium-mediated transformation in Hi-II maize (Zea mays) using standard binary vectors. *Plant Cell Rep*, **27**, 297-305.

Vieira, P., de Waal-Malefyt, R., Dang, M.N., Johnson, K.E., Kastelein, R., Fiorentino, D.F., deVries, J.E., Roncarolo, M.G., Mosmann, T.R. and Moore, K.W. (1991) Isolation and expression of human cytokine synthesis inhibitory factor cDNA clones: homology to Epstein-Barr virus open reading frame BCRFI. *Proc Natl Acad Sci U S A*, **88**, 1172-1176.

Villani, M.E., Morgun, B., Brunetti, P., Marusic, C., Lombardi, R., Pisoni, I., Bacci, C., Desiderio, A., Benvenuto, E. and Donini, M. (2009) Plant pharming of a full-sized, tumour-targeting antibody using different expression strategies. *Plant Biotechnol J*, **7**, 59-72.

Vitale, A. and Pedrazzini, E. (2005) Recombinant pharmaceuticals from plants: the plant endomembrane system as bioreactor. *Mol Interv*, **5**, 216-225.

Wakkach, A., Cottrez, F. and Groux, H. (2000) Can interleukin-10 be used as a true immunoregulatory cytokine? *Eur Cytokine Netw*, **11**, 153-160.

Walmsley, A.M., Alvarez, M.L., Jin, Y., Kirk, D.D., Lee, S.M., Pinkhasov, J., Rigano, M.M., Arntzen, C.J. and Mason, H.S. (2003) Expression of the B subunit of Escherichia coli heat-labile enterotoxin as a fusion protein in transgenic tomato. *Plant Cell Rep*, **21**, 1020-1026.

Walsh, S.R. and Shear, N.H. (2004) Psoriasis and the new biologic agents: interrupting a T-AP dance. *Cmaj*, **170**, 1933-1941.

Walter, M.R. and Nagabhushan, T.L. (1995) Crystal structure of interleukin 10 reveals an interferon gamma-like fold. *Biochemistry*, **34**, 12118-12125.

Wang, D.J., Brandsma, M., Yin, Z., Wang, A., Jevnikar, A.M. and Ma, S. (2008a) A novel platform for biologically active recombinant human interleukin-13 production. *Plant Biotechnol J*, **6**, 504-515.

Wang, X., Brandsma, M., Tremblay, R., Maxwell, D., Jevnikar, A.M., Huner, N. and Ma, S. (2008b) A novel expression platform for the production of diabetes-associated autoantigen human glutamic acid decarboxylase (hGAD65). *BMC Biotechnol*, **8**, 87.

Wogensen, L., Lee, M.S. and Sarvetnick, N. (1994) Production of interleukin 10 by islet cells accelerates immune-mediated destruction of beta cells in nonobese diabetic mice. *J Exp Med*, **179**, 1379-1384.

Wolfraim, L.A. (2006) Treating autoimmune diseases through restoration of antigen-specific immune tolerance. *Arch Immunol Ther Exp (Warsz)*, **54**, 1-13.

Wu, H., Doherty, A. and Jones, H.D. (2009) Agrobacterium-mediated transformation of bread and durum wheat using freshly isolated immature embryos. *Methods Mol Biol*, **478**, 93-103.

Wurbs, D., Ruf, S. and Bock, R. (2007) Contained metabolic engineering in tomatoes by expression of carotenoid biosynthesis genes from the plastid genome. *Plant J*, **49**, 276-288.

Yoon, S.I., Jones, B.C., Logsdon, N.J. and Walter, M.R. (2005) Same structure, different function crystal structure of the Epstein-Barr virus IL-10 bound to the soluble IL-10R1 chain. *Structure*, **13**, 551-564.

Yusibov, V., Hooper, D.C., Spitsin, S.V., Fleysh, N., Kean, R.B., Mikheeva, T., Deka, D., Karasev, A., Cox, S., Randall, J. and Koprowski, H. (2002) Expression in plants and immunogenicity of plant virus-based experimental rabies vaccine. *Vaccine*, **20**, 3155-3164.

Yusibov, V., Rabindran, S., Commandeur, U., Twyman, R.M. and Fischer, R. (2006) The potential of plant virus vectors for vaccine production. *Drugs R D*, **7**, 203-217.

Zdanov, A., Schalk-Hihi, C., Gustchina, A., Tsang, M., Weatherbee, J. and Wlodawer, A. (1995) Crystal structure of interleukin-10 reveals the functional dimer with an unexpected topological similarity to interferon gamma. *Structure*, **3**, 591-601.

Zdanov, A., Schalk-Hihi, C., Menon, S., Moore, K.W. and Wlodawer, A. (1997) Crystal structure of Epstein-Barr virus protein BCRF1, a homolog of cellular interleukin-10. *J Mol Biol*, **268**, 460-467.

Zhao, J., Onduka, T., Kinoshita, J.Y., Honsho, M., Kinoshita, T., Shimazaki, K. and Ito, A. (2003) Dual subcellular distribution of cytochrome b5 in plant, cauliflower, cells. *J Biochem (Tokyo)*, **133**, 115-121.

Zhou, F., Badillo-Corona, J.A., Karcher, D., Gonzalez-Rabade, N., Piepenburg, K., Borchers, A.M., Maloney, A.P., Kavanagh, T.A., Gray, J.C. and Bock, R. (2008) High-level expression of human immunodeficiency virus antigens from the tobacco and tomato plastid genomes. *Plant Biotechnol J*, **6**, 897-913.

Zhou, F., Karcher, D. and Bock, R. (2007) Identification of a plastid intercistronic expression element (IEE) facilitating the expression of stable translatable monocistronic mRNAs from operons. *Plant J*, **52**, 961-972.

Zikakis, J.P., Rzucidlo, S.J. and Biasotto, N.O. (1977) Persistence of bovine milk xanthine oxidase activity after gastric digestion in vivo and in vitro. *J Dairy Sci*, **60**, 533-541.